Innovation, Sciences et Développement économique Canada
Office de la Propriété Intellectuelle du Canada

Innovation, Science and Economic Development Canada
Canadian Intellectual Property Office

CA 3124838 A1 2020/07/09

(21) 3 124 838

(12) DEMANDE DE BREVET CANADIEN
CANADIAN PATENT APPLICATION

(13) A1

(86) Date de dépôt PCT/PCT Filing Date: 2019/12/31
(87) Date publication PCT/PCT Publication Date: 2020/07/09
(85) Entrée phase nationale/National Entry: 2021/06/23
(86) N° demande PCT/PCT Application No.: US 2019/069145
(87) N° publication PCT/PCT Publication No.: 2020/142547
(30) Priorité/Priority: 2018/12/31 (US62/786,970)

(51) Cl.Int./Int.Cl. *A61K 31/416* (2006.01)

(71) Demandeur/Applicant:
THE BOARD OF TRUSTEES OF THE LELAND STANFORD JUNIOR UNIVERSITY, US

(72) Inventeurs/Inventors:
GREEN, MICHAEL J., US;
JAHANGIR, ALAM, US;
MOORE, TEREZA, US;
COWAN, TINA M., US;
ENNS, GREGORY M., US;
SHAMLOO, MEHRDAD, US;
YANES, ROLANDO E., US

(74) Agent: GOWLING WLG (CANADA) LLP

(54) Titre : METHODES ET FORMULATIONS POUR TRAITER UN DYSFONCTIONNEMENT MITOCHONDRIAL
(54) Title: METHODS AND FORMULATIONS TO TREAT MITOCHONDRIAL DYSFUNCTION

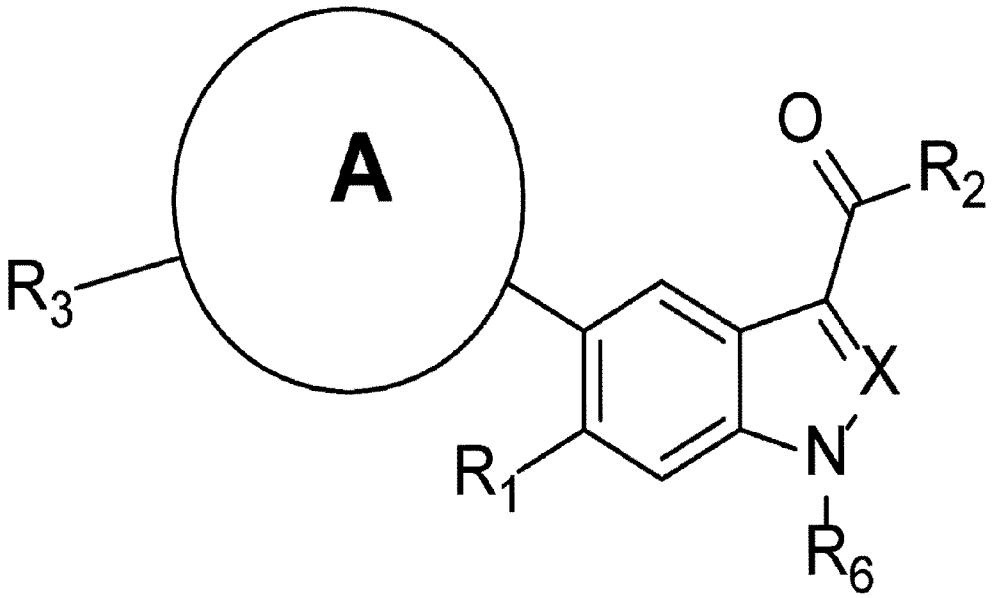

Fig. 12A

(57) Abrégé/Abstract:
Methods of treatment and pharmaceutical formulations configured to treat primary and secondary mitochondrial dysfunction are provided. The methods and treatments use an agonist of AMPK. The agonist activates AMPK to activate ATP-producing pathways and inhibiting ATP-consuming pathways, thus allowing for the alleviation of symptoms associated with mitochondrial dysfunctions.

(12) INTERNATIONAL APPLICATION PUBLISHED UNDER THE PATENT COOPERATION TREATY (PCT)

CORRECTED VERSION

(19) World Intellectual Property Organization
International Bureau

(43) International Publication Date
09 July 2020 (09.07.2020)

WIPO | PCT

(10) International Publication Number
WO 2020/142547 A8

(51) International Patent Classification:
A61K 31/416 (2006.01)

(21) International Application Number:
PCT/US2019/069145

(22) International Filing Date:
31 December 2019 (31.12.2019)

(25) Filing Language: English

(26) Publication Language: English

(30) Priority Data:
62/786,970 31 December 2018 (31.12.2018) US

(71) Applicant: **THE BOARD OF TRUSTEES OF THE LELAND STANFORD JUNIOR UNIVERSITY** [US/US]; Office of the General Counsel Building 170, 3rd Floor, Main Quad, P.O. Box 20386, Stanford, CA 94305-2038 (US).

(72) Inventors; and

(71) Applicants: **GREEN, Michael J.**; 400 Balboa Boulevard, Half Moon Bay, CA 94019 (US). **JAHANGIR, Alam**; 3655 Valley Ridge Lane, San Jose, CA 95148 (US).

(72) Inventors: **MOORE, Tereza**; 3375 Hillview Avenue, Palo Alto, CA 94304 (US). **COWAN, Tina, M.**; 3375 Hillview Avenue, Room 2101, Mail Code: 5324, Palo Alto, CA 94304 (US). **ENNS, Gregory, M.**; 300 Pasteur Drive, Suite H-315, Palo Alto, CA 94304 (US). **SHAMLOO, Mehrdad**; Office of the General Counsel Building 170, 3rd Floor, Main Quad, P.O. Box 20386, Stanford, CA 94305-2038 (US).

(74) Agent: **HANS, Christian, S.**; KPPB LLP, 2190 S. Towne Centre Place, Suite 300, Anaheim, CA 92806 (US).

(81) Designated States *(unless otherwise indicated, for every kind of national protection available)*: AE, AG, AL, AM, AO, AT, AU, AZ, BA, BB, BG, BH, BN, BR, BW, BY, BZ, CA, CH, CL, CN, CO, CR, CU, CZ, DE, DJ, DK, DM, DO, DZ, EC, EE, EG, ES, FI, GB, GD, GE, GH, GM, GT, HN, HR, HU, ID, IL, IN, IR, IS, JO, JP, KE, KG, KH, KN, KP,

(54) Title: METHODS AND FORMULATIONS TO TREAT MITOCHONDRIAL DYSFUNCTION

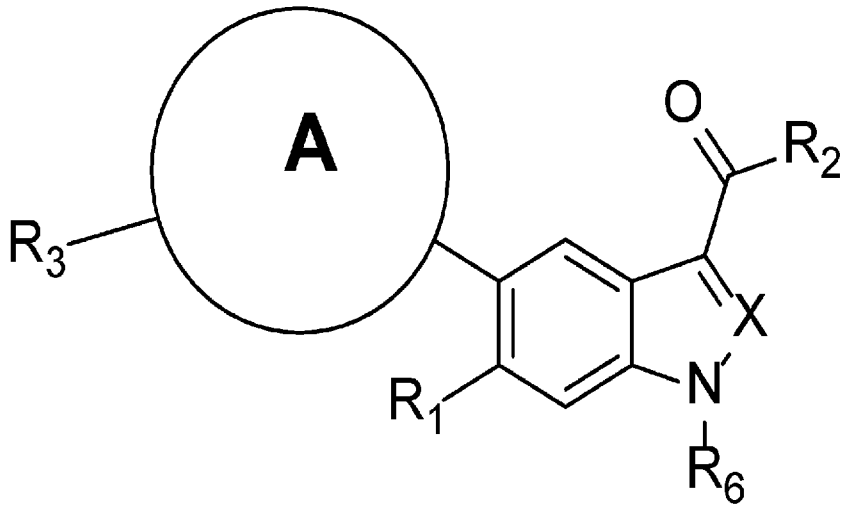

Fig. 12A

(57) Abstract: Methods of treatment and pharmaceutical formulations configured to treat primary and secondary mitochondrial dysfunction are provided. The methods and treatments use an agonist of AMPK. The agonist activates AMPK to activate ATP-producing pathways and inhibiting ATP-consuming pathways, thus allowing for the alleviation of symptoms associated with mitochondrial dysfunctions.

WO 2020/142547 A8

[Continued on next page]

WO 2020/142547 A8

KR, KW, KZ, LA, LC, LK, LR, LS, LU, LY, MA, MD, ME, MG, MK, MN, MW, MX, MY, MZ, NA, NG, NI, NO, NZ, OM, PA, PE, PG, PH, PL, PT, QA, RO, RS, RU, RW, SA, SC, SD, SE, SG, SK, SL, SM, ST, SV, SY, TH, TJ, TM, TN, TR, TT, TZ, UA, UG, US, UZ, VC, VN, ZA, ZM, ZW.

(84) Designated States *(unless otherwise indicated, for every kind of regional protection available)*: ARIPO (BW, GH, GM, KE, LR, LS, MW, MZ, NA, RW, SD, SL, ST, SZ, TZ, UG, ZM, ZW), Eurasian (AM, AZ, BY, KG, KZ, RU, TJ, TM), European (AL, AT, BE, BG, CH, CY, CZ, DE, DK, EE, ES, FI, FR, GB, GR, HR, HU, IE, IS, IT, LT, LU, LV, MC, MK, MT, NL, NO, PL, PT, RO, RS, SE, SI, SK, SM, TR), OAPI (BF, BJ, CF, CG, CI, CM, GA, GN, GQ, GW, KM, ML, MR, NE, SN, TD, TG).

Published:

— *with international search report (Art. 21(3))*

(48) Date of publication of this corrected version:
27 August 2020 (27.08.2020)

(15) Information about Correction:
see Notice of 27 August 2020 (27.08.2020)

METHODS AND FORMULATIONS TO TREAT MITOCHONDRIAL DYSFUNCTION

CROSS REFERENCE TO RELATED APPLICATIONS

[0001] This application claims priority to U.S. Provisional Application Ser. No. 62/786,970, entitled "Methods and Formulations to Treat Mitochondrial Dysfunction" to Moore et al., filed December 31, 2018; the disclosure of which is herein incorporated by reference in its entirety.

FIELD OF THE INVENTION

[0002] The present invention relates to methods of treatment and pharmaceutical formulations to treat primary and secondary mitochondrial dysfunction.

BACKGROUND

[0003] Previously studied drug candidates were conventional AMP-dependent AMPK activators, with the mechanism of action requiring elevations of AMP caused either by RC inhibition (*e.g.*, metformin, resveratrol) or conversion into AMP mimetics (*e.g.*, AICAR). The indirect mechanism involving RC inhibition is not suitable for cases with underlying mitochondrial dysfunction, and AMP-dependent activation of AMPK results in the activation of other AMP-regulated enzymes, thereby compounding pleiotropic effects. Additionally, previous studies have identified direct, AMP-independent AMPK agonists for the purpose of treating diabetes, obesity, and metabolic syndrome.

[0004] Primary mitochondrial diseases are a clinically heterogeneous group of disorders that are usually progressive, multi-systemic, and are associated with a high mortality rate in children. They are caused by inherited deficiencies in the mitochondrial respiratory chain (RC), leading to an increased production of reactive oxygen and nitrogen species (ROS and RNS) as well as a deficiency in overall energy production. These resulting metabolic imbalances lead to cellular damage and ultimately to cell death.

[0005] There is currently no curative treatment for primary mitochondrial disease. Only supportive treatment is available and involves treating specific symptoms (*e.g.*, Diabetes, cardiac disease, and ptosis) and a "mitochondrial cocktail" consisting of

vitamin cofactors and antioxidants. Unfortunately, meta-analyses have shown that the available supportive interventions lacks efficacy, highlighting the need for a novel treatment. (*See, e.g.*, Pfeffer et al, Cochrane Database Sys Rev. 2012 Apr 18;4; Chinnery et al, 2006, Cochrane Database Sys Rev. 2006 Jan 25;(1); the disclosures of which are incorporated herein by reference in their entirety).

[0006] Secondary mitochondrial diseases also demonstrate mitochondrial dysfunction but, unlike primary mitochondrial diseases, are not caused by genes related to the mitochondrial respiratory chain. Secondary mitochondrial diseases, such as Parkinson's disease or Alzheimer's disease, are due to acquired mitochondrial abnormalities caused by other diseases, conditions, or environmental factors that indirectly damage the mitochondria. Consequently, any treatment identified for primary mitochondrial disease, would be expected to also benefit disorders and conditions associated with secondary mitochondrial dysfunction, including neurodegenerative, neuromuscular, and muscle wasting disorders.

SUMMARY OF THE INVENTION

[0007] Methods and Formulations to treat mitochondrial dysfunction in accordance with embodiments of the invention are disclosed.

[0008] In one embodiment, a method of treating a patient with mitochondrial dysfunction includes identifying a mitochondrial dysfunction in an individual and providing an AMPK agonist to the individual.

[0009] In another embodiment, the mitochondrial dysfunction is a primary mitochondrial dysfunction.

[0010] In a further embodiment, the primary mitochondrial dysfunction is selected from the group consisting of Autosomal Dominant Optic Atrophy (ADOA), Alpers-Huttenlocher syndrome (nDNA defect), Ataxia neuropathy syndrome, (nDNA defect), Barth syndrome/ Lethal Infantile Cardiomyopathy (LIC), Co-enzyme Q deficiency, Complex I, complex II, complex III, complex IV and complex V deficiencies (either single deficiencies or any combination of deficiency), Chronic progressive external ophthalmoplegia (CPEO), Diabetes mellitus and deafness, Kearns-Sayre syndrome (mtDNA defect), Leukoencephalopathy with Brainstem and Spinal Cord Involvement

and Lactate Elevation (LBSL- leukodystrophy), Leigh syndrome (mtDNA and nDNA defects), Leber's hereditary optic neuropathy (LHON), Luft Disease, Mitochondrial myopathy, encephalopathy, lactic acidosis, and stroke syndrome (MELAS) (mtDNA defect), Mitochondrial Enoyl CoA Reductase Protein-Associated Neurodegeneration (MEPAN), Myoclonic epilepsy with ragged red fibers (MERRF), mitochondrial recessive ataxia syndrome (MIRAS), mtDNA deletion syndrome, mtDNA Depletion syndrome, mtDNA maintenance disorders, mtDNA/RNA translation defects, Mitochondrial tRNA synthetase deficiencies, Mitochondrial Myopathy, Mitochondrial neurogastrointestinal encephalopathy syndrome (MNGIE), Neurogenic muscle weakness, ataxia, and retinitis pigmentosa (NARP), Pearson syndrome, Pyruvate dehydrogenase complex deficiency (PDCD/PDH) , DNA polymerase gamma deficiency (POLG), Pyruvate carboxylase deficiency, and Thymidine kinase 2 deficiency (TK2).

[0011] In still a further embodiment, the mitochondrial dysfunction is a secondary mitochondrial dysfunction.

[0012] In still another embodiment, the secondary mitochondrial dysfunction is selected from the group consisting of Amyotrophic Lateral Sclerosis (ALS), Alzheimer's disease (AD) and other dementias, Friedreich's ataxia (FA), Huntington's disease (HD), Motor neuron diseases (MND), N-glycanase deficiency (NGLY1), Organic acidemias, Parkinson’s disease (PD) and PD-related disorders, Prion disease, Spinal muscular atrophy (SMA), Spinocerebellar ataxia (SCA), Becker muscular dystrophy , Congenital muscular dystrophies, Duchenne muscular dystrophy, Emery-Dreifuss muscular dystrophy, Facioscapulohumeral muscular dystrophy, Myotonic dystrophy, Oculopharyngeal muscular dystrophy, Charcot-Marie-Tooth disease, Congenital myopathies, Distal myopathies, Endocrine myopathies (hyperthyroid myopathy, hypothyroid myopathy), Giant axonal neuropathy, Hereditary spastic paraplegia , Inflammatory myopathies (dermatomyositis, inclusion-body myositis, polymyositis), Metabolic myopathies, Neuromuscular junction diseases:, Autism, Cancer, Diabetes, Metabolic syndrome, Chronic fatigue syndrome, an inflammatory disorder, arthritis, and aging.

[0013] In yet another embodiment, the AMPK agonist is a direct AMPK agonist.

[0014] In a further embodiment again, the direct AMPK agonist is selected from the group consisting of PT1, ETC-1002, Salicylate, C991, C13, D561-0775, MT 63-78, A-769662, ZLN024, C24, MK-8722, PF-739, and PF-06409577.

[0015] In another embodiment again, the AMPK agonist is an AMP-dependent agonist.

[0016] In a further additional embodiment, the AMP-dependent agonist is selected from the group consisting of metformin, resveratrol, and AICAR.

[0017] In another additional embodiment, the AMPK agonist is provided in a pharmaceutical formulation.

[0018] In a still yet further embodiment, the pharmaceutical formulation comprises the AMPK agonist and at least one of the group consisting of a binding agent, a lubricating agent, a buffer, and a coating.

[0019] In still yet another embodiment, the providing step comprises orally administering the AMPK agonist to the individual.

[0020] In a still further embodiment again, the providing step comprises administering the AMPK agonist daily for at least one week.

[0021] In still another embodiment again, the method further includes assessing the efficacy of the AMPK agonist in the individual.

[0022] In a still further additional embodiment, the providing step is accomplished by administrating the AMPK agonist by at least one of the group consisting of: oral administration, subcutaneous administration, intravenous administration, intraperitoneal administration, intranasal administration, dermal administration, and inhalation.

[0023] In still another additional embodiment, a method of treating mitochondrial disorders includes identifying a disorder in an individual and modulating AMPK activity in the individual.

[0024] In a yet further embodiment again, the modulating step is accomplished by activating AMPK in the individual.

[0025] In yet another embodiment again, the activating step is accomplished by phosphorylating AMPK or providing an agonist to AMPK.

[0026] In a yet further additional embodiment, the modulating step is accomplished by inhibiting AMPK in the individual.

[0027] In yet another additional embodiment, the disorder is associated with mitochondrial dysfunction.

[0028] In a further additional embodiment again, the mitochondrial dysfunction is a primary mitochondrial dysfunction.

[0029] In another additional embodiment again, the mitochondrial dysfunction is a secondary mitochondrial dysfunction.

In a still yet further embodiment again, an AMPK agonist includes a molecule of formula

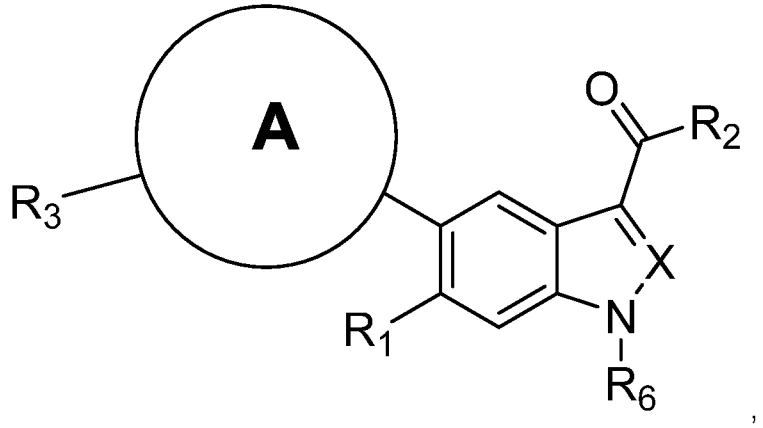

,

where:

A is selected from a 5-membered ring heterocyclic, either unsubstituted or substituted with one or more C_{1-6} alkyl or fluoro substituents

X is CR_5 or N;

R_1 is H, CF_3, or halo;

R_2 is OR_5, NHOH, $NHSO_2R_4$, OCH_2OCOR_4, or COR_2 is a C-linked tetrazole,

R_3 is C_{1-10} alkyl, C_{3-7} cycloalkyl, C_{4-12} alkylcycloalkyl, C_{4-10} cycloalkylalkyl, C_{3-7} heterocycloalkyl, C_{4-12} alkylheterocycloalkyl, C_{4-10} heterocycloalkylalkyl, aryl or heteroaryl either unsubstituted or substituted with one to three substituents selected from halo, OH and $OCOR_7$;

R_4 is C_{1-10} alkyl, C_{3-7} cycloalkyl, C_{4-12} alkylcycloalkyl, C_{4-10} cycloalkylalkyl either unsubstituted or substituted with one to three halogen substituents;

R_5 is R_4 or H;

R_6 is H, C_{1-6} alkyl, C_{3-6} cycloalkyl, or two R_6 groups, together with the nitrogen atom to which they are attached can form a four to seven membered

heterocycloalkyl ring, all of which can be optionally substituted with 1 to 3 fluorine atoms; and

R_7 is C_{1-10} alkyl, C_{3-7} cycloalkyl, C_{4-12} alkylcycloalkyl unsubstituted or substituted with one to three substituents selected from fluoro, C_{1-10} alkyl, and NR_6, R_6.

[0030] In still yet another embodiment again, A is selected from the group consisting of

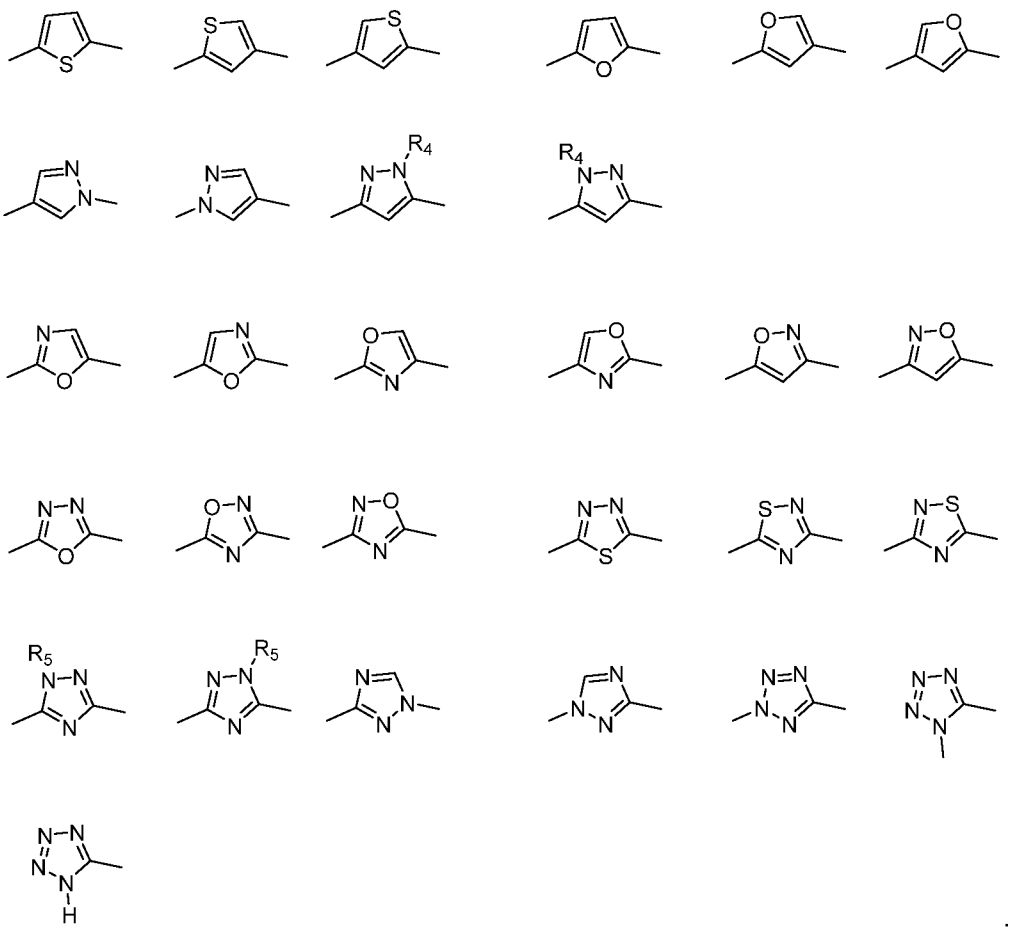

[0031] In a still yet further additional embodiment, A is selected from the group consisting of:

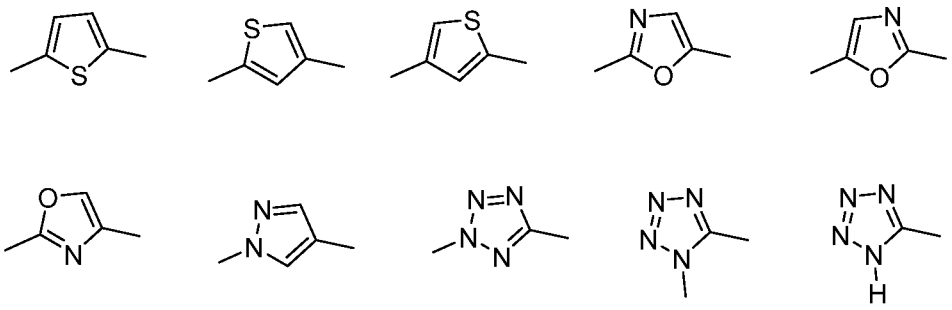

[0032] In still yet another additional embodiment, A is selected from the group consisting of:

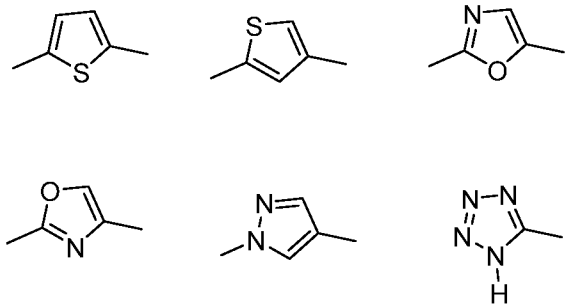

[0033] In a yet further additional embodiment again, X is CH, R_6 is H, R_1 is Cl, and R_2 is OH.

[0034] In yet another additional embodiment again, the molecule has a formula as illustrated in one of Figures 13A-13Z and Figures 14A-14O.

[0035] In a still yet further additional embodiment again, the molecule has the formula:

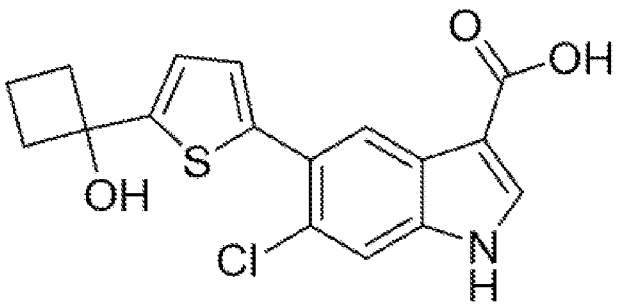

[0036] In still yet another additional embodiment again, an AMPK agonist includes a molecule of formula:

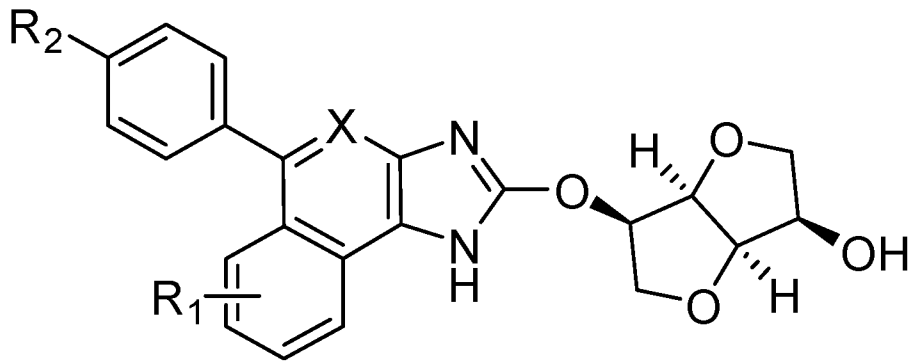

where:

X is CH or N;

R_1 is small alkyl (C1-C4) or halogen (e.g., Cl, Br, or F);

R_2 is phenyl, alkyl C1-C10, cycloalkyl (C3-C10), hydroxyalkyl (C1-C6), heteroaromatic (e.g., pyridyl, pyrazolyl, pyrolyl, pyrimidyl, thiophenyl, furanyl, or triazole), or heterocyclic C4-C6;

where phenyl is optionally substituted with halogens (e.g., Cl, Br, or F),

where an alkyl is linear or branched and optionally substituted with OH, OMe, OEt,

where cycloalkyl is optionally substituted with one or more OH,

where hydroxy alkyl is linear or branched

where heteroaromatic is optionally substituted with small alkyls (C1-C6) or hydroxyalkyls (C1-C6), where alkyls and hydroxyalkyls are linear or branched,

where heteroatom in hetrocyclic is optionally O, S, or NR_4, where R_4 is a linear or branched C1-C6 alkyl or hydroxyalkyl; and

R_4 is a linear or branched C1-C6 alkyl or hydroxyalkyl.

[0037] In another further embodiment, the molecule has the formula of:

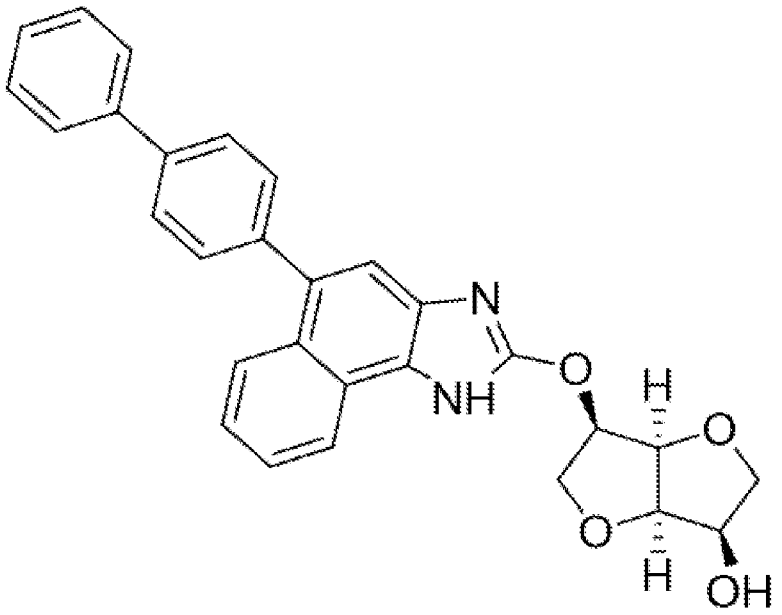

[0038] In still another further embodiment, an AMPK agonist includes a molecule of formula:

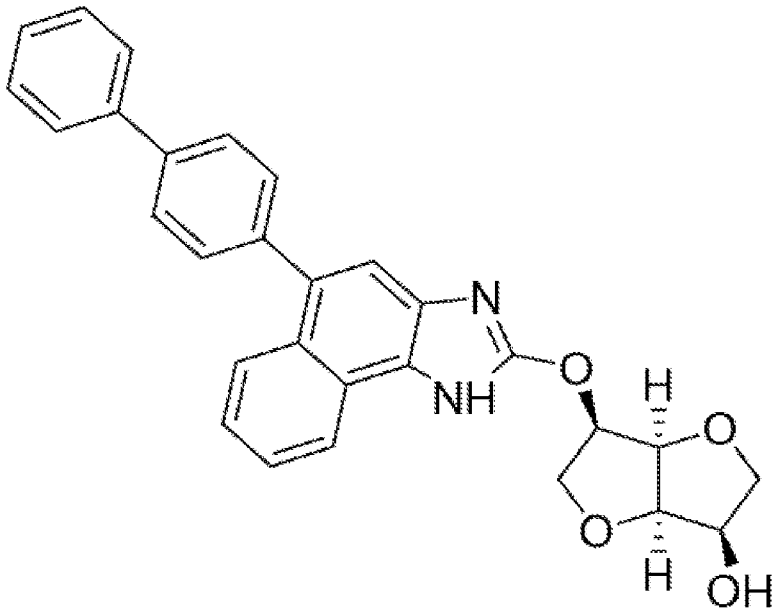

where:

A is a fused ring (e.g., C3-C10 cycloalkyl);

X is CH or N;

Y is O, S, NH, NR_3;

R_1 is small alkyl (C1-C4) or halogen (e.g., Cl, Br, or F);

R_2 is phenyl, alkyl C1-C10, cycloalkyl (C3-C10), hydroxyalkyl (C1-C6), heteroaromatic (e.g., pyridyl, pyrazolyl, pyrolyl, pyrimidyl, thiophenyl, furanyl, or triazole), or heterocyclic C4-C6;

where phenyl is optionally substituted with halogens (e.g., Cl, Br, or F),

where an alkyl is linear or branched and optionally substituted with OH, OMe, OEt,

where cycloalkyl is optionally substituted with one or more OH,

where hydroxy alkyl is linear or branched

where heteroaromatic is optionally substituted with small alkyls (C1-C6) or hydroxyalkyls (C1-C6), where alkyls and hydroxyalkyls are linear or branched,

where heteroatom in hetrocyclic is optionally O, S, or NR_4;

R_3 is a C1-C6 alkyl (linear or branched); and

R_4 is a linear or branched C1-C6 alkyl or hydroxyalkyl.

[0039] In yet another further embodiment, A is selected from a C6 phenyl ring or one of the following:

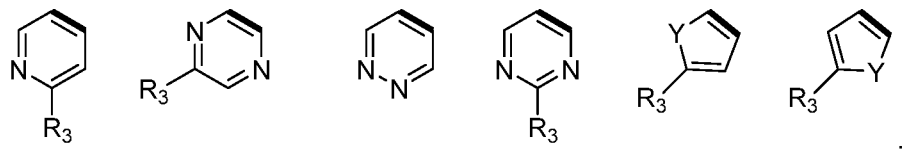

[0040] In another further embodiment again, the molecule has the formula of:

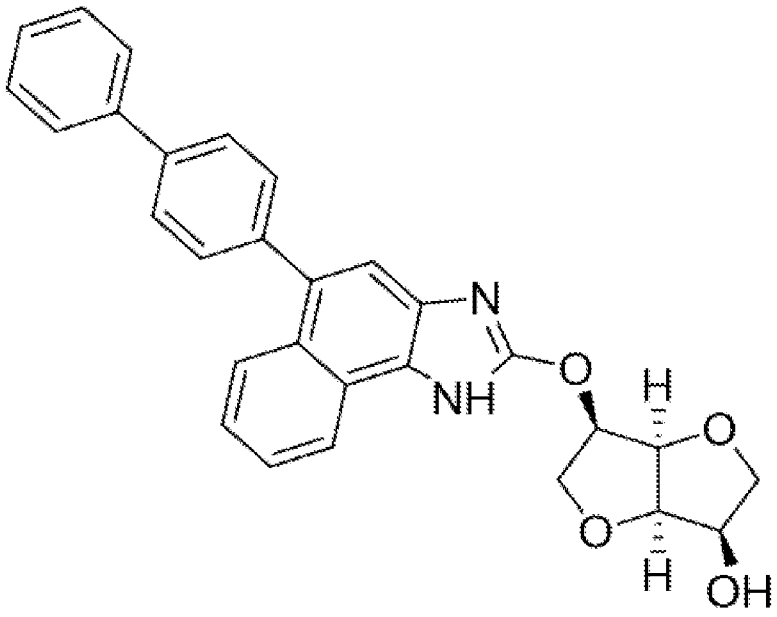

BRIEF DESCRIPTION OF THE DRAWINGS

[0041] These and other features and advantages of the present invention will be better understood by reference to the following detailed description when considered in conjunction with the accompanying drawings where:

[0042] Figure 1A illustrates pathways activated and inhibited by AMPK in accordance with various embodiments.

[0043] Figures 1B-1D illustrate structures of AMPK agonists in accordance with various embodiments.

[0044] Figures 2A-2F illustrate results of cell viability assays under various treatments in accordance with various embodiments.

[0045] Figures 3A-3N illustrate cellular morphology of fibroblasts under various treatments in accordance with various embodiments.

[0046] Figure 4A illustrates pAMPK concentration in a knockdown assay in accordance with various embodiments.

[0047] Figure 4B illustrates cell viability results in a knockdown study with various treatments in accordance with various embodiments.

[0048] Figures 4C-4F illustrate cellular morphology results in a knockdown study with various treatments in accordance with various embodiments.

[0049] Figure 5A illustrates pAMPK concentration after a treatment assay in accordance with various embodiments.

[0050] Figure 5B-5D illustrate gene expression levels after a treatment assay in accordance with various embodiments.

[0051] Figures 6A-6H illustrate cellular respiration results with and without treatment on various deficient fibroblast lines in accordance with various embodiments.

[0052] Figures 7A-7C illustrate ATP concentrations with and without treatment of various deficient fibroblast lines in accordance with various embodiments.

[0053] Figures 7D-7F illustrate reactive oxygen species (ROS) concentrations with and without treatment of various deficient fibroblast lines in accordance with various embodiments.

[0054] Figure 8A illustrates lipofuscin levels in control and NGLY1 deficient fibroblast lines in accordance with various embodiments.

[0055] Figure 8B illustrates lipofuscin levels in an NGLY1 deficient fibroblast line and with and without treatment in accordance with various embodiments.

[0056] Figure 9A illustrates funduscopy images of retinas with and without treatment in a control and an induced AMD model in accordance with various embodiments.

[0057] Figure 9B illustrates retinal section images of retinas with and without treatment in a control and an induced AMD model in accordance with various embodiments.

[0058] Figure 9C illustrates ONL thickness measurements of retinas with and without treatment in a control and an induced AMD model in accordance with various embodiments.

[0059] Figure 9D illustrates electroretinography images of retinas with and without treatment in a control and an induced AMD model in accordance with various embodiments.

[0060] Figure 9E illustrates reduced retinal degradation after treatment with AMPK agonists in accordance with various embodiments.

[0061] Figure 10A illustrates percent of infarct tissue in treated and untreated ischemic tissue in accordance with various embodiments.

[0062] Figures 10B and 10C illustrate brain slices with infarct tissue in treated and untreated ischemic tissue in accordance with various embodiments.

[0063] Figures 11A-11C illustrate locomotor performance in treated and untreated mice in accordance with various embodiments.

[0064] Figures 11D and 11E illustrate mitochondrial function and glycogen storage in treated and untreated mice in accordance with various embodiments.

[0065] Figures 11F and 11G illustrate results of ACC phosphorylation assays performed on treated and untreated mice in accordance with various embodiments.

[0066] Figure 12A illustrates a generalized structure of AMPK agonists in accordance with various embodiments.

[0067] Figure 12B-12D illustrate schematics methods of synthesis of AMPK agonists in accordance with various embodiments.

[0068] Figures 13A-13Z illustrate structures of AMPK agonists in accordance with various embodiments.

[0069] Figures 14A-14O illustrate structures of AMPK agonists in accordance with various embodiments.

[0070] Figures 15A-15B illustrate generalized structures of AMPK agonists in accordance with various embodiments.

[0071] Figure 15C illustrates a schematic of a method of synthesis of AMPK agonists in accordance with various embodiments.

[0072] Figure 15D illustrates a structure of an AMPK agonist in accordance with various embodiments.

[0073] Figure 16A illustrates results of ACC phosphorylation assay performed on mitochondrial deficient cells in accordance with various embodiments.

[0074] Figure 16B illustrates AMPK activity of AMPK agonists used in determining EC50 in accordance with various embodiments.

[0075] Figure 17 illustrates a method of treating an individual in accordance with various embodiments.

[0076] Figure 18 illustrates a method of modulating AMPK activity in an individual in accordance with various embodiments.

DETAILED DESCRIPTION

[0077] Turning now to the data and description, methods of treatment, and pharmaceutical formulations configured to treat mitochondrial disorders, diseases, and/or dysfunctions are described. In various embodiments, the methods and formulations use agonists of AMP-activated protein kinase (AMPK). AMPK is a master regulator of cellular energy homeostasis and is activated during energy deficiency to restore adenosine triphosphate (ATP) levels. Generally, AMPK restores energy homeostasis by activating ATP-producing pathways (*e.g.*, Glycolysis, mitochondrial biogenesis) and inhibiting ATP-consuming pathways (*e.g.*, Gluconeogenesis and fatty acid synthesis). Additional pathways or processes promoted by AMPK include antioxidant enzymes, autophagy, fatty acid metabolism, and muscle regeneration. Figure 1 illustrates a variety of pathways activated or inhibited by AMPK. AMPK's regulation of glucose and fatty acid pathway has made it an attractive therapeutic target for diabetes, obesity and metabolic syndrome, leading to the identification of AMPK agonists for this purpose.

[0078] To combat the defects in indirect AMPK agonists, certain embodiments are directed to direct, AMP-independent AMPK agonists to treat disorders and conditions with underlying mitochondrial dysfunction. Direct AMPK activating compounds, including PT1, ETC-1002, Salicylate, C991, C13, D561-0775, MT 63-78, A-769662, ZLN024, C24, MK-8722 (Figure 1B), PF-739 (Figure 1C), and PF-06409577 (Figure 1D) allosterically activate AMPK by directly binding to either the alpha or beta subunit, and in some cases were shown to improve lipid and glucose profiles *in vivo*. (*See e.g.*, Cool et al, Cell Metab. 2006 Jun;3(6):403-16; Pang et al, J Biol Chem. 2008 Jun 6;283(23):16051-60; Hawley et al, Science. 2012 May 18;336(6083):918-22; Li et al, Toxicol Appl Pharmacol. 2013 Dec 1;273(2):325-34; Zhang et al, PLoS One. 2013 Aug 20;8(8); Xiao et al, Nat Commun. 2013;4:3017; Zadra et al, EMBO Mol Med. 2014 Apr;6(4):519-38; Hunter et al, Chem Biol. 2014 Jul 17;21(7):866-79; Pinkosky et al, Nat Commun. 2016 Nov 28;7:13457; Cameron et al, 2016 Sep 8;59(17):8068-81; Myers et

al, Science. 2017 Aug 4;357(6350):507-511; Cokorinos et al, Cell Metab. 2017 May 2;25(5):1147-1159; Xi et al, Oncotarget. 2017 Nov 10; 8(56): 96089–96102; the disclosures of which are incorporated herein by reference in their entirety.)

[0079] Treatments using various embodiments of direct AMPK agonists increase cellular respiration and ATP levels and reduce oxidative stress, resulting in consistent and effective improvement in viability of cells from patients with both primary and secondary mitochondrial disease, including a wide-range of disorders and conditions associated with secondary mitochondrial dysfunction. Diseases and disorders associated with primary and secondary mitochondrial dysfunction are listed in Tables 1 and 2, respectively. Additionally, direct AMPK agonists provide protection against retinal degeneration in age related macular degeneration (AMD), neuroprotectivity in ischemic stroke, and is sufficient to enhance motor performance. Further, direct AMPK agonists mitigate known negative effects, such as retinal damage, neuronal degeneration and muscle wasting, associated with mitochondrial dysfunction in both primary and secondary mitochondrial disorders. As such, certain embodiments are directed to the treatment of N-glycanase (NGLY1) deficiency, age-related macular degeneration (AMD), ischemic stroke, muscular dystrophies (*e.g.*, Duchenne and Becker), Friedreich ataxia (FA), autoimmune disorders with muscle involvement (*e.g.*, inclusion body myositis, Polymyositis, and Dermatomyositis), and/or neurodegenerative disorders (*e.g.*, Amyotrophic Lateral Sclerosis (ALS), Parkinson's Disease, and Alzheimer's Disease). Additionally, AMPK activation in cardiac tissue can result in reversible cardiac hypertrophy, thus various embodiments are directed to the treat diseases associated with dilated cardiomyopathy. (*See, e.g.*, Arad et al, Circ Res. 2007 Mar 2;100(4):474-88; Myers et al, Science. 2017 Aug 4;357(6350):507-511; the disclosures of which are incorporated herein by reference in their entirety.)

Table 1: Diseases and disorders associated with primary mitochondrial dysfunction
Autosomal Dominant Optic Atrophy (ADOA)
Alpers-Huttenlocher syndrome (nDNA defect)
Ataxia neuropathy syndrome, (nDNA defect)
Barth syndrome/ Lethal Infantile Cardiomyopathy (LIC)
Co-enzyme Q deficiency
Complex I, complex II, complex III, complex IV and complex V deficiencies (either single deficiencies or any combination of deficiency)

Chronic progressive external ophthalmoplegia (CPEO)
Diabetes mellitus and deafness
Kearns-Sayre syndrome (mtDNA defect)
Leukoencephalopathy with Brainstem and Spinal Cord Involvement and Lactate Elevation (LBSL- leukodystrophy)
Leigh syndrome (mtDNA and nDNA defects)
Leber's hereditary optic neuropathy (LHON)
Luft Disease
Mitochondrial myopathy, encephalopathy, lactic acidosis, and stroke syndrome (MELAS) (mtDNA defect)
Mitochondrial Enoyl CoA Reductase Protein-Associated Neurodegeneration (MEPAN)
Myoclonic epilepsy with ragged red fibers (MERRF)
mitochondrial recessive ataxia syndrome (MIRAS)
mtDNA deletion syndrome
mtDNA Depletion syndrome
mtDNA maintenance disorders
mtDNA/RNA translation defects
Mitochondrial tRNA synthetase deficiencies
Mitochondrial Myopathy
Mitochondrial neurogastrointestinal encephalopathy syndrome (MNGIE)
Neurogenic muscle weakness, ataxia, and retinitis pigmentosa (NARP)
Pearson syndrome
Pyruvate dehydrogenase complex deficiency (PDCD/PDH)
DNA polymerase gamma deficiency (POLG)
Pyruvate carboxylase deficiency
Thymidine kinase 2 deficiency (TK2)

Table 2: Diseases and disorders associated with secondary mitochondrial dysfunction	
Neurodegenerative:	
	Amyotrophic Lateral Sclerosis (ALS)
	Alzheimer's disease (AD) and other dementias
	Friedreich's ataxia (FA)
	Huntington's disease (HD)
	Motor neuron diseases (MND)
	N-glycanase deficiency (NGLY1)
	Organic acidemias
	Parkinson’s disease (PD) and PD-related disorders
	Prion disease
	Spinal muscular atrophy (SMA)
	Spinocerebellar ataxia (SCA)
Muscular dystrophies:	
	Becker muscular dystrophy
	Congenital muscular dystrophies

	Duchenne muscular dystrophy
	Emery-Dreifuss muscular dystrophy
	Facioscapulohumeral muscular dystrophy
	Myotonic dystrophy
	Oculopharyngeal muscular dystrophy
Myopathies:	
	Charcot-Marie-Tooth disease
	Congenital myopathies
	Distal myopathies
	Endocrine myopathies (hyperthyroid myopathy, hypothyroid myopathy)
	Giant axonal neuropathy
	Hereditary spastic paraplegia
	Inflammatory myopathies (dermatomyositis, inclusion-body myositis, polymyositis)
	Metabolic myopathies
	Neuromuscular junction diseases:
Other:	
	Autism
	Cancer
	Diabetes
	Metabolic syndrome
	Chronic fatigue syndrome
	Inflammatory disorders (e.g., arthritis)
	Aging (e.g., lifespan)

Characterization of AMPK Agonist Properties

[0080] Properties of selected AMPK agonists are provided below to characterize the performance of exemplary embodiments of the invention. Although some specific agonists are discussed, it will be understood that the results are meant only to provide an overview of agonist functions and are not meant to be limiting.

Effect of Direct AMPK Agonists on Cell Viability and Morphology

[0081] Various embodiments utilized direct AMPK agonists to increase cell viability and morphology in individuals having mitochondrial dysfunction. Figures 2A-2F illustrate the effect on cell viability of direct AMPK agonists of some embodiments. Figures 2A-2D illustrate cell viability in four fibroblast lines deficient for Cytochrome C Oxidase Assembly Factor (SURF1, Figure 2A), Heme A:Farnesyltransferase Cytochrome C Oxidase Assembly Factor (COX10, Figure 2B), Mitochondrial Complex I (CI, Figure 2C),

and Mitochondrial DNA Polymerase Gamma (POLG, Figure 2D). In Figure 2A, four direct AMPK agonists, PT1, A-769662, ZLN024, and C24 of various embodiments demonstrate a 35-55% increase in viability compared to untreated cells (*e.g.*, cells treated with the vehicle, DMSO). Figures 2B-2D illustrate the effect on cell viability for mitochondrial dysfunctions encompassing components of the respiratory chain and mitochondrial DNA (mtDNA) replication machinery. Turning to Figures 2B-2D, the direct AMPK agonist, PT1, improves survival in these mutant lines despite the different pathogenic mechanisms of the gene deficiencies. Additionally, the remaining compounds showed variable responses among the mutant lines: A-769662 improved survival in CI and POLG-deficient cells, ZLN024 improved survival in CI-deficient cells, and C24 improved survival in SURF1-deficient cell but not in any of the other lines. Additionally, the indirect AMPK agonist, AICAR, does not improve cell viability in any of the other lines except SURF1 (Figure 2A), indicating that AICAR is not as effective as direct AMPK agonists. The direct AMPK agonist, PT1, showed similar results in fibroblasts exhibiting NGLY-1 deficiency, as seen in Figure 2E. Figure 2E illustrates fibroblasts deficient in NGLY-1 isolated from three individuals. The fibroblasts treated with PT1 (+PT1) exhibit up to a 60% improvement in viability versus the untreated (-PT1) cells. Additionally, Figure 2F shows the effect of cell viability of three newer AMPK agonists of various embodiments. In Figure 2F, the AMPK agonists, MK-8722, PF-739, and PF-06409577 show increasing levels of cellular viability in SURF1 deficient fibroblasts in a dose dependent manner. Thus, direct AMPK agonists of various embodiments improve cell viability across a range of primary and secondary mitochondrial disease etiologies.

[0082] Turning to Figures 3A-3N, cellular morphology of fibroblasts with various deficiencies are illustrated, in accordance with many embodiments. Specifically, Figures 3A and 3B illustrate fibroblasts deficient in SURF1, where Figure 3A illustrates cellular morphology without treatment (DMSO only), while figure 3B illustrates SURF1 deficient fibroblasts treated with PT1, showing improved cellular morphology over the untreated cells in Figure 3A. Similarly, Figures 3C-3J illustrate similar results in cellular morphology, when treated with PT1, where Figures 3C and 3D illustrate fibroblasts deficient for COX10, Figures 3E and 3F illustrate fibroblasts deficient for CI, Figures 3G

and 3H illustrate fibroblasts deficient for POLG, and Figures 3I and 3J illustrate fibroblasts deficient for NGLY-1. Similarly, Figures 3C, 3E, 3G, and 3I illustrate the untreated deficient fibroblasts, while Figures 3D, 3F, 3H, and 3J illustrate fibroblasts treated with PT1. Additionally, Figures 3K-3N illustrate the effect of newly developed AMPK agonists, MK-8722, PF-739, and PF-06409577, on SURF1-deficient fibroblasts. In particular, Figure 3K shows SURF1-deficient fibroblasts treated only with the vehicle, DMSO, while Figure 3L shows improved cellular morphology following treatment with MK-8722, Figure 3M shows improved cellular morphology following treatment with PF-739, and Figure 3N shows improved cellular morphology following treatment with PF-06409577. Thus, direct AMPK agonists of various embodiments improve cellular morphology across a range of primary and secondary mitochondrial disease etiologies.

[0083] Turning now to Figures 4A-4F, direct AMPK agonists of certain embodiments are specific to AMPK activation and not nonspecific interactions. Figure 4A illustrates a protein blot (western blot) of phosphorylated AMPK (pAMPK) demonstrating the relative level of pAMPK to tubulin after treatment after transfecting COX10 deficient fibroblasts with small interfering RNA (siRNA). A siRNA specific for the AMPK alpha subunit gene, PRKAA1, resulted in a decrease in pAMPK levels over cells transfected with a nonspecific siRNA used as a control (siCNT). Figure 4B illustrates cell viability in the COX10 deficient fibroblasts with and without PT1 treatment and with and without siRNA transfection, showing that PT1 treatment alone (PT1) and PT1 treatment with the nonspecific siCNT (siCNT + PT1) have increased viability over untreated cells (DMSO) and cells treated with PT1 and transfected with siAMPK (siAMPK + PT1). Additionally, treatment with PT1 together with selective knockdown of AMPK (siAMPK + PT1) results in a 63% decrease in pAMPK levels and 41% decrease in cell viability compared to control conditions (siCNT + PT1), consistent with the idea that cellular response to PT1 is mediated by AMPK activation. Figures 4C-4F illustrate cellular morphology under the same conditions as present in Figure 4B. Specifically, Figure 4C illustrates untreated COX10 deficient fibroblasts; Figure 4D illustrates COX10 deficient fibroblasts treated with PT1; Figure 4E illustrates COX10 deficient fibroblasts transfected with siAMPK and treated with PT1; and Figure 4F illustrates COX10 deficient fibroblasts transfected with the control siCNT and treated with PT1.

[0084] Turning to Figures 5A-5D, certain embodiments of direct AMPK agonists address metabolic disruptions caused by mitochondrial dysfunction. Figure 5A illustrates pAMPK levels normalized to actin in SURF1 deficient fibroblasts treated with PT1 for 0 hours, 2 hours, 24 hours, and 48 hours. Figure 5A illustrates that pAMPK levels increase within 2 hours post PT1 treatment and peaked at 24 hours post PT1 treatment. Additionally, pAMPK levels return to baseline positions after 48 hours post PT1 treatment. In Figures 5B-5D, the effect of PT1 treatment, in accordance with various embodiments, increase gene expression of mitochondrial biosynthesis and antioxidant genes. Figure 5B shows a 2.4-fold increase in expression of peroxisome proliferator-activated receptor gamma coactivator 1-alpha (PGC-1α), while Figures 5C and 5D illustrate a 1.3-fold increase in manganese superoxide dismutase (SOD2) expression and a 1.5-fold increase in catalase expression, respectively.

Effect of Direct AMPK Agonists on Cellular Respiration

[0085] Various embodiments improve cellular respiration in individuals with mitochondrial dysfunction. As noted above, certain embodiments increase PGC-1α expression. PGC-1α stimulates the biogenesis of new mitochondria that possess increased respiratory function as compared to aged mitochondria having accrued secondary mtDNA mutations and reactive oxygen species (ROS). Turning to Figures 6A-H, improved respiratory function caused by direct AMPK agonists of some embodiments is illustrated. Figures 6A-6C show basal oxygen consumption rates (OCR) in SURF1, POLG, and NGLY1 deficient fibroblasts, respectively. Despite etiological differences in each gene, SURF1, POLG, and NGLY1 deficient fibroblasts showed an approximately 30% improvement for SURF1 and POLG deficient fibroblasts and 16% improvement in NGLY1 deficient fibroblasts in basal respiration when treated with PT1 over untreated (DMSO), in accordance with various embodiments. Additionally, Figures 6D and 6E illustrate the fraction of basal mitochondrial oxygen consumption used for ATP synthesis (ATP-coupled respiration) in SURF1 (Figure 6D) and POLG (Figure 6E) deficient fibroblasts. In this situation, the treatment with PT1 shows an improvement of approximately 40% in SURF1 deficient fibroblasts (Figure 6D) and 30% in POLG deficient fibroblasts (Figure 6E) over the untreated (DMSO) fibroblasts, in line with

certain embodiments. Further, treatment with PT1 in accordance with some embodiments improves maximal respiration capacity, which reflects the ability to of cells to respond to increased ATP demand, as illustrated in Figures 6F-6H. In Figures 6F, SURF1 deficient fibroblasts show an approximately 50% improvement in maximal respiration in cells treated with the direct AMPK agonist, PT1 over the untreated (DMSO) fibroblasts. Similarly, Figure 6G illustrates that POLG deficient fibroblasts show an improvement of approximately 20% in maximal respiration in cells treated with the direct AMPK agonist, PT1 over the untreated (DMSO) fibroblasts. And, Figure 6H shows an approximately 40% improvement in maximal respiration NGLY1 deficient fibroblasts when treated with the direct AMPK agonist, PT1 over the untreated (DMSO) fibroblasts.

Effect of Direct AMPK Agonists on Oxidative Stress and Energy Status

[0086] Turning now to Figures 7A-7F, various embodiments improve ATP production and reduce reactive oxygen species (ROS) levels in mitochondrial dysfunction. Specifically, Figures 7A, 7B, and 7C show increases in ATP production of 35% in SURF1 deficient fibroblasts, 36% in POLG deficient fibroblasts, and 40% inNGLY1 deficient fibroblasts treated with the direct AMPK agonist, PT1, over untreated (DMSO) fibroblasts, respectively. Further, Figures 7D, 7E, and 7F illustrate reductions in ROS levels of 10% in SURF1 deficient fibroblasts, 15% in POLG deficient fibroblasts, and 18% in NGLY1 deficient fibroblasts treated with the direct AMPK agonist, PT1, over untreated (DMSO) fibroblasts, respectively. Mitochondrial dysfunction causes an incomplete electron transfer through the respiration chain (RC), leading to decreased ATP synthesis and over-production of reactive oxygen species (ROS). (*See, e.g.*, Atkuri et al, Proc Natl Acad Sci U S A. 2009 Mar 10;106(10):3941-5; Enns et al, PLoS One. 2014 Jun 18;9(6); the disclosures of which are incorporated herein by reference in their entirety.) ATP and ROS content reflect cellular energy and oxidative status, both of which are dependent on effective ATP-coupled respiration and overall mitochondrial function. Cellular responses to these metabolic disruptions involve activating pathways that improve cellular respiration (*e.g.*, mitochondrial biogenesis) and upregulating the expression of endogenous antioxidants to neutralize ROS and decrease oxidative

stress. Thus, improvements in ATP production and reduction in ROS levels, as shown in Figures 7A-7F, show the ability of various embodiments to improve the oxidative stress and energy status of mitochondrial dysfunction.

Effect of Direct AMPK Agonists on Lipofuscin Levels

[0087] Some embodiments decrease accumulation of aberrant glycoproteins as seen in Figures 8A-8B. Certain mitochondrial dysfunctions, including those caused by NGLY1 deficiencies, produce an accumulation of proteins and lipids, called lipofuscin. (*See, e.g.,* Jobst, et al., J Clin Pathol. 1991 May; 44(5): 437–438; the disclosure of which is incorporated herein by reference in its entirety.) As seen in Figure 8A, NGLY1 deficient fibroblasts exhibit approximately 60% higher levels of lipofuscin than normal fibroblasts (Control). Figure 8B illustrates that treatment with the direct AMPK agonist, PT1, in accordance with various embodiments, reduces lipofuscin levels by approximately 36% in NGLY1 deficient fibroblasts.

AMPK Activation Attenuates Retinal Degeneration in AMD

[0088] Turning now to Figures 9A-9E, various embodiments attenuate retinal damage caused by mitochondrial dysfunction. In particular, Figure 9A shows funduscopic images of retinas treated with and without sodium iodate (SI) and with and without the direct AMPK agonist, PT1, in accordance with certain embodiments. SI is a toxin that selectively induces oxidative stress and mitochondrial dysfunction in retinal pigment epithelium (RPE). As such, SI treated tissue simulates retinal disorders caused by mitochondrial dysfunction, such as AMD. As seen in Figure 9A, the tissue without SI treatment (-SI) with and without PT1 (+PT1 and -PT1) have similar, normal tissue. However, tissue treated with SI and without PT1 (+SI; -PT1) shows signs of retinal degeneration, including white deposits. However, tissue treated with both SI and PT1 (+SI; +PT1) show improved signs of retinal degeneration. Thus, indicating that direct AMPK agonists of various embodiments attenuate retinal degeneration. Similarly, Figure 9B shows similar results from H&E staining of retinal sections. As illustrated, tissue without SI treatment (-SI; -PT1 and –SI, +PT1) have similar appearances. However, the –SI; +-PT1 tissue shows signs of retinal degeneration, including thinning

of the photoreceptor outer nuclear level (ONL), disorganization of the inner and photoreceptor outer/inner segments (IS/OS), and presence of melanin debris. With treatment of PT1 in the SI treated tissue, these disease indications are reduced, including a protection against ONL thinning (white bars), alterations in photoreceptor morphology, and decreased melanin debris (black arrows). Measurements of ONL thickness are illustrated in Figure 9C, where the tissue not treated with SI (SI-, PT1- and SI-, PT1+) and the SI and PT1 treated tissue (SI+, PT1+) show greater thickness than the SI treated tissue without PT1 treatment (SI+, PT1-). Further, Figure 9D demonstrates improved electrical response of retinal tissue treated with both SI and PT1 (PT1+; SI+) to levels similar to normal tissue (PT1-; SI- and PT1+; SI-) over the tissue treated with SI and without PT1 (PT1-; SI+).

[0089] Further, Figure 9E illustrates retinal thickness in wild type mice (WT/WT) as mice that are possess knock-out and/or knock-in alleles of the cytochrome C oxidase assembly protein, SCO2, where the knock-in allele represented an E129K mutation on the SCO2 protein. In particular, the mice are heterozygous knock-in and wild type (KI/WT) or heterozygous knock-out and knock-in (KO/KI). Figure 9E illustrates how treated (MK8722) mice demonstrate less degradation than mice treated with only a vehicle (VEH) mice.

[0090] Mitochondrial dysfunction in the eye of patients with mitochondrial disease result in ophthalmic manifestations such as retinopathy and optic atrophy, and compromised mitochondrial function has also been shown to be associated with the age-related macular degeneration (AMD). Given that the eye is one of the most energy-dependent tissues in the body, both primary and secondary mitochondrial diseases with ophthalmological findings are expected to benefit from AMPK activation. (*See, e.g.*, Calaza, et al, Neurobiol Aging. 2015 Oct;36(10):2869-76; the disclosure of which is incorporated by reference herein in its entirety.) Thus, the direct AMPK agonists of various embodiments will be used to treat patients with ophthalmic diseases associated with mitochondrial dysfunction.

Neuroprotection in Ischemic Stroke

[0091] Some embodiments provide neuroprotection in individuals with ischemic stroke. Impairment of mitochondrial energy metabolism in neurons is the key pathogenic factor in ischemic stroke and a number of neurodegenerative disorders, including certain primary mitochondrial diseases, AD, PD, and ALS (Schon et al, J Clin Invest. 2003 Feb 1; 111(3): 303–312; the disclosure of which is incorporated herein by reference in its entirety). Figures 10A-10C demonstrate the neuroprotective effect of direct AMPK on individuals suffering ischemic stroke. In particular, Figure 10A shows the percent of infarct tissue in brain tissue suffering ischemic stroke. As seen in Figure 10A, treatment with PT1 shows a marked improvement over individuals treated with only the vehicle DMSO (Vehicle). Turning to Figures 10B and 10C, illustrate TCC-stained brain slices, where individuals treated with only the vehicle (Figure 10B) show high levels of ischemic tissue in white, whereas the individuals treated with PT1 (Figure 10C), in accordance with various embodiments, show much lower amounts of ischemic tissue in white.

Effect of AMPK Agonists on Motor Performance and Skeletal Muscle

[0092] Various embodiments will be used to improve motor performance in individuals with mitochondrial dysfunction as well as muscle wasting diseases, such as muscular dystrophies and autoimmune myositis disorders. Figures 11A-11C illustrate improvements in muscle performance using the AMPK agonists MK-8722, in accordance with various embodiments. Figure 11A illustrates distance travelled in an activity chamber by mice with various genotypes in the SCO2 gene treated with an AMPK agonist and with a delivery vehicle only. Specifically, Figure 11A illustrates heterozygous knock-in and wild-type mice treated with only a vehicle (1102), heterozygous knock-in and knock-out mice treated with only a vehicle (1104), heterozygous knock-in and wild-type mice treated with an AMPK agonist (1106), and heterozygous knock-in and knock-out mice treated with an AMPK agonist (1108). As illustrated in Figure 11A, heterozygous knock-in and wild-type mice show similar levels of activity, regardless of whether they are treated with an AMPK agonist (1106) or vehicle-only (1102), while mice that are heterozygous for knock-out and knock-in alleles

show reduced activity when treated with a vehicle only (1104), but activity in the knock-out/knock-in mice treated with an AMPK agonist (1108) returns to levels comparable with knock-in/wild-type mice.

[0093] Figure 11B illustrates rotarod performance improvements in knock-out/knock-in mice using an AMPK agonist (1108) over knock-out/knock-in mice with vehicle-only treatment (1104). Additionally, the knock-out/knock-in mice using an AMPK agonist (1108) show levels higher than the knock-in/wild-type mice treated with an AMPK agonist (1106) or vehicle treated (1102). Similarly, Figure 11C illustrates results from a hanging wire assay illustrating that AMPK agonists of many embodiments improve muscle performance. In particular, AMPK agonists are capable of improving wire hang time in knock-out/knock-in mice (1108) to levels higher than the knock-in/wild-type (1102, 1106) as well as the vehicle-treated knock-out/knock-in (1104). Collectively, Figures 11A-11C illustrate that AMPK activation from AMPK agonists of many embodiments can enhance strength, endurance, and overall locomotor function in muscle-degenerative disorders associated with mitochondrial dysfunction.

[0094] Many embodiments are further capable of increasing mitochondrial function and/or glycogen storage in skeletal muscle, as indicated in Figures 11D-11E. Figure 11D illustrates that histological staining indicative of mitochondrial cytochrome C oxidase (CtyoC) and succinate dehydrogenase (SDH) activities. The darker staining in embodiments treating with an AMPK agonist indicates increased activity over the lighter stained vehicle-only treated samples. Similarly, the darker staining of glycogen in Figure 11E illustrates an increased presence of stored glycogen in samples treated with an embodiment of an AMPK agonist. The combination of increased mitochondrial function and glycogen content indicates that embodiments are capable of normalizing energy levels within skeletal muscle, thereby preventing degeneration and weakness.

[0095] Turning to Figures 11F-11G, the increased phosphorylation of ACC in skeletal muscle. In particular, Figure 11F illustrates a western blot of phosphorylated ACC (pACC) in mice treated with a vehicle only (KI/KO Veh) as well as in mice treated an AMPK agonist of many embodiments (KI/KO MK8722). Figure 11G summarizes the western blots by normalizing pACC to 1 in mice treated with a vehicle only (KI/KO Veh) and mice treated an AMPK agonist of many embodiments (KI/KO MK8722). Figures

11F-11G thus indicate that AMPK agonists of many embodiments are capable of activating AMPK in skeletal muscle.

Embodiments of AMPK Agonists

[0096] Many embodiments are directed to highly potent, selective and stable small molecule agonists of AMPK. Many such embodiments are directed to molecules having a generalized structure as illustrated in Figure 12A. A number of embodiments will modify the generalized structure in Figure 12A to generate derivative molecules based on the structure in Figure 12A. Derived molecules can be tested for activity in a number of ways known in the art or described herein, such as measuring pACC in a sample, as in indicator of increasing AMPK activity. By varying certain fragments, R-groups, etc., it is possible to develop a systematic understanding of how each fragment influences AMPK activity.

[0097] Derivative molecules of certain embodiments are developed from the structure in 12A. In many embodiments, moieties, R-groups, or other fragments may be substituted by one or more of the following:

- A is selected from 5-membered ring heterocyclics either unsubstituted or substituted with one or more C_{1-6} alkyl or fluoro substituents;
- X is CR_5 or N;
- R_1 is H, CF_3 or halo;
- R_2 is OR_5. NHOH, $NHSO_2R_4$, OCH_2OCOR_4 or COR_2 is a C-linked tetrazole,
- R_3 is C_{1-10} alkyl, C_{3-7} cycloalkyl, C_{4-12} alkylcycloalkyl, C_{4-10} cycloalkylalkyl, C_{3-7} heterocycloalkyl, C_{4-12} alkylheterocycloalkyl, C_{4-10} heterocycloalkylalkyl, aryl or heteroaryl either unsubstituted or substituted with one to three substituents selected from halo, OH and $OCOR_7$;
- R_4 is C_{1-10} alkyl, C_{3-7} cycloalkyl, C_{4-12} alkylcycloalkyl, C_{4-10} cycloalkylalkyl either unsubstituted or substituted with one to three halogen substituents;
- R_5 is R_4 or H;
- R_6 is H, C_{1-6} alkyl, C_{3-6} cycloalkyl, or two R_6 groups, together with the nitrogen atom to which they are attached can form a four to seven membered

heterocycloalkyl ring, all of which can be optionally substituted with 1 to 3 fluorine atoms;

- R_7 is C_{1-10} alkyl, C_{3-7} cycloalkyl, C_{4-12} alkylcycloalkyl unsubstituted or substituted with one to three substituents selected from fluoro, C_{1-10} alkyl and NR_6,R_6.

[0098] In many embodiments, A is selected from the group consisting of:

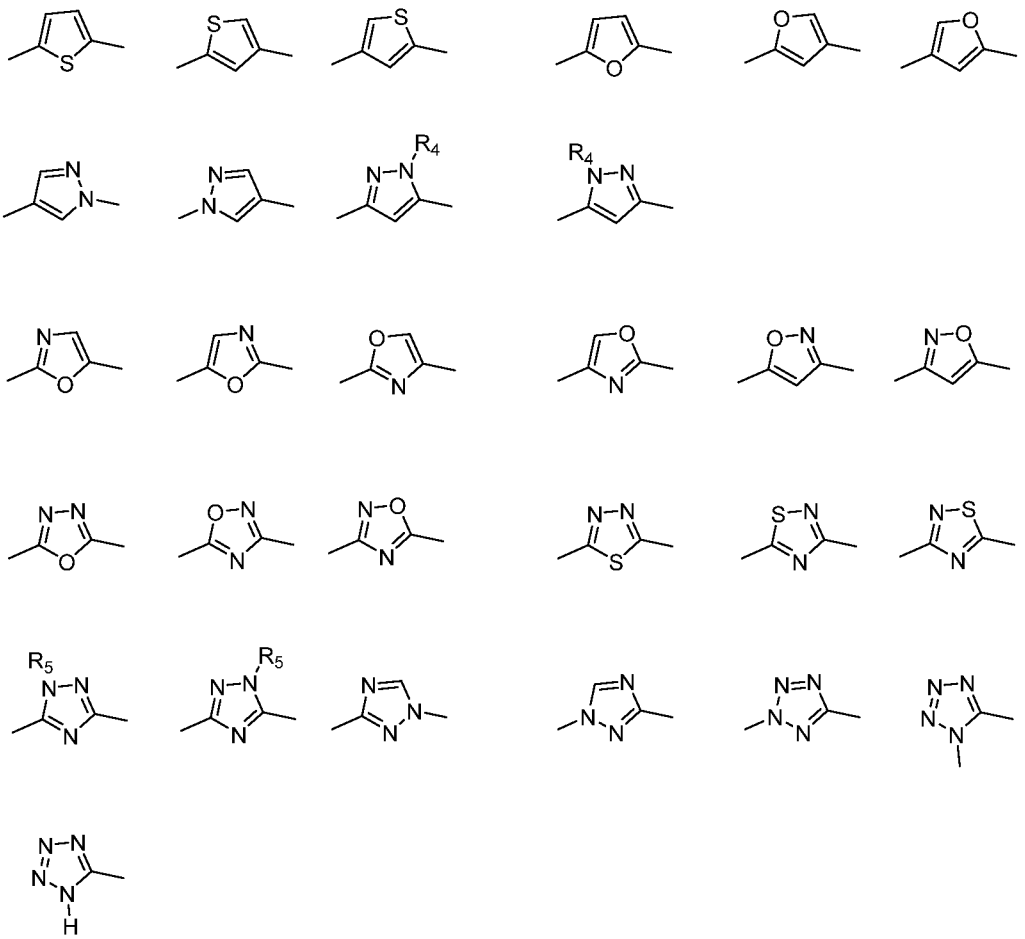

[0099] A number of embodiments can be manufactured or synthesized, such as by using a method as illustrated in Figures 12B-12D. Figure 12B illustrates a method to synthesize the compound illustrated in Figure 13A. In particular, Figure 12B illustrates a step 1 of combining cyclobutanone with 2,5-dibromothiophene to generate 1-(5-bromothiophen-2-yl)cyclobutan-1-ol. At Step 2, Bispinacalatodiboron is added to the result of Step 1 to generate 1-(5-(4,4,5,5-tetramethyl-1,3,2-dioxaborolan-2-yl)thiophen-2-yl)cyclobutan-1-ol. Step 3 combines this product with methyl 5-bromo-6-chloro-1H-indole-3-carboxylate and K_2CO_3 to generate methyl 6-chloro-5-(5-(1-

hydroxycyclobutyl)thiophen-2-yl)-1H-indole-3-carboxylate. Finally, Step 4 generates 6-chloro-5-(5-(1-hydroxycyclobutyl)thiophen-2-yl)-1H-indole-3-carboxylic acid (Figure 13A), by combining the product of step 3 with NaOH and ethanol. While the process of Figure 12B generates the compound illustrated in Figure 13A, it should be noted that additional compounds can be generated in a similar manner (e.g., the processes illustrated in Figures 12C-12D), such as the compounds illustrated in Figures 13B-13Z and 14A-14O.

[00100] Additional embodiments will be prepared by the method shown in Figure 12C, such that the boron group is attached first to the indole ring of these embodiments, then coupled to the A Ring (as shown in Figure 12A).

[00101] Further embodiments will be prepared by the method of Figure 12D, where the A Ring contains four nitrogen atoms.

[00102] Further embodiments can possess different structures while still maintaining the ability to activate AMPK. Some embodiments will possess a generalized structure, such as illustrated in Figures 15A-15B.

[00103] Derivative molecules of certain embodiments are developed from the structure in 15A. In many embodiments, moieties, R-groups, or other fragments may be substituted by one or more of the following:

- X is CH or N;
- R_1 is small alkyl (C1-C4) or halogen (e.g., Cl, Br, or F);
- R_2 is phenyl, alkyl C1-C10, cycloalkyl (C3-C10), hydroxyalkyl (C1-C6), heteroaromatic (e.g., pyridyl, pyrazolyl, pyrolyl, pyrimidyl, thiophenyl, furanyl, or triazole), or heterocyclic C4-C6;
    - where phenyl is optionally substituted with halogens (e.g., Cl, Br, or F),
    - where an alkyl is linear or branched and optionally substituted with OH, OMe, OEt,
    - where cycloalkyl is optionally substituted with one or more OH,
    - where hydroxy alkyl is linear or branched
    - where heteroaromatic is optionally substituted with small alkyls (C1-C6) or hydroxyalkyls (C1-C6), where alkyls and hydroxyalkyls are linear or branched,

- where heteroatom in hetrocyclic is optionally O, S, or NR_4, where R_4 is a linear or branched C1-C6 alkyl or hydroxyalkyl; and
- R_4 is a linear or branched C1-C6 alkyl or hydroxyalkyl.

[00104] Derivative molecules of certain embodiments are developed from the structure in 15B. In many embodiments, moieties, R-groups, or other fragments may be substituted by one or more of the following:

- A is a fused ring (e.g., C3-C10 cycloalkyl);
- X is CH or N;
- Y is O, S, NH, NR_3;
- R_1 is small alkyl (C1-C4) or halogen (e.g., Cl, Br, or F);
- R_2 is phenyl, alkyl C1-C10, cycloalkyl (C3-C10), hydroxyalkyl (C1-C6), heteroaromatic (e.g., pyridyl, pyrazolyl, pyrolyl, pyrimidyl, thiophenyl, furanyl, or triazole), or heterocyclic C4-C6;
  - where phenyl is optionally substituted with halogens (e.g., Cl, Br, or F),
  - where an alkyl is linear or branched and optionally substituted with OH, OMe, OEt,
  - where cycloalkyl is optionally substituted with one or more OH,
  - where hydroxy alkyl is linear or branched
  - where heteroaromatic is optionally substituted with small alkyls (C1-C6) or hydroxyalkyls (C1-C6), where alkyls and hydroxyalkyls are linear or branched,
  - where heteroatom in hetrocyclic is optionally O, S, or NR_4;
- R_3 is a C1-C6 alkyl (linear or branched); and
- R_4 is a linear or branched C1-C6 alkyl or hydroxyalkyl.

[00105] In a number of embodiments, A is a C6 phenyl ring. In many embodiments, A is selected from the group consisting of:

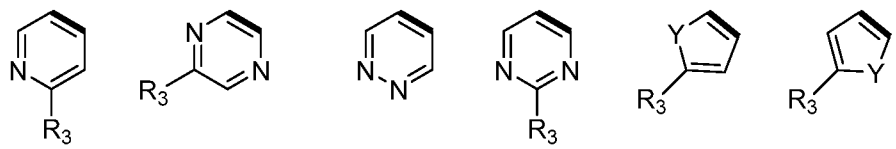

[00106] Turning to figure 15C, a method of synthesizing embodiments is illustrated. Specifically, Figure 15C illustrates a method to synthesize the embodiment illustrated in Figure 15D (also referred to as EV8017). While the process of Figure 15C generates

the compound illustrated in Figure 15D, it should be noted that additional compounds can be generated in a similar manner.

[00107] Turning to Figure 16A, the biological effect of a novel AMPK agonist illustrated in Figure 13A. In particular, Figure 16A illustrates a western blot of phosphorylated ACC (pACC) in mitochondrial-defective patient cells treated with the embodiment illustrated in Figure 13A (labeled EV8016) and vehicle-only treated cells (labeled DMSO). As noted above, in relation to Figure 11F, phosphorylation of ACC is indicative of AMPK activation, thus indicating that compounds in accordance with many embodiments are capable of activating AMPK.

[00108] Turning to Figure 16B, EC50 of various embodiments of AMPK agonists can be determined. In the exemplary embodiment EV8016 (Figure 13A), the EC50 was determined to be 232nM, while the PF-06409577 embodiment (Figure 1D) was determined to be 96nM. One of skill in the art would appreciate and understand how to determine EC50 of additional embodiments.

Methods of Treating Individuals with AMPK Agonists

[00109] Turning now to Figure 17, various embodiments are directed to treating mitochondrial dysfunction in an individual in process 1700. In some embodiments, a mitochondrial dysfunction is identified in the individual at step 1702. In certain embodiments, individuals with dysfunction are discovered by exhibited symptoms, such as N-glycanase (NGLY1) deficiency, age-related macular degeneration (AMD), ischemic stroke, muscular dystrophies (*e.g.*, Duchenne and Becker), Friedreich ataxia (FA), autoimmune disorders with muscle involvement (*e.g.*, inclusion body myositis, Polymyositis, and Dermatomyositis), neurodegenerative disorders (*e.g.*, Amyotrophic Lateral Sclerosis (ALS), Parkinson's Disease, and Alzheimer's Disease), diabetes, metabolic disorder, and/or obesity. In other embodiments, mitochondrial dysfunction will be identified based on molecular signatures of disease or dysfunction, such that protein blots (western blots), polymerase chain reaction (PCR), genotyping using genetic markers (e.g., single nucleotide polymorphisms (SNPs), expressed sequence tags (ESTs), simple sequence repeats (SSRs), etc.) will identify a particular disease or dysfunction present in the individual.

[00110] At step 1704, the individual is treated with an AMPK agonist in various embodiments. In some embodiments, the AMPK agonist is a direct (or AMP-independent) agonist, while in other embodiments, the AMPK agonist is an AMP-dependent agonist. Examples of direct agonists include PT1, ETC-1002, Salicylate, C991, C13, D561-0775, MT 63-78, A-769662, ZLN024, C24, MK-8722, PF-739, and PF-06409577. Examples of ATP-dependent agonists include metformin, resveratrol, and AICAR. In certain embodiments, the AMPK agonist is supplied to an individual at a therapeutically effective dose, where the therapeutically effective dose reduces, eliminates, or alleviates the consequences of mitochondrial dysfunction during and/or after commencement of the therapy. In some embodiments, the AMPK agonist is provided orally, subcutaneously, intravenously, intraperitoneal injection, intranasal administration, dermal administration, via inhalation, intraocular (including intravitreal), and/or any method that provides a therapeutic effect. In certain embodiments, the AMPK agonist is formulated to provide a therapeutic effect. In some embodiments, the AMPK formulation includes a binding agent, a lubricating agent, a buffer, and/or a coating, which allows for a pharmacokinetic release of the AMPK agonist to provide the therapeutic effect.

[00111] Further, the AMPK agonist and/or formulation will be provided to the individual an appropriate dose and dosing schedule to provide a therapeutic effect. In some embodiments, the AMPK agonist will be provided as a single dose, while some embodiments will provide multiple doses over a course of time. In various embodiments, dosing will be accomplished as a concentration of a total volume, such that a dose will be 10nM, 30nM, 100nM, 1μM, 100μM, or more, depending on the therapeutic effect. In additional embodiments, dosing will be in a ratio of mass of an AMPK agonist to mass of the individual being treated, such that a dose will be 1mg/kg, 5mg/kg, 10mg/kg, 20mg/kg, 50mg/kg, 100mg/kg, or more, depending on the therapeutic effect. In multiple-dosing embodiments, the dosing schedule can be 1 dose/day, 2 doses/day, 3 doses/day, or more and can continue for as long as necessary, such that the dosing can go for 1 week, 2 weeks, 3 weeks, 4 weeks, 5 weeks, 10 weeks, 20 weeks, or in perpetuity for the lifetime of the individual.

[00112] In further embodiments, the dose and/or dosing regimen will vary over the course of treatment depending on various factors, including achieving a threshold of enzyme activity. In some embodiments, a higher dose will be used to treat an individual and will be reduced after an amount of time, such that in various embodiments, a daily dose of 100μM will be used for an amount of time, such as 1 week, 2 weeks, 4 weeks, or more, then the dose will be reduced for continuing treatment of an individual. In certain embodiments, the dosing regimen will change, such that the time between doses will change over the course of a treatment. For example, certain embodiments will provide daily doses of an AMPK agonist to an individual for an amount of time (e.g., 1 week, 2 weeks, 4 weeks, etc.) then will increase the amount of time between doses, such that subsequent doses will occur semi-weekly, weekly, or monthly for the rest of the treatment.

[00113] At step 1706, various embodiments will assess the individual for efficacy of the AMPK agonist. In certain embodiments, this step is accomplished by assessing the disease symptoms, such as those listed for step 1702, while in other embodiments, this step will be accomplished by looking at molecular profiles, such as genotyping, gene expression, and other methods as disclosed in reference to step 1702.

Methods of Modulating AMPK activity

[00114] Turning now to Figure 18, various embodiments are directed to modulating AMPK activity to treat diseases or disorders in an individual, as illustrated in process 1800. In some embodiments, a disorder or disease is identified that is associated with mitochondrial dysfunction at step 1802. Examples of these diseases and/or disorders include the diseases and disorders identified in Tables 1-2, such that the disease and/or/ disorder is associated with mitochondrial dysfunction, such as primary mitochondrial dysfunction and/or secondary mitochondrial dysfunction. In various embodiments, the diseases and disorders are identified based on symptoms exhibited by an individual, while in some embodiments, diseases and disorders will be identified based on molecular signatures of disease or dysfunction, such that protein blots (western blots), polymerase chain reaction (PCR), genotyping using genetic markers

(e.g., single nucleotide polymorphisms (SNPs), expressed sequence tags (ESTs), simple sequence repeats (SSRs), etc.).

[00115] At Step 1804, various embodiments will modulate AMPK activity. Modulating AMPK activity can be activating AMPK or inhibiting AMPK activity. In certain embodiments, AMPK activity will be activated by phosphorylating AMPK or providing an AMPK agonist. In certain embodiments, modulating is accomplished by inhibiting AMPK activity. Inhibition of AMPK can be accomplished using a competitive inhibitor or an allosteric inhibitor, which prevent AMPK from catalyzing a reaction.

[00116] At Step 1806, various embodiments will assess the individual for efficacy of the treatment. In certain embodiments, this step is accomplished by assessing the disease symptoms, such as those listed for step 1802, while in other embodiments, this step will be accomplished by looking at molecular profiles, such as genotyping, gene expression, and other methods as disclosed in reference to step 1802

EXEMPLARY EMBODIMENTS

[00117] Experiments were conducted to demonstrate the capabilities of the assays and inhibitors in accordance with embodiments. These results and discussion are not meant to be limiting, but merely to provide examples of operative devices and their features.

Materials & Methods

[00118] Fibroblasts previously derived from four patients with primary mitochondrial disease (Surf1, Complex I, Cox10, Polg), three patients with NGLY1 deficiency and four normal controls were used for the study. All samples were obtained with informed consent and approved by the Stanford IRB. Fibroblasts were maintained in DMEM medium containing 8.3mM glucose and supplemented with 10% fetal bovine serum (FBS)(Fisher Scientific), 1% Penicillin-Streptomycin (10,000U/mL)(Life Technologies), 1% glutaMAX (Life Technologies), 1% uridine (5mg/ml) and 1% pyruvate (11mg/ml) at 37°C, 5% CO_2.

[00119] For the screening of various compounds, $15x10^3$ cells/500ul media were seeded in quadruplets on 24 well microtiter plates. The following day, the medium was

removed, wells washed with PBS and replaced with a mitochondrial stressor media containing DMEM, 1% Penicillin-Streptomycin (10,000U/mL)(Life Technologies), 10% FCS (Fisher Scientific), 1mM Galactose (Sigma Aldrich), and 25μM sodium azide with or without the following compounds: 1mM AICAR (Medchem Express), 1mM Metformin (Sigma Aldrich), 100μM PT1 (Santa Cruz Biotechnology), 100μM A-769662 (Medchem Express), 100μM C24 (Medchem Express). Following treatment with the various compounds, tissue cultures were analyzed for growth, oxygen consumption rate, and ATP levels.

Example 1: Cell Growth and Viability

[00120] *Methods:* Cell growth was measured by a fluorometric method using Calcein AM (Anaspec). Mitochondrial stressor media was removed, wells washed with PBS and then incubated with 500ul/well of 800nM Calcein AM in PBS for 30min at 37C, 5% CO2. Cell viability was measured by values obtained using a 485 nm excitation with the Flouroskan Ascent Microplate Fluorometer (Thermo Scientific).

[00121] Cellular ATP content was measured by LC-MS. Cells were trypsonized, washed with cold PBS, and lysed using NH4AC (0.05M pH6). The lysate was transferred to a molecular weight cut-off filter (Chromsystems) and spun for 20min at 4C, 800xg. Following centrifugation, the supernatant was analyzed for DNA quantitation using the NanoDrop ND-1000 (Nanodrop Technologies) and ATP quantitation by a 6400 Series Triple Quad LC/MS System (Agilent Technologies).

[00122] Fibroblasts in tissue culture were visualized by phase-contrast microscopy with a Leica DM IRB microscope at ×10 magnification, and images were taken with the Hamamatsu ORCA-ER camera.

[00123] Statistical significance ($p<0.05$) was calculated by 2-tailed student's t-test.

[00124] *Results:* Four direct activators of AMPK, PT1, A-769662, ZLN024, and C24, were tested on SURF1-deficient fibroblasts. The AMP analog AICAR, previously shown to improve mitochondrial function in vitro (Golubitzky, et al, PLoS One. 2011;6(10); the disclosure of which is incorporated by reference herein in its entirety;) was included in the study design as a positive control. Mutant cells treated with direct AMPK agonists demonstrated a 35-55% increase in viability compared with untreated cells (i.e., cells

treated with the vehicle DMSO) (Figures 2A), with PT1 showing the largest improvement. A smaller but still significant effect was also seen in SURF1 cells treated with AICAR compared to the corresponding untreated control (*i.e.*, cells treated with PBS), with mean cell survival increased by 57%.

[00125] To assess whether these findings extend to mitochondrial disorders beyond SURF1 deficiency, similar studies using fibroblasts from patients with deficiencies of mitochondrial complex I (CI), heme A:farnesyltransferase cytochrome c oxidase assembly factor (COX10), and mitochondrial DNA polymerase gamma (POLG) were performed. These studies therefore assessed a broad range of mitochondrial disruptions encompassing different components of the respiratory chain and mtDNA replication machinery. One compound, PT1, consistently and significantly improved survival in all mutant lines despite their different pathogenic mechanisms (Figures 2B-2D). The remaining compounds showed variable responses among the mutant lines: A-769662 improved survival in CI and POLG-deficient cells, ZLN024 improved survival in CI-deficient cells, and C24 improved survival in SURF1-deficient cell but not in any of the other lines. Interestingly, AICAR treatment also did not improve survival in any of the other lines except SURF1. Similar results were observed with fibroblasts from patients with NLGY-1 deficiency with up to 60% improvement in viability (Figure 2E). Additionally, the newly developed AMPK agonists, MK-8722, PF-739, and PF-04609577, were tested and showed they improved the viability of surf1 patient cells similar to PT1, and that this improvement occurred in a dose dependent manner (Fig 2E). Additionally, the cell morphology improved with treatment with PT1 on SURF1 (Figure 3B), COX10 (Figure 3D), CI (Figure 3F), POLG (Figure 3H), and NGLY1 Figure 3J) deficient fibroblasts over untreated cells (Figures 3A, 3C, 3E, 3G, AND 3I), where the untreated cells show exhibit bright apoptotic cells. Additionally, MK-8722 (Figure 3L), PF-739 (Figure 3M), and PF-04609577 (Figure 3N) improved cell morphology in SURF1-deficient fibroblasts over untreated fibroblasts (Figures 3K), where the untreated cells show exhibit bright apoptotic cells are illustrated.

[00126] *Conclusion*: These results indicate that direct AMPK activation improves cell viability across a range of primary and secondary mitochondrial disease etiologies,

which is supported by improved cell morphology seen in mutant cells treated with PT1 compared to cells treated with DMSO.

Example 2: Measuring AMPK agonist on AMPK

[00127] *Methods*: Western blotting was performed to identify pAMPK levels in cells treated with PT1. Cells were lysed with RIPA buffer supplemented with Na-Orthovanadate, PMSF, and Protease Inhibitor cocktail. Whole cell extracts were fractionated by SDS-PAGE and transferred to a polyvinylidene difluoride membrane using a transfer apparatus according to the manufacturer's protocols (Bio-Rad). After incubation with 5% nonfat milk in TBST (10 mM Tris, pH 8.0, 150 mM NaCl, 0.5% Tween 20) for 60 min, the membrane was washed once with TBST and incubated with antibodies against AMPK (1:1,000), pAMPK (1:1,000), actin (1:10,000) at 4°C overnight. Membranes were washed three times for 5 min and incubated with a 1:10,000 dilution of horseradish peroxidase-conjugated anti-mouse or anti-rabbit antibodies for 2h. Blots were washed with TBST three times and developed with the ECL system (Thermo Scientific) according to the manufacturer's protocols.

[00128] To test whether the cellular response to PT1 is a result of AMPK activation itself, or is merely a result of nonspecific interactions, an siRNA knockdown strategy was used. siRNA for PRKAA1 (s101) and a negative control (Life Technologies) were incubated with Hiperfect reagent (Qiagen) in media containing DMEM, 1% Penicillin-Streptomycin (10,000U/mL) (Life Technologies), 1% glutaMAX (Life Technologies) but no serum and allowed to complex for 10 min at room temperature. The complex was then added to COX10 patient tissue cultures in 6-well microtiter plates (final siRNA concentration of 10 nM of each siRNA) and incubated for 72hr at 37°C, 5% CO_2. At the end of the incubation period, the cells were analyzed for levels of AMPK and pAMPK by western blot analysis (see protocol above) or incubated for six additional days with PT1 (or DMSO as untreated control) and assessed for viability by Calcein AM. COX10-deficient fibroblasts were treated with PT1 and either siAMPK or siCNT, and responses were evaluated for pAMPK protein expression by western blotting (Figure 4A), cell viability by Calcein AM fluorescence assay (Figure 4B), and cell morphology by phase contrast microscopy (Figures 4C-4F)

[00129] *Results*: Cultured fibroblasts from SURF1 deficient patient cells were treated with PT1 for 0hr, 2hr, 24hr and 48hr and pAMPK levels measured. pAMPK levels increased by 2 hours post-PT1 treatment, and peaked at 24hr with return to baseline at 48hrs (Fig 5A). Treatment with PT1 together with selective knockdown of AMPK (PT1+siAMPK) resulted in a 63% decrease in pAMPK levels and 41% decrease in cell viability compared to control conditions (PT1+siCNT), consistent with the idea that cellular response to PT1 is mediated by AMPK activation. Following 48hr treatment with PT1, the peroxisome proliferator-activated receptor gamma coactivator 1-alpha (PGC-1α), a master regulator of mitochondrial biogenesis, increased by 2.4- fold (Figure 5B). Similarly, catalase and manganese superoxide dismutase (SOD2), two of the main antioxidant genes regulated by AMPK, increased by 1.3-fold and 1.5-fold, respectively (Figures 5C-5D).

[00130] *Conclusion*: PT1's mechanism of action addresses the main metabolic disruptions caused by mitochondrial dysfunction; therefore stimulating mitochondrial biogenesis and triggering the oxidative stress response through AMPK activation.

Example 3: Oxygen Consumption and Cellular Respiration

[00131] *Background*: To determine if the upregulation of PGC-1 with PT1 treatment was associated with improved mitochondrial respiration, oxygen consumption rates (OCR) were evaluated in both SURF1 and POLG patient fibroblasts.

[00132] *Methods*: Oxygen consumption rate (OCR) was measured using an XF96 extracellular flux analyzer (Seahorse Biosciences). Fibroblasts were seeded at 10x103 cell/well in 100ul media containing 8.3mM glucose and supplemented with 10% fetal bovine serum (FBS) (Fisher Scientific), 1% Penicillin-Streptomycin (10,000U/mL)(Life Technologies), 1% glutaMAX (Life Technologies), 1% uridine (5mg/ml) and 1% pyruvate (11mg/ml) on an XF 96 well plate at 37°C, 5% CO2. The following day the medium was replaced with the mitochondrial stressor media (details above) with or without PT1, A-769662, and AICAR. After 48 hours the stressor media was replaced with 175µl unbuffered XF base DMEM medium (Fisher Scientific) with the same constituents as the mitochondrial stressor medium and incubated at 37°C for 30min for equilibrium before the measurements. OCR Baseline measurements were measured three times,

once every five minutes. After the experiment, cell content was estimated by Calcein AM fluorescence intensity (FI) and OCR was calculated as OCR divided by FI.

[00133] *Results*: Despite distinct etiologic differences, both Surf1 and POLG patient cells treated with PT1 demonstrated a roughly 30% improvement in basal respiration (Figures 6A-6B), while PT1 demonstrated a 16% increase in basal OCR in NGLY1 patient cells (Figure 6C).

[00134] The fraction of basal mitochondrial oxygen consumption used for ATP synthesis (ATP-coupled respiration) also improved by 40% in Surf1 and 30% in POLG, demonstrating PT1's positive effect on the coupling efficiency of oxidative phosphorylation (Figures 6D-6E).

[00135] Maximal respiration capacity, which reflects the cells' ability to respond to increased ATP demand, improved in both Surf1 and POLG cells, with a 50% and 20% increase, respectively (Figures 6F-6G), while PT1 demonstrated a 40% increase in maximal OCR in NGLY1 patient cells (Figure 6H).

[00136] *Conclusion*: Activating AMPK through an AMP-independent mechanism may be a more suitable mechanism by which to target mitochondrial dysfunction.

Example 4: Measuring Oxidative Stress and Energy Status

[00137] *Background*: ATP and ROS content reflect cellular energy and oxidative status, both of which are dependent on effective ATP-coupled respiration and overall mitochondrial function. Mitochondrial dysfunction causes an incomplete electron transfer through the RC, leading to decreased ATP synthesis and over-production of reactive oxygen species (ROS). (Atkuri et al, Proc Natl Acad Sci USA. 2009 Mar 10;106(10):3941-5; Enns et al, PLoS One. 2014 Jun 18;9(6); the disclosures of which are incorporated by reference herein in their entirety.)

[00138] *Methods*: SURF1, POLG, and NGLY1 patient cells were supplemented with PT1 or DMSO (untreated control) for 48hrs (n=3) and ATP levels measured by the CellTiter-Glo ATP Assay or for 72hrs (n=3) and ROS levels were measured by the CellROX Deep Red Flow Cytometry Assay. Results were normalized to total protein concentration. Data are represented as the mean $\pm$ standard error of the mean. Statistical significance was measured to $p<0.05$.

[00139] *Results*: ATP content increased with treatment by 35% in Surf1, 36% in POLG, and 40% in NGLY1 patient cells, and compared to DMSO treated cells, ROS levels decrease by 10%, 15%, and 18% respectively (Figures 7A-7F).

[00140] *Conclusion*: Consistent with the observed upregulation of ATP-coupled respiration and expression of the antioxidants Catalase and SOD2 (Example 2; Figures 5C-5D), both the energy deficiency and oxidative stress improved with PT1 treatment in cells from patients with either primary or secondary mitochondrial dysfunction.

Example 5: Measuring Effect on AMD

[00141] *Methods*: To generate an AMD model, mice were treated with 100mg/kg of PT1 (or vehicle) 24hrs and 12hrs prior to SI (or vehicle) treatment, then treated every 24hrs for 3 days post-SI. Both PT1 and SI were delivered by intraperitoneal (IP) injections and animals were phenotyped 3 days post-SI administration.

[00142] Mice were anesthetized and their pupils dilated using 1% atropine sulfate, 2.5% phenylephrine hydrochloride, and 0.5% proparacaine hydrochloride. Funduscopy was performed using the Micron III small animal retinal imaging AD camera (Phoenix Research Laboratories, INC).

[00143] Retinal function was evaluated by recording of dark- and light-adapted ERG (Espion E2 System, Diagnosys LLC). Mice were dark adapted overnight before ERG recording, and all procedures were performed in the dark or under dim red light. Mice were anesthetized and their pupils dilated as described above. For the ERG recordings, electrodes were placed on the center of cornea. A ground needle electrode was placed in the base of the tail, and reference needle electrode was placed subdermally between the eyes. The a-wave amplitude was measured from the baseline to the trough of the a-wave, and b-wave amplitude was measured from the trough of the a-wave to the peak of the b-wave.

[00144] *Results*: Fewer white deposits are observed in PT1 treated mice (+SI;+PT1) compared to untreated mice (+SI;-PT1) (n=5 mice per group). PT1 treatment alone (-SI;+PT1) does not alter funduscopy results, closely resembling control mice (-SI;-PT1) (Figure 9A). H&E staining of retinal sections shows PT1 treatment (+SI;+PT1) protects against ONL thinning (white bars), prevents alterations in photoreceptor IS/OS

morphology, and decreases melanin debris (black arrows) compared to untreated mice (+SI;-PT1) (n=5 mice per group) (Figure 9B). ONL thickness in PT1 treated mice (+SI;+PT1) is similar to control mice (-SI;-PT1) and is significantly improved compared to untreated mice (+SI;-PT1). PT1 treatment alone does not alter ONL thickness (-SI; +PT1 vs. -SI;-PT1)(n=3-4 mice per group) (Figure 9C). Electroretinography demonstrates significantly increased rod responses (scotopic a-wave and b-wave) in PT1 treated mice (+SI;+PT1) compared to untreated mice (+SI;-PT1) (n=3-4 mice per group) (Figure 9D).

[00145] *Conclusion*: PT1 demonstrates improvements in retinas exhibiting AMD, thus indicating a positive use of AMPK agonists as a treatment for AMD.

Example 6: Neuroprotection in Ischemic Stroke

[00146] *Methods*: To generate an ischemic stroke model, ischemic lesions were induced by transiently occluding the middle cerebral artery for 45 minutes, followed by reperfusion. Mice were then injected intraperitoneally with either 100mg/kg of PT1 or vehicle in two doses, 1 hour and 24 hours post-occlusion, and sacrificed one hour later for terminal tissue collection.

[00147] Isolated brains were placed in cold saline for 20 minutes, sliced in seven coronal slices (2 mm thick), and stained in a 1.0% 2,3,5- triphenyltetrazolium chloride (TTC) solution in saline at 37°C for 30 minutes. The stained brain tissues were fixed in 10% formalin in phosphate-buffered saline. The images were captured using a CCD camera (Panasonic Corporation, Japan) and the unstained damaged areas were defined as infarcted tissue and were quantified using Image Pro Plus 4.1 software (Media Cybernetics, Silver Spring, MD).

[00148] *Results*: TCC-stained brain slices from mice treated with PT1 showed a reduction in size of the infarcted regions (white) compared to mice treated with vehicle (Figures 10B-10C).

[00149] *Conclusion*: PT1 treatment showed a striking attenuation of the ischemic (stroke) area in brain slices from mice treated with PT1 compared with untreated controls.

Example 7: Enhancement of Motor Performance

[00150] *Background*: As a high-energy demand organ, the eye is particularly susceptible to the consequences of mitochondrial damage. Similarly, skeletal muscle is also a high-energy organ that relies on both oxidative phosphorylation and glycolysis for energy production.

[00151] *Methods*: To examine the effects of AMPK agonists on in vivo systems with mitochondrial dysfunction, MK8722 was used to treat a mouse model of mitochondrial disease. These mice have mitochondrial Complex IV deficiency caused by deficient cytochrome C oxidase assembly protein, SCO2, and harbor a Sco2 knock-out (KO) allele and a Sco2 knock-in (KI) allele expressing an E→K mutation at position 129 (E129K). The E129K mutation corresponds to the E140K mutation found in almost all human SCO2-mutated patients. (*See e.g.*, Yang et al, Analysis of mouse models of cytochrome c oxidase deficiency owing to mutations in Sco2. Hum Mol Genet. 2010 Jan 1;19(1):170-80; the disclosure of which is incorporated by reference herein in its entirety.) The predominant phenotype of Sco2 deficient mice is reduced locomotor function and ocular defects, both common findings in patients with primary mitochondrial disease. The Sco2 mice were grouped into four treatment groups: Sco2 KI/KO+MK8722, Sco2 KI/KO+DMSO (vehicle), Control KI/WT+MK8722, Control KI/WT+DMSO with 7-9 mice per group. 1.5-month old Sco2 mice were treated once daily by oral gavage with MK8722 (10mg/kg) or vehicle (DMSO) for 14 weeks. Locomotor function was evaluated using the activity chamber, rotarod, and hanging-wire tests and ocular structure using optical coherence tomography (OCT).

[00152] *Results*: As a result of this sensitivity to mitochondrial dysfunction, ocular structure measured in vivo by Optical Coherence Tomography (OCT) revealed retinal defects in both Sco2 KI/KO as well as the heterozygous KI/WT littermates. The thickness of the retinal nerve fiber layer (RNFL) was reduced in Sco2 KI/KO and KI/WT mice compared to WT/WT controls (KI/KO Veh: 74.1μm and KI/WT Veh: 72.7 μm versus WT/WT Veh: 76.2μm). By contrast, the RNFL in the MK8722-treated mice was thicker than the vehicle-treated Sco2 KO/KI and KI/WT mice (KI/KO Veh: 74.1μm versus KI/KO MK8722: 77μm and KI/WT Veh: 72.7μm vs. KI/WT MK8722: 74.7μm) (see Fig. 9E).

[00153] In the locomotor function studies evaluating muscle performance, MK8722-treated Sco2 KI/KO mutant mice outperformed the vehicle-treated Sco2 KI/KO mutant mice in the activity chamber (See Figure 11A), rotarod running test (See Figure 11B), and fore limb wire hang test (See Figure 11C). As seen in Figure 11A, vehicle-treated Sco2 KI/KO mice moved less distance in the activity chamber compared to the KI/WT littermate controls and 8 weeks of MK8722 treatment restored their activity to control levels (KO/KI Veh: 1516.7cm; KO/KI MK8722: 2337.8cm; KI/WT Veh: 2337cm). Figure 11B illustrates that MK8722 treatment also improved the rotarod running time of KI/KO mutant mice compared to vehicle-treated mice to levels similar to the controls (KO/KI Veh: 176.1sec; KO/KI MK8722: 248.1sec; KI/WT Veh: 235.7sec). For the hanging wire test, Figure 11C shows that MK8722 treatment increased the length of time Sco2 KO/KI mutant mice could hang by their four limbs to levels even above that of the KI/WT controls (KO/KI Veh: 173.2sec; KO/KI MK8722: 312.5sec; KI/WT Veh: 145.5sec).

[00154] Figure 11D shows the intensity of histological stains indicative of mitochondrial cytochrome C oxidase (CytoC) and succinate dehydrogenase (SDH) activities are increased in the skeletal muscle tissue of MK8722-treated Sco2 KI/KO mutant mice compared to vehicle-treated mutant mice. Similarly, Figure 11E shows an increased glycogen content upon histological assessment of skeletal muscle in Sco2 KI/KO mutant mice treated with MK8722 compared to untreated mice. The increase in locomotor function (Figures 11A-11C) and mitochondrial function (Figures 11D-11E), was associated with an increase in ACC phosphorylation, as seen in Figure 11F.

[00155] *Conclusion*: The retinal study (Figure 9E) demonstrates that activation of AMPK can improve and/or prevent ocular damage associated with mitochondrial dysfunction. Additionally, the locomotor studies (Figures 11A-11C) demonstrate that AMPK activation can enhance strength, endurance, and overall locomotor function in muscle degenerative disorders associated with mitochondrial dysfunction. Further, the increased mitochondrial function (Figure 11D) and glycogen content (Figure 11E) may play an integral part of the mechanism of action by which energy levels are normalized within the skeletal muscle, thereby preventing degeneration and weakness. Coupled with the increased ACC phosphorylation indicative of increased AMPK activation, these

results demonstrate the ability of AMPK agonists of many embodiments to have many pharmacological benefits.

Example 8: Synthesizing 6-chloro-5-(5-(1-hydroxycyclobutyl)thiophen-2-yl)-1H-indole-3-carboxylic acid and analogs thereof

[00156] *Background*: Figure 12A illustrates a generalized structure of a compound capable of activating AMPK. The synthesis of four derivatives (Figures 13A-13B and Figure 14J-14K) are described in this example.

[00157] *Methods*: A graphical illustration of this example is illustrated in Figure 12B, and while this example illustrates the synthesis of the compound illustrated in Figure 13A, one of skill in the art would understand the use of different reagents, reactants, conditions, etc. to generate derivative compounds, including those illustrated in Figures 13B-13Z and Figures 14A-14O.

[00158] Step 1: 1-(5-bromothiophen-2-yl)cyclobutan-1-ol—To a stirred solution of 2,5-dibromothiophene (0.95 g, 3.922 mmol) in dry THF at -78°C, n-butyl lithium was added (2.69 ml, 4.314 mmol) drop wise at -78°C and the mixture was allowed to stir for another 30 min at the same temp. Then a solution of cyclobutanone (0.27 g, 3.922 mmol) was slowly added over 2 min and the reaction mixture was allowed to stir at -78°C for 1 h and then quenched with ammonium chloride. The product was extracted into ethyl acetate, dried over sodium sulfate, evaporated under reduced pressure and then purified by Flash chromatography (230 – 400 mesh, 10% EA in PE) to give 1-(5-bromothiophen-2-yl)cyclobutan-1-ol (0.6g; 66%) as a colorless liquid.

[00159] Step 2: 1-(5-(4,4,5,5-tetramethyl-1,3,2-dioxaborolan-2-yl)thiophen-2-yl)cyclobutan-1-ol—A mixture of the product of Step 1 (2.0 g, 8.579 mmol), Bispinacalatodiboron (3.2 g, 12.87 mmol) and KOAc (2.25 g, 25.7 mmol) in 1,4-dioxane (20 ml) was purged with N_2 gas for 5 minutes and then $Pd(dppf)Cl_2$ (0.32 g, 0.429 mmol) was added. After stirring for 16 h at 90° C the solvent was removed by evaporation under reduced pressure and the residue was purified by column chromatography over florisil, eluting with 0-10% EA/PE, to give 1-(5-(4,4,5,5-tetramethyl-1,3,2-dioxaborolan-2-yl)thiophen-2-yl)cyclobutan-1-ol (0.6g; 25%) as a gummy solid.

[00160] Step 3: Methyl 6-chloro-5-(5-(1-hydroxycyclobutyl)thiophen-2-yl)-1H-indole-3-carboxylate—A mixture of the product of Step 2 (0.275 g, 0.977 mmol), methyl 5-bromo-6-chloro-1H-indole-3-carboxylate (0.282 g, 0.977 mmol), K2CO3 (0.40 g, 2.931 mmol) in 1,4-dioxane (5 ml) and water (1 ml) was purged with N_2 gas for 5 minutes. Pd(dppf)Cl_2.DCM (0.04 g, 0.048 mmol) was then added and the resulting solution was stirred for 16 h at 100°C. The solvent was removed by evaporation under reduced pressure and the residue was purified by column chromatography over florisil by eluting with 0-10% EA/PE, to give methyl 6-chloro-5-(5-(1-hydroxycyclobutyl)thiophen-2-yl)-1H-indole-3-carboxylate (0.15g; 91%) as an off white solid.

[00161] Step 4: 6-chloro-5-(5-(1-hydroxycyclobutyl)thiophen-2-yl)-1H-indole-3-carboxylic acid—To a stirred solution of the product of Step 3 (0.150 g, 0.414 mmol) in ethanol and 6N NaOH solution (10 ml) was stirred for 16 h at 80°C. The solvent was removed by evaporation under reduced pressure and the residue was acidified with citric acid and the product was extracted into ethyl acetate. After washing the extract with water and drying with sodium sulfate the solvent was removed under reduced pressure and the crude residue was purified by prep-HPLC to give 6-chloro-5-(5-(1-hydroxycyclobutyl)thiophen-2-yl)-1H-indole-3-carboxylic acid (0.06g; 42%) as an off-white powder.

[00162] By altering certain reagents, the methodology described above in relation to Figure 12B were also be used to generate 6-chloro-5-(5-(1-hydroxycyclobutyl)thiophen-3-yl)-1H-indole-3-carboxylic acid (Figure 13B), 6-chloro-5-(1-methyl-1H-pyrazol-4-yl)-1H-indole-3-carboxylic acid (Figure 14J), and 6-chloro-5-(1-phenyl-1H-pyrazol-4-yl)-1H-indole-3-carboxylic acid (Figure 14K).

[00163] *Results*: Step 1 produced 1-(5-bromothiophen-2-yl)cyclobutan-1-ol with the following characteristics: ^{1}H NMR (400 MHz, CDCl3): δ 6.91 (d, J = 3.6 Hz, 1H), 6.81 (d, J = 4.0 Hz, 1H), 2.49 – 2.36 (m, 4H), 2.21(s, 1H), 1.96 – 1.91 (m, 1H), 1.76 – 1.69 (m, 1H). LCMS: 97.6% (217.07, M-18).

[00164] Step 3 produced Methyl 6-chloro-5-(5-(1-hydroxycyclobutyl)thiophen-2-yl)-1H-indole-3-carboxylate with the following characteristics: ^{1}H NMR (400 MHz, CDCl3): δ 8.56 (bs, 1H), 8.29 (s, 1H), 7.93 (d, J = 2.8 Hz, 1H), 7.54 (s, 1H), 7.16 (d, J = 3.6 Hz,

1H), 7.06 (d, J = 3.6Hz, 1H), 3.92 (s, 3H), 2.65 – 2.58 (m, 2H), 2.51 – 2.44 (m, 2H), 2.31 (s, 1H), 1.99 – 1.91 (m, 1H), 1.84 – 1.80 (m, 1H). LCMS: 95.63% (344.23, M-18).

[00165] Step 4 produced 6-chloro-5-(5-(1-hydroxycyclobutyl)thiophen-2-yl)-1H-indole-3-carboxylic acid with the following characteristics: ^{1}H NMR (400 MHz, DMSO-d6): δ 12 (br s, 1H), 8.12 (s, 1H), 8.07 (s, 1H), 7.63 (s, 1H), 7.12 (d, J= 3.6 Hz,1H), 7.06 (d, J = 3.6 Hz, 1H), 5.96 (s, 1H), 2.45 – 2.31 (m, 4H), 1.91 – 1.82 (m, 1H), 1.78 – 1.68 (m, 1H). LCMS: 99.06 % (465.30 [M+H]+), melting range: 228-232°C.

[00166] Figure 13B illustrates 6-chloro-5-(5-(1-hydroxycyclobutyl)thiophen-3-yl)-1H-indole-3-carboxylic acid, which has ^{1}H NMR (400 MHz, DMSO-d6): δ 11.90 (bs, 1H), 8.04 (s, 1H), 7.60 (s, 1H), 7.42 (d, J = 1.2 Hz, 1H), 7.20 (d, J= 1.6 Hz, 1H), 5.96 (s, 1H), 2.44 – 2.32 (m, 4H), 1.91 – 1.82 (m, 1H), 1.77 – 1.70 (m, 1H), LCMS: 97.92 % (346.51 [M+H]+), and Melting Range: 248-252°C.

[00167] Figure 14J illustrates 6-chloro-5-(1-methyl-1H-pyrazol-4-yl)-1H-indole-3-carboxylic acid, which has ^{1}H NMR (400 MHz, DMSO-d6): δ 12.09 (s, 1H), 11.87 (s, 1H), 8.04 (d, J = 2.4 Hz, 2H), 8.01 (s, 1H), 7.67 (s, 1H), 7.59 (s, 1H), 3.90 (s, 1H), LCMS: 99.32 % (276.31 [M+H]+), and Melting range: 241-245°C

[00168] Figure 14K illustrates 6-chloro-5-(1-phenyl-1H-pyrazol-4-yl)-1H-indole-3-carboxylic acid, which has ^{1}H NMR (400 MHz, DMSO-d6): δ 11.86 (br s, 1H), 8.77 (s, 1H), 8.20 (br s, 1H), 8.00 (s, 2H), 7.93 (d, J = 7.6 Hz, 1H), 7.63 (s, 1H), 7.52(t, 2H), 7.33 (t, 1H), LCMS: 97.20 % (338.13 [M+H] +), and Melting Range: 245-249°C.

[00169] *Conclusion*: Embodiments are capable of synthesizing novel AMPK agonists and derivates thereof, such as those illustrated in Figures 13B-13Z and Figures 14A-14O.

Example 9: Synthesizing Analogs of EV8016 (Figure 13A)

[00170] *Background*: Figure 12A illustrates a generalized structure of a compound capable of activating AMPK. The synthesis of additional derivatives (Figure 13F and Figures 14L-14M) are described in this example.

[00171] *Methods*: A graphical illustration of this example is illustrated in Figure 12C, and while this example illustrates the synthesis of the compound illustrated in Figure 14L, one of skill in the art would understand the use of different reagents, reactants,

conditions, etc. to generate derivative compounds, including those illustrated in Figures 13A-13Z and Figures 14A-14O.

[00172] *Results*: Figure 13F illustrates 6-chloro-5-(5-(1-(hydroxymethyl)cyclopropyl)thiophen-2-yl)-1H-indole-3-carboxylic acid which has ^{1}H NMR (400 MHz, DMSO-d6): δ 11.65 (bs, 1H), 8.24 (bs, 1H), 7.89 (bs, 1H), 7.55 (d, J = 9.2 Hz, 1H), 705 (s, 1H), 6.88 (d, J = 3.6 Hz, 1H), 4.90 (s, 1H), 3.57 (s, 2H),, 1.00 – 0.87 (m, 4H) and LCMS: 99.06 % (465.30 $[M+H]^+$).

[00173] Figure 14L illustrates 6-chloro-5-(2-phenyloxazol-5-yl)-1H-indole-3-carboxylic acid, which has ^{1}H NMR (400 MHz, DMSO) δ 12.08 (s, 2H), 8.53 (s, 1H), 8.13 (s, 1H), 8.06 (d, J = 6.6 Hz, 2H), 7.81 (s, 1H), 7.72 (s, 1H), 7.59 (t, J = 7.1 Hz, 3H), LCMS: 91.95 % (339.35 [M+H]+), and Melting range: 261-265°C

[00174] Figure 14M illustrates 6-chloro-5-(4-phenylthiophen-2-yl)-1H-indole-3-carboxylic acid which has ^{1}H NMR (400 MHz, DMSO-d6): δ 11.77 (bs, 1H), 8.31 (s, 1H), 7.91 (s, 1H), 7.88 (s, 1H), 7.76 (d, J= 7.6 Hz, 2H), 7.66 (d, J = 1.2 Hz, 1H), 7.61 (s, 1H), 7.43 (t, 2H), 7.31 (t, 1H), LCMS: 99.55 % (354.10 $[M+H]^+$) and Melting range: 195 – 199 °C.

[00175] *Conclusion*: Embodiments are capable of synthesizing novel AMPK agonists and derivates thereof, such as those illustrated in Figures 13A-13Z and Figures 14A-14O.

Example 10: Synthesizing Additional Analogs of EV8016 (Figure 13A)

[00176] *Background*: Figure 12A illustrates a generalized structure of a compound capable of activating AMPK. The synthesis of additional derivatives (Figures 14N-14O) are described in this example.

[00177] *Methods*: A graphical illustration of this example is illustrated in Figure 12D, and while this example illustrates the synthesis of the compounds illustrated in Figures 14N-14O, one of skill in the art would understand the use of different reagents, reactants, conditions, etc. to generate derivative compounds, including those illustrated in Figures 13A-13Z and Figures 14A-14O.

[00178] *Results*: Figure 14N illustrates methyl 6-chloro-5-(1H-tetrazol-5-yl)-1H-indole-3-carboxylate, which is the product after Step 2 of Figure 12D. This compound has ^{1}H

NMR (400 MHz, DMSO-d6): δ 12.03 (br s, 1H), 8.25 (s, 1H), 8.15 (s, 1H), 7.60 (s, 1H), 7.01-7.00 (br s, 1H), 3.81 (s, 3H), and LCMS: 93.9% (278.07 [M+H] +).

[00179] Figure 14O illustrates 6-chloro-5-(1H-tetrazol-5-yl)-1H-indole-3-carboxylic acid, which a product of Step 3 of Figure 12D. This compound has ^{1}H NMR (400 MHz, DMSO-d6): δ 16.73 (s, 1H), 12.34 (s, 1H), 12.21 (s, 1H), 8.36 (s, 1H), 8.19 (d, *J* = 2.9 Hz, 1H), 7.78 (s, 1H) and melting range: 268-272°C.

[00180] *Conclusion*: Embodiments are capable of synthesizing novel AMPK agonists and derivates thereof, such as those illustrated in Figures 13A-13Z and Figures 14A-14O.

Example 11: Synthesizing (3R,3aR,6R,6aR)-6-((5-([1,1'-biphenyl]-4-yl)-1H-naphtho[1,2-d]imidazol-2-yl)oxy)hexahydrofuro[3,2-b]furan-3-ol

[00181] *Methods*: A graphical illustration of this example is shown in Figure 15A. Additionally, while this example illustrates the synthesis of the compound illustrated in Figure 15B, one of skill in the art would understand the use of different reagents, reactants, conditions, etc. to generate derivative compounds.

[00182] Step 1: Synthesizing N-(4-bromonaphthalen-1-yl)acetamide (Compound 2)—To a stirred solution of Compound-1 (5.0 g, 22.520 mmol) in Methanol, was added Acetic acid (4.2 mL, 45.040 mmol), at RT and the reaction mixture was allowed to stir at 70 °C for 2 h. The reaction progress was monitored by TLC. Upon completion, reaction mixture was poured into ice cold water and the precipitated solid was filtered off, dried under vacuo to afford compound-2 as a yellow solid (4.5g, 75%).

[00183] Step 2: Synthesizing N-(4-bromo-2-nitronaphthalen-1-yl)acetamide (Compound 3)—To a stirred solution of Compound-2 (4.0 g, 15.150 mmol) in acetic acid (40 mL) at room temperature, was added Fuming HNO_3 (0.72 mL, 16.660 mmol) and the reaction mixture was stirred at 75°C for 2 h. The reaction progress was monitored by TLC. Upon completion, reaction mixture was poured into ice cold water, precipitated solid was filtered off, washed with plenty of water and dried under vacuo to afford compound-3 as yellow solid (3.52g, 72%).

[00184] Step 3: Synthesizing N-(4-([1,1'-biphenyl]-4-yl)-2-nitronaphthalen-1-yl)acetamide (Compound 5):

[00185] To a stirred solution of Compound-3 (20.0 g, 64.720 mmol) and Compound-4 (19.2 g, 97.080 mmol) in Dioxane and Water (9:1), was added K2CO3 (22.30 g, 161.800 mmol), the reaction mixture was purged for 15 min with nitrogen, then added Pd(PPh3)4 (3.73 g, 3.230 mmol) and again purged for 10 min with nitrogen, then the reaction mixture was stirred at 90°C for 2 h. The reaction progress was monitored by TLC. Upon completion of reaction, reaction mixture was filtered through Celite, filtrate was concentrated under reduced pressure, residue was triturated with water and the precipitated solid was filtered. Solid was recrystallized from 2-propanol, obtained solid was filtered and dried under vacuo to afford compound-5 as yellow solid (11.1g, 40%). Compound 5 was used as such in Step 6.

[00186] Step 4: Synthesizing 4-([1,1'-biphenyl]-4-yl)-2-nitronaphthalen-1-amine (Compound 6)—To a stirred solution of Compound-5 (5.0 g, 13.089 mmol) in 1, 4 Dioxane (500 mL), was added Conc. HCl (50 mL) and the reaction mixture was stirred at 100°C for 48 h. The reaction progress was monitored by TLC. Upon completion of reaction, Dioxane was evaporated under reduced pressure, the aqueous residue was diluted with ice cold water and the precipitated solid was filtered. The solid was washed with plenty of water and dried under vacuo to afford compound-6 (4.05g, 91.0%) as yellow solid. This compound was used in the next step without further purification.

[00187] Step 5: Synthesizing 4-([1,1'-biphenyl]-4-yl)naphthalene-1,2-diamine (Compound 7)—To a solution of compound-6 (5.0 g, 14.662 mmol) and in a mixture of THF (400 mL) and Ethanol (100 mL,), were added 10% w/w wet Pd-C (1.0 g,) the resulting reaction mixture was hydrogenated in a Parr apparatus, under 80psi pressure of hydrogen for 16 h at RT. The progress of the reaction was monitored by TLC. After completion of reaction, filtered through Celite and the filtrate was concentrated under reduced pressure. The crude product was triturated with n-pentane and precipitated solid was filtered, dried under vacuo to afford compound-7 as a yellow solid (3.5g crude). This compound was used a such immediately in the next step.

[00188] Step 6: Synthesizing 5-([1,1'-biphenyl]-4-yl)-1,3-dihydro-2H-naphtho[1,2-d]imidazole-2-thione (Compound 8)—To a stirred solution of Compound-7 (3.5 g, 11.290 mmol) in THF (70 mL), was added DMAP (2.75 g 22.80 mmol) followed by thiophosgene (0.89 mL, 11.290 mmol) at 0°C and the resulting reaction mixture was

stirred for 3 h at RT. Reaction progress was monitored by TLC. Upon completion of reaction, solvent was evaporated under reduced pressure, residue was partitioned between ethyl acetate and water. Organic layer was washed with brine, dried over anhydrous Na_2SO_4, filtered and concentrated under reduced pressure to afford crude compound-8 (3.2g) as a yellow solid.

[00189] Step 7: Synthesizing 5-([1,1'-biphenyl]-4-yl)-2-(methylthio)-1H-naphtho[1,2-d]imidazole (Compound 9)—To a stirred solution of Compound-8 (3.0 g, 8.522 mmol) in Acetone (100 mL), was added K_2CO_3 (1.41 g, 10.226 mmol) at 0°C, stirred for 10–15 min, was added Methyl iodide (0.55 mL, 8.522 mmol) and the resulting reaction mixture was allowed to stir for 3 h at RT. Reaction progress was monitored by TLC. Upon completion of reaction, solvent was evaporated under reduced pressure and the residue was partitioned between ethyl acetate and water. Organic layer was washed with brine, dried over anhydrous Na_2SO_4, filtered and concentrated under reduced pressure to afford crude. The crude was purified by Flash chromatography (230x400 mesh, 15–20% EA in PE) to afford 1.1g (35.3%) compound-9 as a yellow solid.

[00190] Step 8: Synthesizing 5-([1,1'-biphenyl]-4-yl)-2-(methylsulfonyl)-1H-naphtho[1,2-d]imidazole (Compound 10)—To a stirred solution of Compound-9 (1.0 g, 2.732 mmol) in dichloromethane (30 mL), was added 3-Chloro perbenzoic acid (1.41 g, 8.196 mmol) at 0°C and the resulting reaction mixture was stirred for 2 h at RT. Reaction progress was monitored by TLC. Upon completion of reaction, reaction mixture was diluted with dichloromethane, washed with 10% aqueous $NaHCO_3$ solution, 10% sodium thiosulphate solution followed by brine. Organic layer was dried over anhydrous Na_2SO_4, filtered and concentrated under reduced pressure to afford 3.5g of crude yellow solid compound 10.

[00191] Step 9: Synthesizing 5-([1,1'-biphenyl]-4-yl)-2-(methylsulfonyl)-1-((2-(trimethylsilyl)ethoxy)methyl)-1H-naphtho[1,2-d]imidazole (Compound 11)—To a stirred solution of Compound-10 (1.3 g, 3.266 mmol) in dichloromethane (50 mL), was added Triethylamine (0.68 mL, 4.899 mmol) followed by SEM chloride (0.65 g, 3.919 mmol), at 0°C and the resulting reaction mixture was stirred for 2 h at RT. Reaction progress was monitored by TLC. Upon completion of reaction, diluted with dichloromethane, washed with 10% aqueous $NaHCO_3$ solution, followed by brine. Organic layer was dried over

anhydrous Na_2SO_4, filtered and concentrated under reduced pressure. The crude product was purified by Flash chromatography (230 x 400 mesh, 10 - 15% EA in PE) to afford compound-11 (0.35g, 20%).

[00192] Step 10: Synthesizing 5-([1,1'-biphenyl]-4-yl)-2-(((3R,3aR,6R,6aS)-6-((tert-butyldimethylsilyl)oxy)hexahydrofuro[3,2-b]furan-3-yl)oxy)-1-((2-(trimethylsilyl)ethoxy)methyl)-1H-naphtho[1,2-d]imidazole (13)—To a stirred solution of Compound-12 (0.34 g, 1.325 mmol) in Tetrahydrofuran (5 mL), was added Potassium tert-butoxide (0.15 g, 1.325 mmol) at 0°C and the resulting reaction mixture was stirred for 1 h at 0°C. To this reaction mixture, was added the solution of Compound-11 in Tetrahydrofuran at 0°C and the resulting reaction mixture was allowed to stir at RT for 2 h. Reaction progress was monitored by TLC. Upon completion of reaction, solvent was evaporated under reduced pressure and the residue was partitioned between ethyl acetate and water. Organic layer was washed with brine, dried over anhydrous Na_2SO_4, filtered and concentrated under reduced pressure to afford crude compound-13 (0.6g) as a brown gummy solid.

[00193] Step 11: Synthesizing (3R,3aR,6R,6aR)-6-((5-([1,1'-biphenyl]-4-yl)-1H-naphtho[1,2-d]imidazol-2-yl)oxy)hexahydrofuro[3,2-b]furan-3-ol (Compound EV8017)—To a stirred solution of Compound-13 (0.6 g, 0.846 mmol) in Formic acid (12 mL), was added solution of $KHSO_4$ (0.11 g, 0.846 mmol) in water (1.0 mL) and the resulting reaction mixture was stirred for 16 h at 60°C. Reaction progress was monitored by TLC and LCMS. Upon completion of reaction, cooled to 0°C, basified with 2N aqueous NAOH solution by adjusting pH to 12–13, stirred the solution at 0°C for further 1 h, neutralized with 2N HCl and extracted with ethyl acetate. Combined organic layer was washed with brine, dried over anhydrous Na_2SO_4, filtered and concentrated under reduced pressure. Crude product was purified by Flash chromatography (C-18 column, 80% MeOH in Water) to afford compound-EV8017 as off white solid (0.14g, 35.7%).

[00194] *Results*: Step 1 produced Compound 2 with the following characteristics: LCMS: 98.8% (266.06 $M+H^+$ & 264.06 $M-H^+$); ^1H NMR (400 MHz, $CDCl_3$): δ 8.31 (d, J = 8.4 Hz, 1H), 7.88 (d, J = 8.0 Hz, 1H), 7.82 – 7.80 (m, 2H), 7.67 – 7.61 (m, 2H), 7.47 (br s, 1H), 2.36 (s, 3H).

[00195] Step 2 produced Compound 3 with the following characteristics: LCMS: 94.0% (309.12 M-H$^+$); ^{1}H NMR (400 MHz, $CDCl_3$): δ 8.72 (br s, 1H), 8.38 (s, 1H), 8.30 (d, J = 8.4 Hz, 1H), 8.06 (d, J = 8.4 Hz, 1H), 7.82 – 7.78 (m, 1H), 7.71 – 7.67 (m, 1H), 2.37 (s, 3H).

[00196] Step 3 produced Compound 5 with the following characteristics: LCMS: 91.85% (381.31 M-H$^+$).

[00197] Step 4 produced Compound 6 with the following characteristics: LCMS: 90.48% (341.29, M+H$^+$).

[00198] Step 5 produced Compound 7 with the following characteristics: LCMS: 52.0 % (311.3 [M+H]$^+$).

[00199] Step 6 produced Compound 8 with the following characteristics: LCMS: 52.0 % (353.2 [M+H]$^+$).

[00200] Step 7 produced Compound 9 with the following characteristics: LCMS: 77.6.0 % (367.29 [M+H]$^+$).

[00201] Step 8 produced Compound 10 with the following characteristics: LCMS: 76.9 % (397.29 [M-H]$^+$).

[00202] Step 9 produced Compound 11 with the following characteristics: LCMS: 88.0 % (529.40 [M+H]$^+$); ^{1}H NMR (400 MHz, $CDCl_3$): δ 8.75 (d, J = 7.6 Hz, 1H), 8.00 (s, 1H), 7.75 (d, J = 6.4 Hz, 2H), 7.71 (m, 3H), 7.67 (s, 1H), 7.60 (d, J = 8.4 Hz, 1H), 7.54 – 7.40 (m, 4H), 6.04 (s, 2H), 3.70 (t, J = 8.0 Hz, 2H), 0.93 (t, J = 8.0 Hz, 2H), -0.47(s, 9H).

[00203] Step 10 produced Compound 13 with the following characteristics: LCMS: 84.8 % (709.70 [M+H]$^+$).

[00204] Step 11 produced Compound EV8017 with the following characteristics: LCMS: 99.89 % (465.30 [M+H]$^+$); HPLC: 99.86%; m.p.; 158-162°C ^{1}H NMR (400 MHz, DMSO-d6): δ 13 - 12 (br s, 1H), 8.29 (br s, 1H), 7.87 (d, J = 8.4 Hz, 1H), 7.83 – 7.77 (m, 4H), 7.59 – 7.50 (m, 6H), 7.42 – 7.35 (m, 2H), 5.52 (d, J = 5.6 Hz, 1H), 4.98 (d, J = 6.8 Hz, 1H), 4.89 (t, J = 4.8 Hz, 1H), 4.41 (t, J = 4.8 Hz, 1H), 4.23 – 4.16 (m, 2H), 3.88 (q, J = 6.8 Hz, 1H), 3.82 (t, J = 6.8 Hz, 1H), 3.48 (t, J = 8.4 Hz, 1H).

[00205] *Conclusion*: Embodiments are capable of synthesizing novel AMPK agonists and derivates thereof, such as those illustrated in Figure 15B.

DOCTRINE OF EQUIVALENTS

[00206] While the above description contains many specific embodiments of the invention, these should not be construed as limitations on the scope of the invention, but rather as an example of one embodiment thereof. Accordingly, the scope of the invention should be determined not by the embodiments illustrated, but by the appended claims and their equivalents.

WHAT IS CLAIMED IS:

1. A method of treating a patient with mitochondrial dysfunction comprising:
identifying a mitochondrial dysfunction in an individual; and
providing an AMPK agonist to the individual.

2 The method of claim 1, wherein the mitochondrial dysfunction is a primary mitochondrial dysfunction.

3. The method of claim 2, wherein the primary mitochondrial dysfunction is selected from the group consisting of Autosomal Dominant Optic Atrophy (ADOA), Alpers-Huttenlocher syndrome (nDNA defect), Ataxia neuropathy syndrome, (nDNA defect), Barth syndrome/ Lethal Infantile Cardiomyopathy (LIC), Co-enzyme Q deficiency, Complex I, complex II, complex III, complex IV and complex V deficiencies (either single deficiencies or any combination of deficiency), Chronic progressive external ophthalmoplegia (CPEO), Diabetes mellitus and deafness, Kearns-Sayre syndrome (mtDNA defect), Leukoencephalopathy with Brainstem and Spinal Cord Involvement and Lactate Elevation (LBSL- leukodystrophy), Leigh syndrome (mtDNA and nDNA defects), Leber's hereditary optic neuropathy (LHON), Luft Disease, Mitochondrial myopathy, encephalopathy, lactic acidosis, and stroke syndrome (MELAS) (mtDNA defect), Mitochondrial Enoyl CoA Reductase Protein-Associated Neurodegeneration (MEPAN), Myoclonic epilepsy with ragged red fibers (MERRF), mitochondrial recessive ataxia syndrome (MIRAS), mtDNA deletion syndrome, mtDNA Depletion syndrome, mtDNA maintenance disorders, mtDNA/RNA translation defects, Mitochondrial tRNA synthetase deficiencies, Mitochondrial Myopathy, Mitochondrial neurogastrointestinal encephalopathy syndrome (MNGIE), Neurogenic muscle weakness, ataxia, and retinitis pigmentosa (NARP), Pearson syndrome, Pyruvate dehydrogenase complex deficiency (PDCD/PDH) , DNA polymerase gamma deficiency (POLG), Pyruvate carboxylase deficiency, and Thymidine kinase 2 deficiency (TK2).

4 The method of claim 1, wherein the mitochondrial dysfunction is a secondary mitochondrial dysfunction.

5. The method of claim 4, wherein the secondary mitochondrial dysfunction is selected from the group consisting of Amyotrophic Lateral Sclerosis (ALS), Alzheimer's disease (AD) and other dementias, Friedreich's ataxia (FA), Huntington's disease (HD), Motor neuron diseases (MND), N-glycanase deficiency (NGLY1), Organic acidemias, Parkinson's disease (PD) and PD-related disorders, Prion disease, Spinal muscular atrophy (SMA), Spinocerebellar ataxia (SCA), Becker muscular dystrophy , Congenital muscular dystrophies, Duchenne muscular dystrophy, Emery-Dreifuss muscular dystrophy, Facioscapulohumeral muscular dystrophy, Myotonic dystrophy, Oculopharyngeal muscular dystrophy, Charcot-Marie-Tooth disease, Congenital myopathies, Distal myopathies, Endocrine myopathies (hyperthyroid myopathy, hypothyroid myopathy), Giant axonal neuropathy, Hereditary spastic paraplegia , Inflammatory myopathies (dermatomyositis, inclusion-body myositis, polymyositis), Metabolic myopathies, Neuromuscular junction diseases:, Autism, Cancer, Diabetes, Metabolic syndrome, Chronic fatigue syndrome, an inflammatory disorder, arthritis, and aging.

6. The method of claim 1, wherein the AMPK agonist is a direct AMPK agonist.

7. The method of claim 6, wherein the direct AMPK agonist is selected from the group consisting of PT1, ETC-1002, Salicylate, C991, C13, D561-0775, MT 63-78, A-769662, ZLN024, C24, MK-8722, PF-739, and PF-06409577.

8. The method of claim 1, wherein the AMPK agonist is an AMP-dependent agonist.

9. The method of claim 8, wherein the AMP-dependent agonist is selected from the group consisting of metformin, resveratrol, and AICAR.

10. The method of claim 1, wherein the AMPK agonist is provided in a pharmaceutical formulation.

11. The method of claim 10, wherein the pharmaceutical formulation comprises the AMPK agonist and at least one of the group consisting of a binding agent, a lubricating agent, a buffer, and a coating.

12. The method of claim 1, wherein the providing step comprises orally administering the AMPK agonist to the individual.

13. The method of claim 1, wherein the providing step comprises administering the AMPK agonist daily for at least one week.

14. The method of claim 1 further comprising assessing the efficacy of the AMPK agonist in the individual.

15. The method of claim 1, wherein the providing step is accomplished by administrating the AMPK agonist by at least one of the group consisting of: oral administration, subcutaneous administration, intravenous administration, intraperitoneal administration, intranasal administration, dermal administration, and inhalation.

16. A method of treating mitochondrial disorders comprising:
identifying a disorder in an individual; and
modulating AMPK activity in the individual.

17. The method of claim 16, wherein the modulating step is accomplished by activating AMPK in the individual.

18. The method of claim 17, wherein the activating step is accomplished by phosphorylating AMPK or providing an agonist to AMPK.

19. The method of claim 16, wherein the modulating step is accomplished by inhibiting AMPK in the individual.

20. The method of claim 16, wherein the disorder is associated with mitochondrial dysfunction.

21. The method of claim 20, wherein the mitochondrial dysfunction is a primary mitochondrial dysfunction.

22. The method of claim 20, wherein the mitochondrial dysfunction is a secondary mitochondrial dysfunction.

23. An AMPK agonist comprising a molecule of formula:

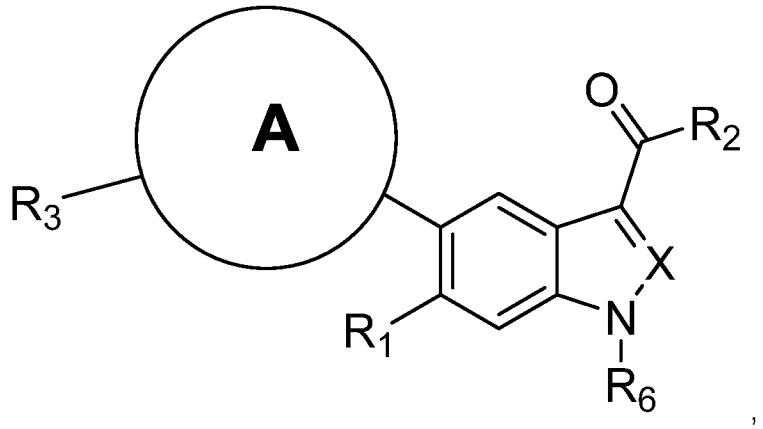

,

where:

A is selected from a 5-membered ring heterocyclic, either unsubstituted or substituted with one or more C_{1-6} alkyl or fluoro substituents

X is CR_5 or N;

R_1 is H, CF_3, or halo;

R_2 is OR_5, NHOH, $NHSO_2R_4$, OCH_2OCOR_4, or COR_2 is a C-linked tetrazole,

R_3 is C_{1-10} alkyl, C_{3-7} cycloalkyl, C_{4-12} alkylcycloalkyl, C_{4-10} cycloalkylalkyl, C_{3-7} heterocycloalkyl, C_{4-12} alkylheterocycloalkyl, C_{4-10} heterocycloalkylalkyl, aryl or heteroaryl either unsubstituted or substituted with one to three substituents selected from halo, OH and $OCOR_7$;

R_4 is C_{1-10} alkyl, C_{3-7} cycloalkyl, C_{4-12} alkylcycloalkyl, C_{4-10} cycloalkylalkyl either unsubstituted or substituted with one to three halogen substituents;

R_5 is R_4 or H;

R_6 is H, C_{1-6} alkyl, C_{3-6} cycloalkyl, or two R_6 groups, together with the nitrogen atom to which they are attached can form a four to seven membered heterocycloalkyl ring, all of which can be optionally substituted with 1 to 3 fluorine atoms; and

R_7 is C_{1-10} alkyl, C_{3-7} cycloalkyl, C_{4-12} alkylcycloalkyl unsubstituted or substituted with one to three substituents selected from fluoro, C_{1-10} alkyl, and NR_6, R_6.

24. The AMPK agonist of claim 23, wherein A is selected from the group consisting of:

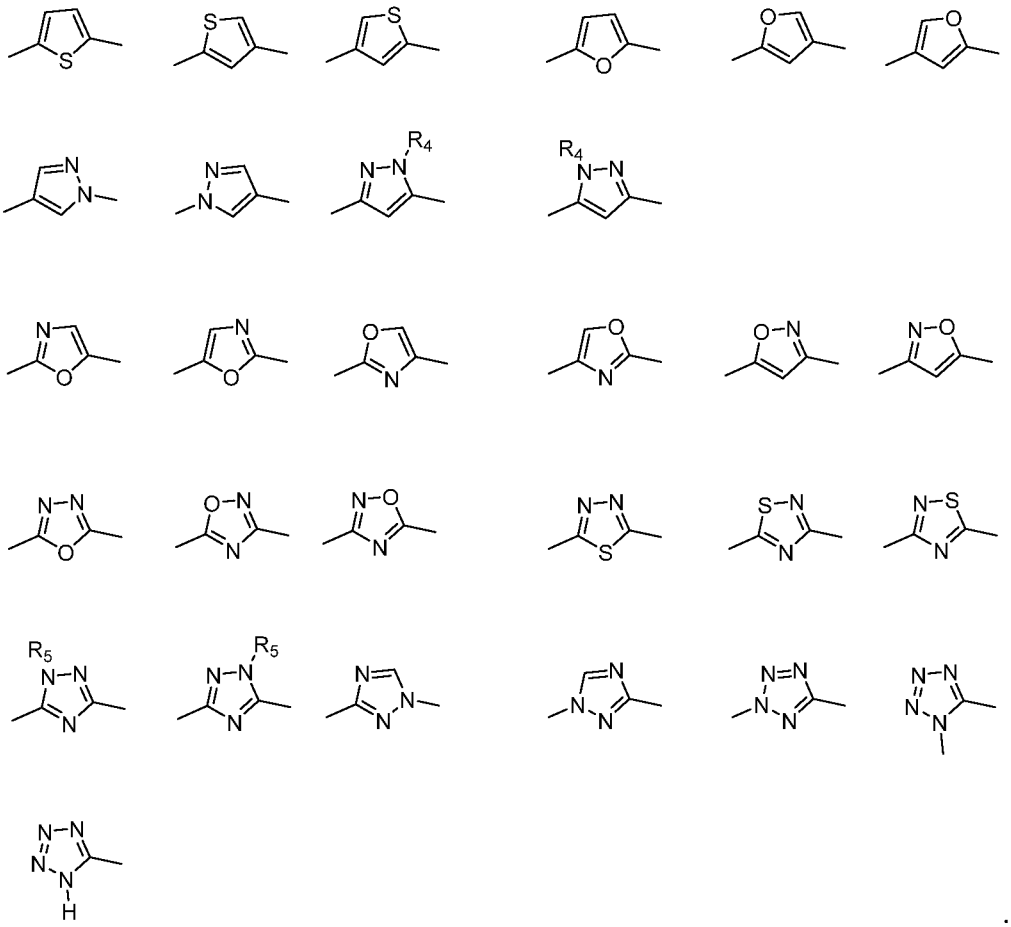

25. The AMPK agonist of claim 23, wherein A is selected from the group consisting of:

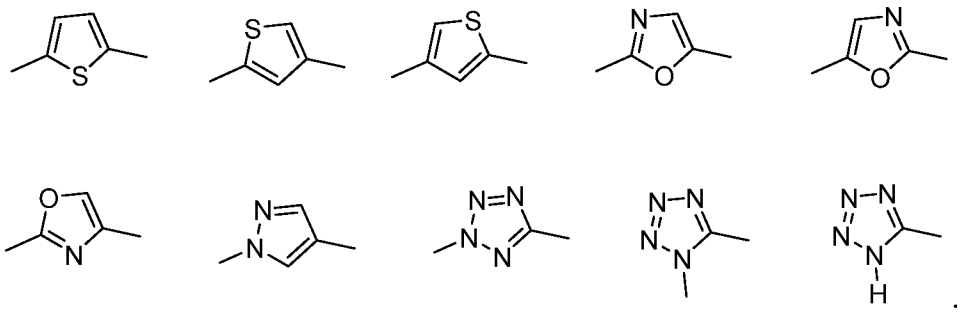

26. The AMPK agonist of claim 23, wherein A is selected from the group consisting of:

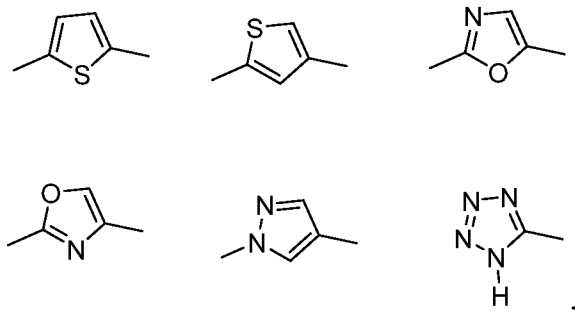

27. The AMPK agonist of claim 26, wherein X is CH, R_6 is H, R_1 is Cl, and R_2 is OH.

28. The AMPK agonist of claim 23, wherein the molecule has a formula as illustrated in one of Figures 13A-13Z and Figures 14A-14O.

29. The AMPK agonist of Claim 23, wherein the molecule has the formula:

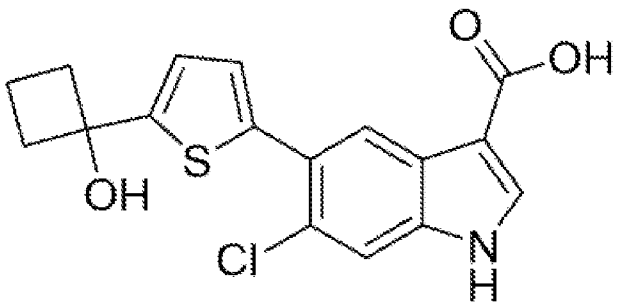

30. An AMPK agonist comprising a molecule of formula:

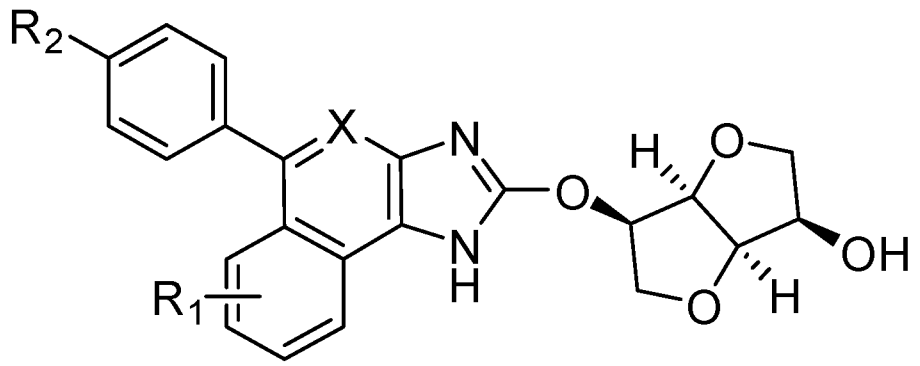

,

where:

X is CH or N;

R_1 is small alkyl (C1-C4) or halogen (e.g., Cl, Br, or F);

R_2 is phenyl, alkyl C1-C10, cycloalkyl (C3-C10), hydroxyalkyl (C1-C6), heteroaromatic (e.g., pyridyl, pyrazolyl, pyrolyl, pyrimidyl, thiophenyl, furanyl, or triazole), or heterocyclic C4-C6;

where phenyl is optionally substituted with halogens (e.g., Cl, Br, or F),

where an alkyl is linear or branched and optionally substituted with OH, OMe, OEt,

where cycloalkyl is optionally substituted with one or more OH,

where hydroxy alkyl is linear or branched

where heteroaromatic is optionally substituted with small alkyls (C1-C6) or hydroxyalkyls (C1-C6), where alkyls and hydroxyalkyls are linear or branched,

where heteroatom in hetrocyclic is optionally O, S, or NR_4, where R_4 is a linear or branched C1-C6 alkyl or hydroxyalkyl; and

R_4 is a linear or branched C1-C6 alkyl or hydroxyalkyl.

31. The AMPK agonist of claim 30, wherein the molecule has the formula of:

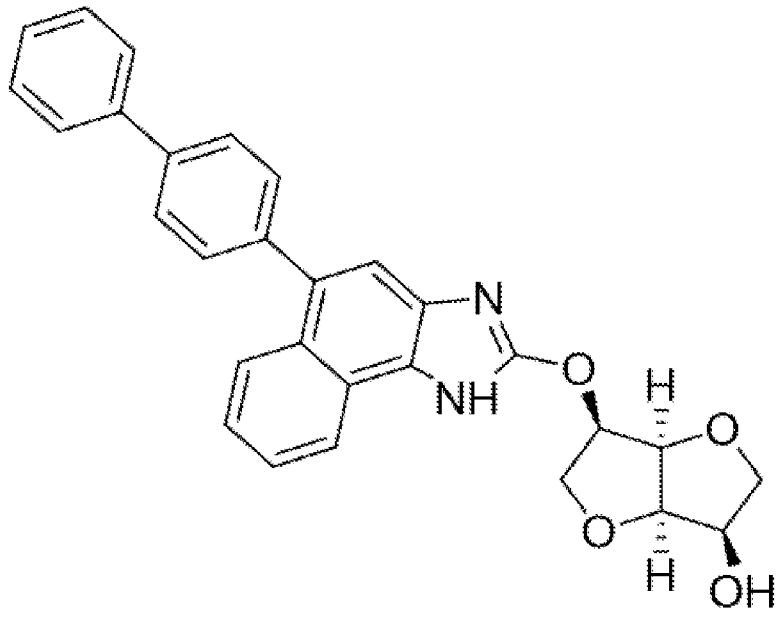

32. An AMPK agonist comprising a molecule of formula :

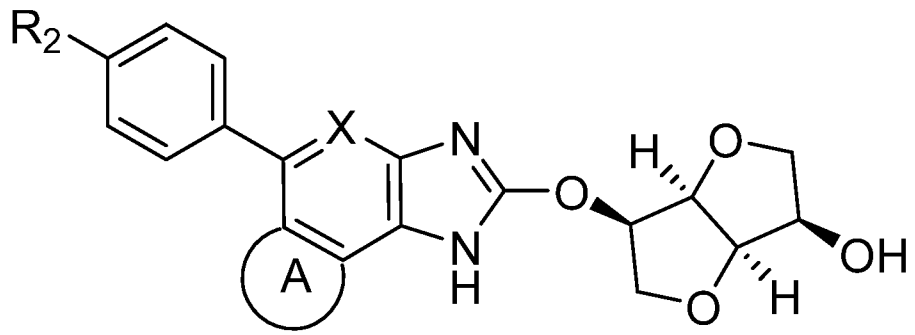

where:

A is a fused ring (e.g., C3-C10 cycloalkyl);

X is CH or N;

Y is O, S, NH, NR_3;

R_1 is small alkyl (C1-C4) or halogen (e.g., Cl, Br, or F);

R_2 is phenyl, alkyl C1-C10, cycloalkyl (C3-C10), hydroxyalkyl (C1-C6), heteroaromatic (e.g., pyridyl, pyrazolyl, pyrolyl, pyrimidyl, thiophenyl, furanyl, or triazole), or heterocyclic C4-C6;

where phenyl is optionally substituted with halogens (e.g., Cl, Br, or F),

where an alkyl is linear or branched and optionally substituted with OH, OMe, OEt,

where cycloalkyl is optionally substituted with one or more OH,

where hydroxy alkyl is linear or branched

where heteroaromatic is optionally substituted with small alkyls (C1-C6) or hydroxyalkyls (C1-C6), where alkyls and hydroxyalkyls are linear or branched,

where heteroatom in hetrocyclic is optionally O, S, or NR_4;

R_3 is a C1-C6 alkyl (linear or branched); and

R_4 is a linear or branched C1-C6 alkyl or hydroxyalkyl.

33. The AMPK agonist of claim 32, wherein A is selected from a C6 phenyl ring or one of the following:

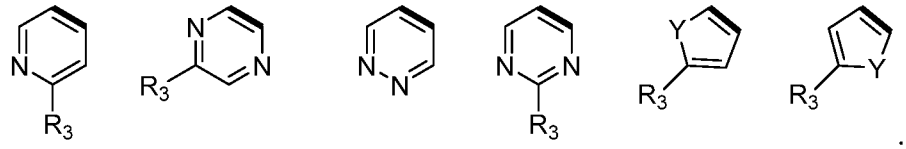

34. The AMPK agonist of claim 32, wherein the molecule has the formula of:

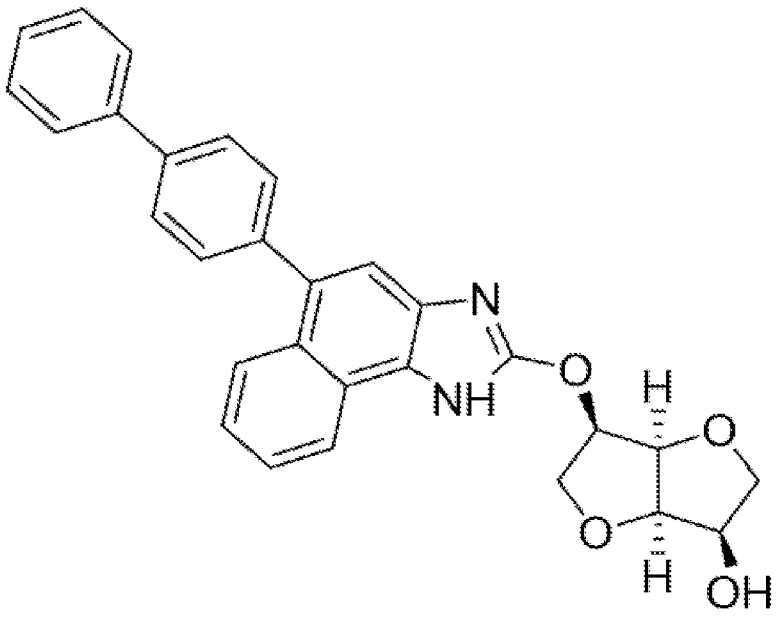

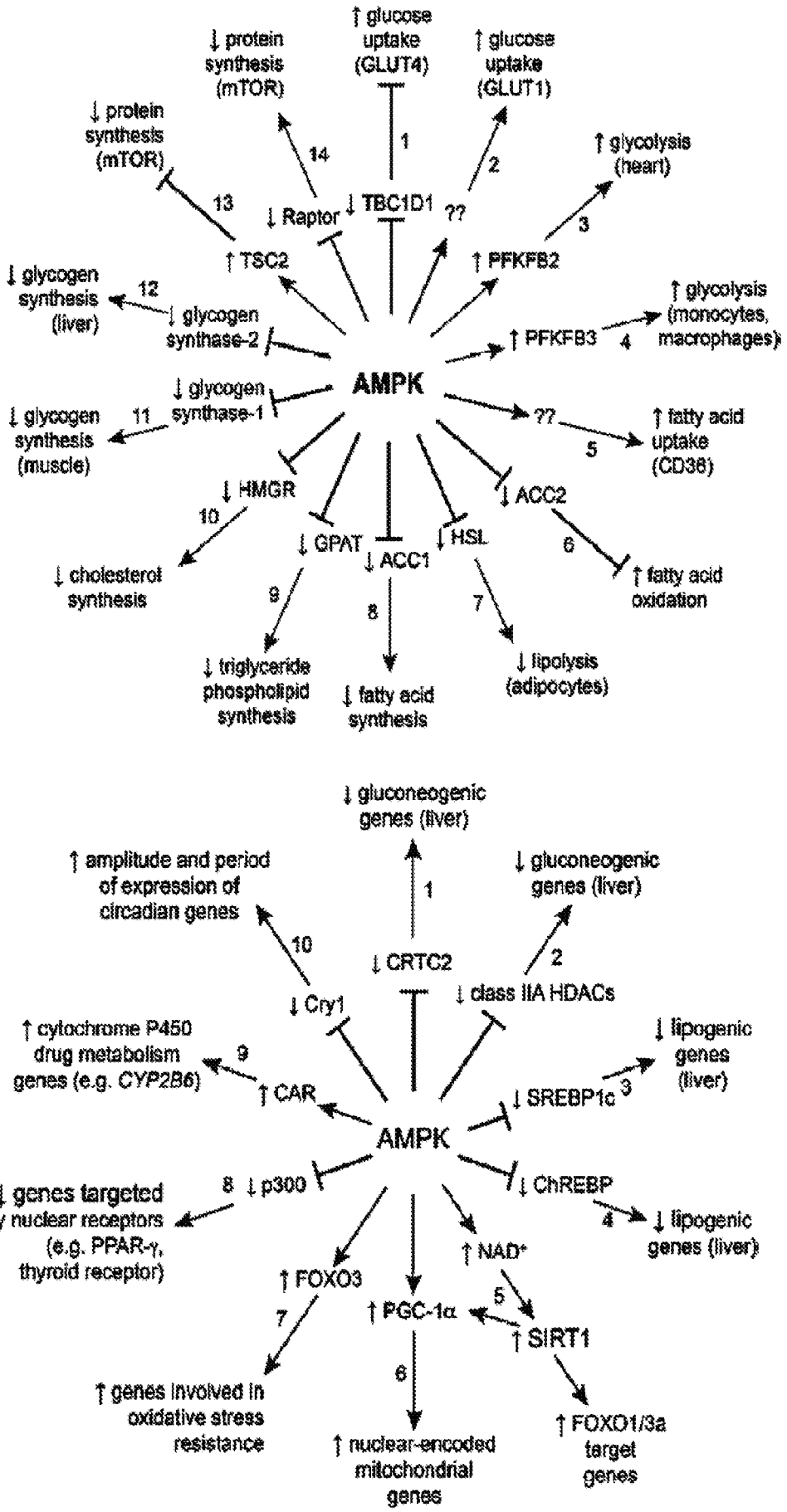
↑ glucose uptake (GLUT4)
↓ protein synthesis (mTOR)
↑ glucose uptake (GLUT1)
↓ protein synthesis (mTOR)
↑ glycolysis (heart)
↓ Raptor
↓ TBC1D1
??
↑ TSC2
↑ PFKFB2
↓ glycogen synthesis (liver)
↓ glycogen synthase-2
↑ glycolysis (monocytes, macrophages)
↑ PFKFB3
AMPK
↓ glycogen synthase-1
↓ glycogen synthesis (muscle)
??
↑ fatty acid uptake (CD36)
↓ HMGR
↓ ACC2
↓ GPAT
↓ ACC1
↓ HSL
↓ cholesterol synthesis
↑ fatty acid oxidation
↓ triglyceride phospholipid synthesis
↓ fatty acid synthesis
↓ lipolysis (adipocytes)
↓ gluconeogenic genes (liver)
↑ amplitude and period of expression of circadian genes
↓ gluconeogenic genes (liver)
↓ CRTC2
↓ class IIA HDACs
↓ Cry1
↑ cytochrome P450 drug metabolism genes (e.g. CYP2B6)
↓ lipogenic genes (liver)
↑ CAR
↓ SREBP1c
AMPK
↓ genes targeted by nuclear receptors (e.g. PPAR-γ, thyroid receptor)
↓ p300
↓ ChREBP
↓ lipogenic genes (liver)
↑ NAD+
↑ FOXO3
↑ PGC-1α
↑ SIRT1
↑ genes involved in oxidative stress resistance
↑ nuclear-encoded mitochondrial genes
↑ FOXO1/3a target genes

FIG. 1A

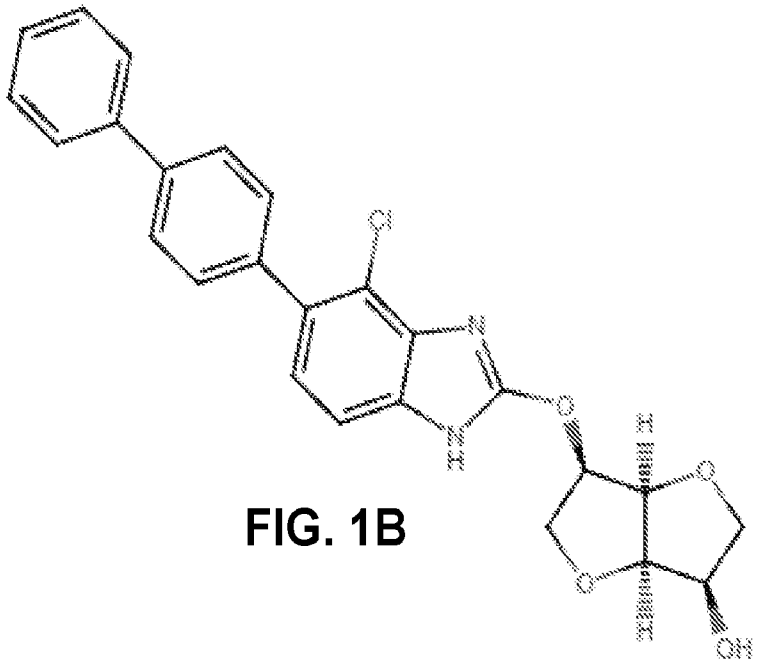

FIG. 1B

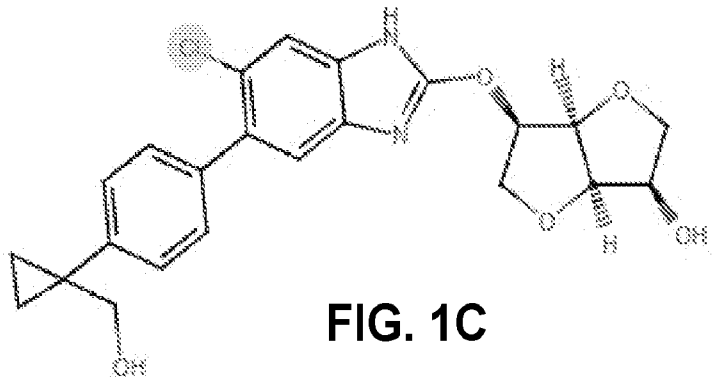

FIG. 1C

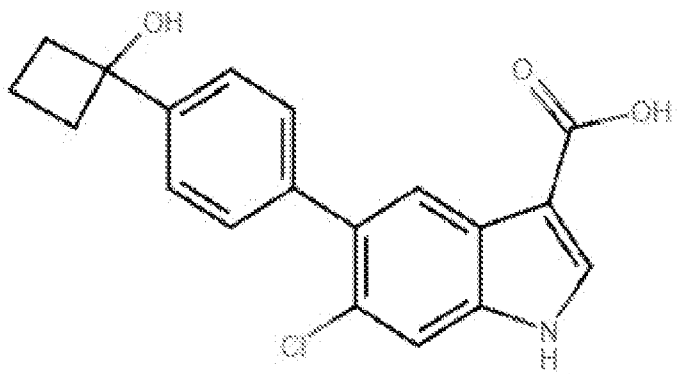

FIG. 1D

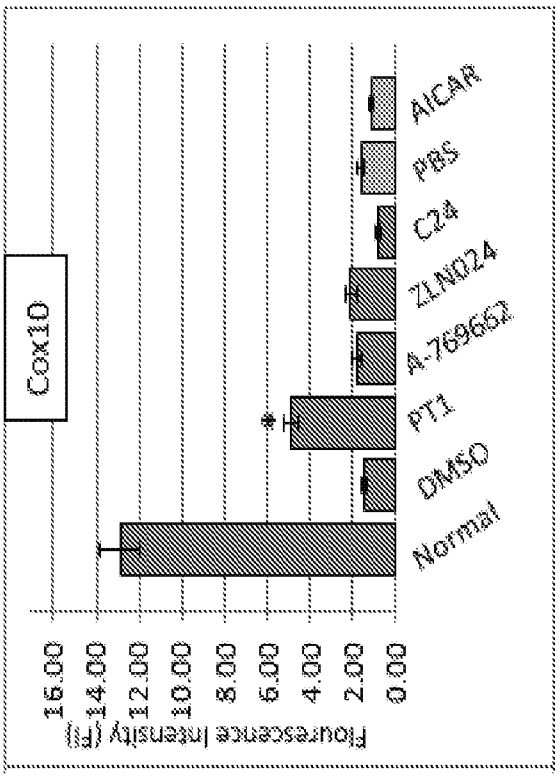

FIG. 2B

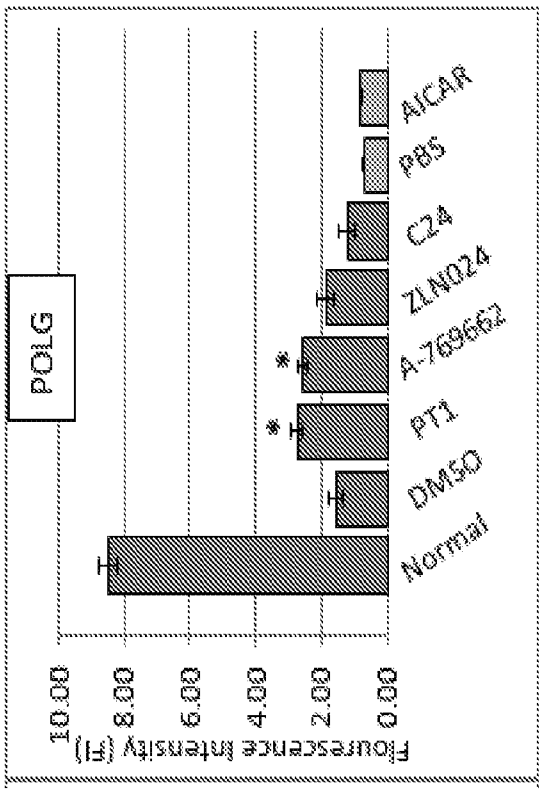

FIG. 2D

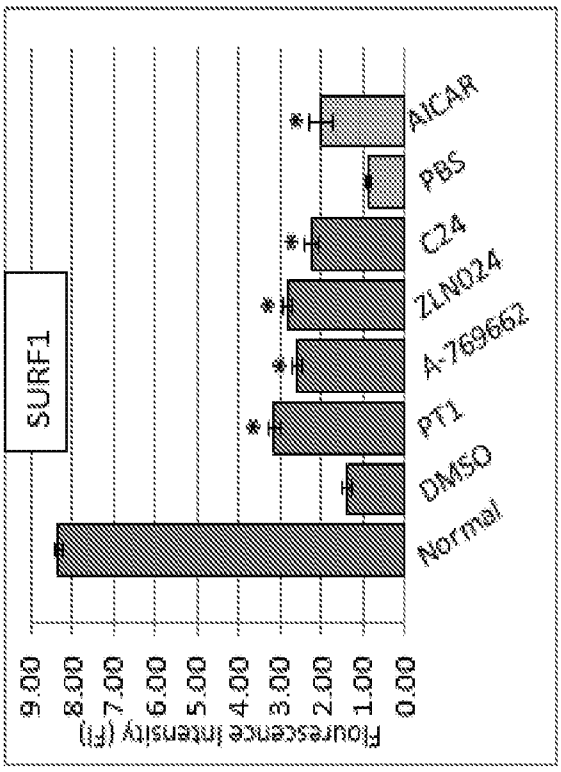

FIG. 2A

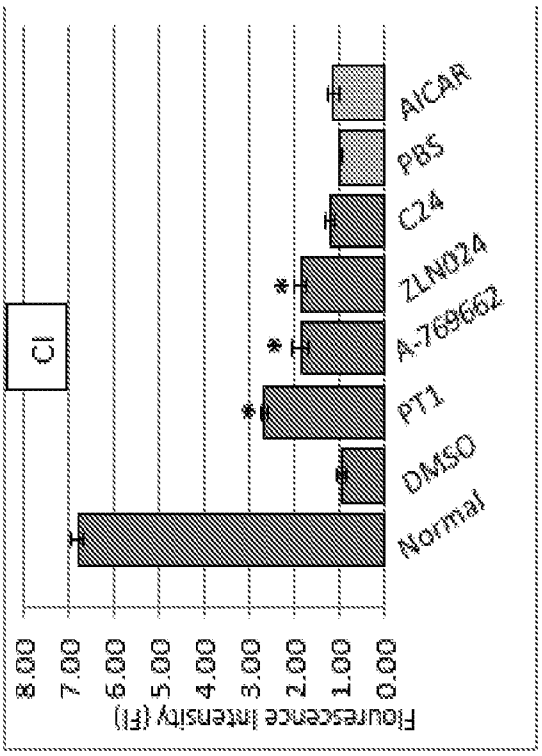

FIG. 2C

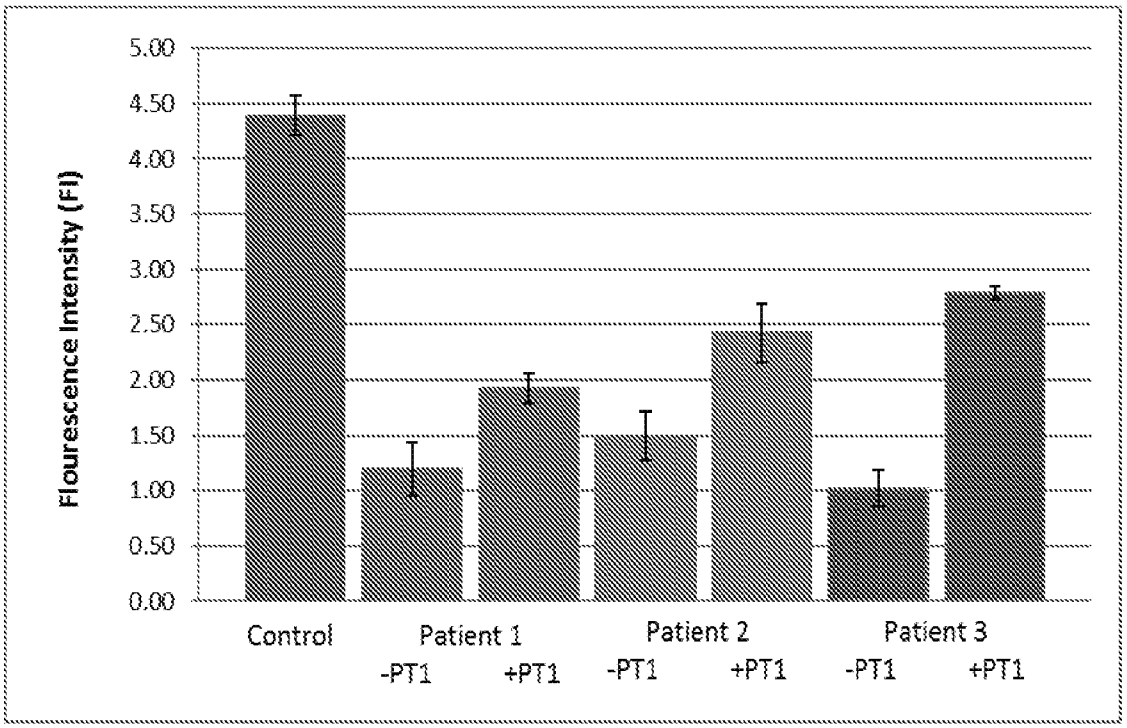
Flourescence Intensity (FI)
5.00
4.50
4.00
3.50
3.00
2.50
2.00
1.50
1.00
0.50
0.00
Control
Patient 1
-PT1
+PT1
Patient 2
-PT1
+PT1
Patient 3
-PT1
+PT1

FIG. 2E

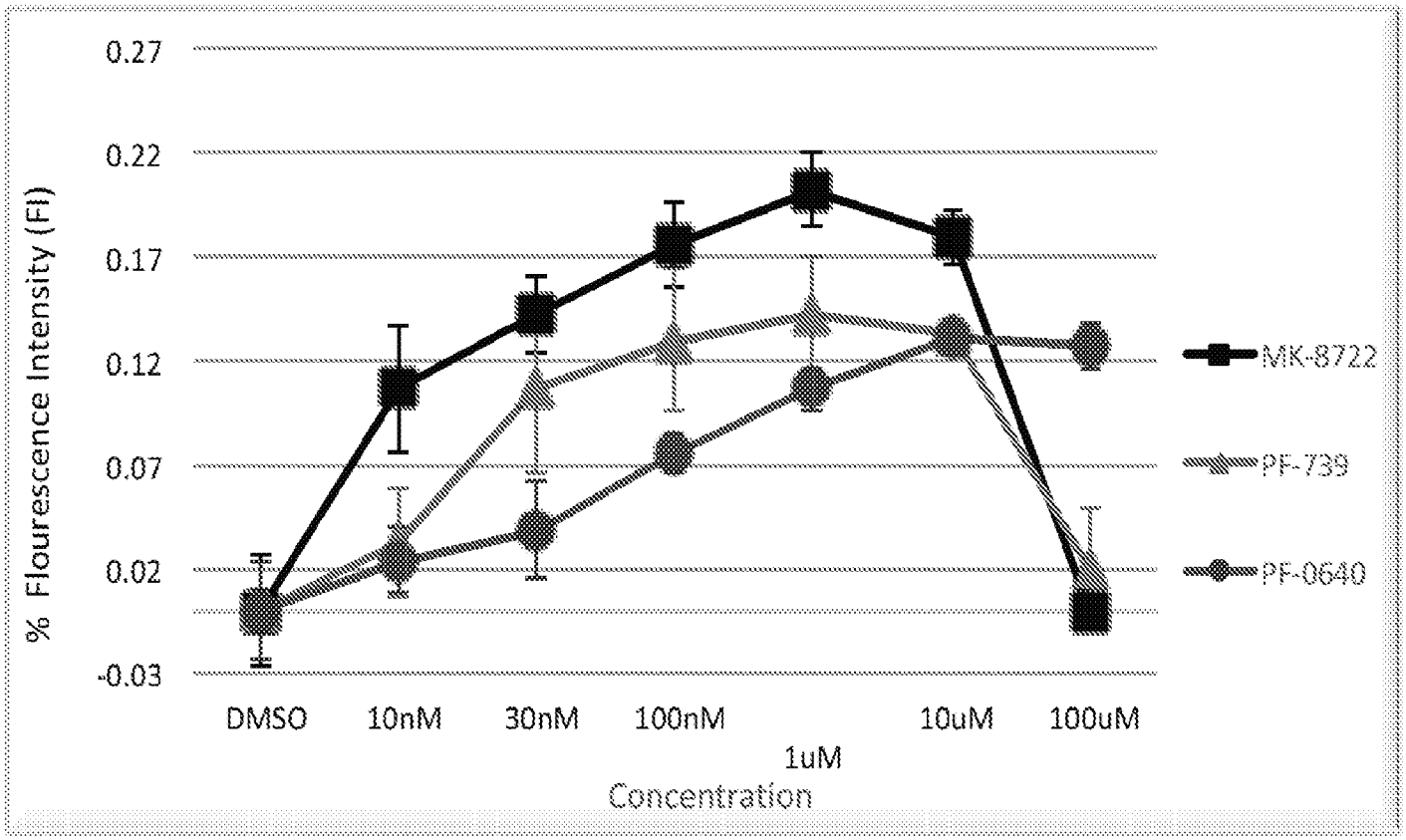
% Flourescence Intensity (FI)
0.27
0.22
0.17
0.12
0.07
0.02
-0.03
DMSO
10nM
30nM
100nM
1uM
10uM
100uM
Concentration
MK-8722
PF-739
PF-0640

FIG. 2F

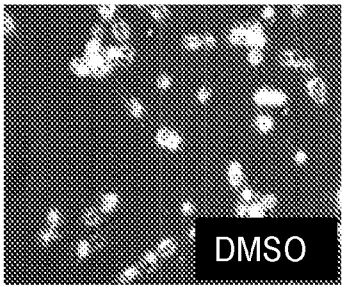

Fig. 3A

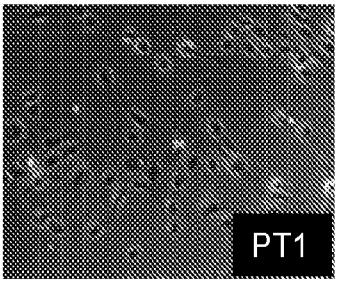

Fig. 3B

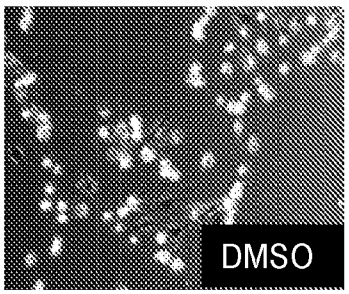

Fig. 3C

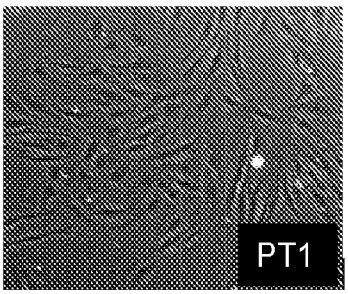

FIG. 3D

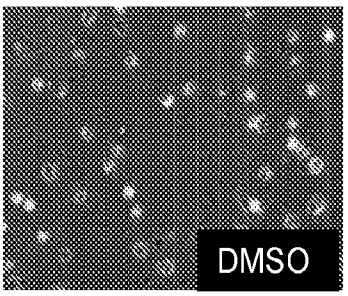

Fig. 3E

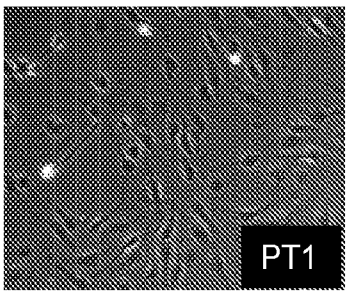

Fig. 3F

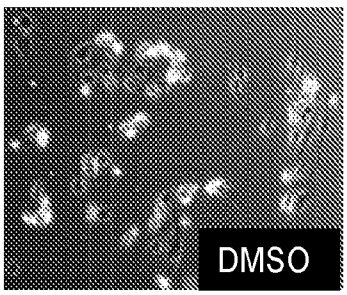

Fig. 3G

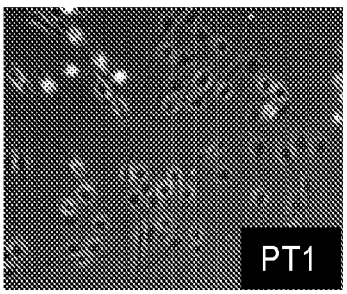

FIG. 3H

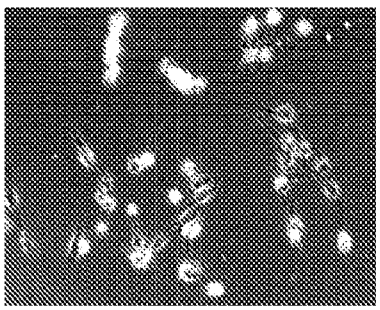

Fig. 3I

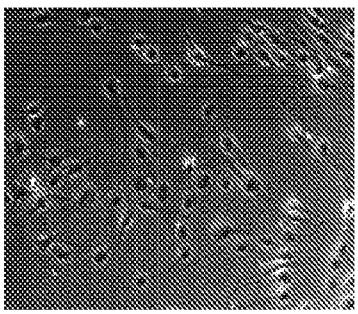

Fig. 3J

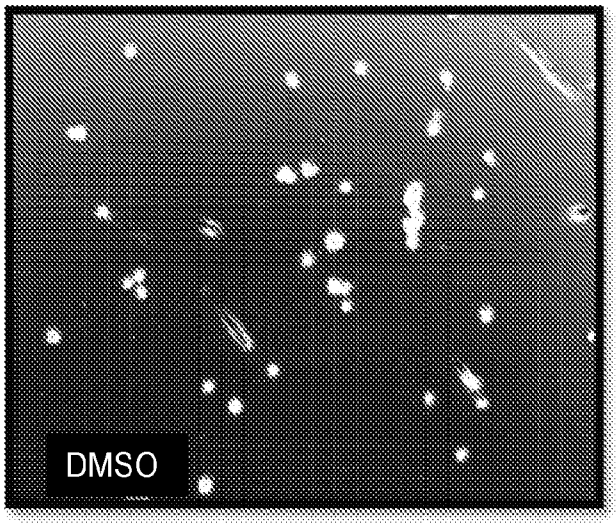

Fig. 3K

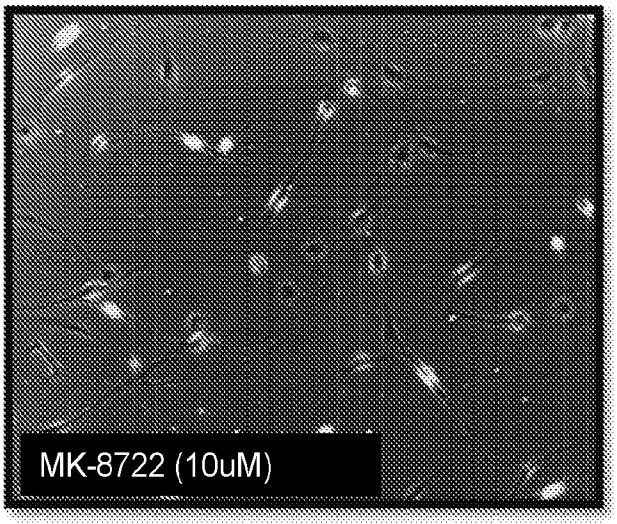

Fig. 3L

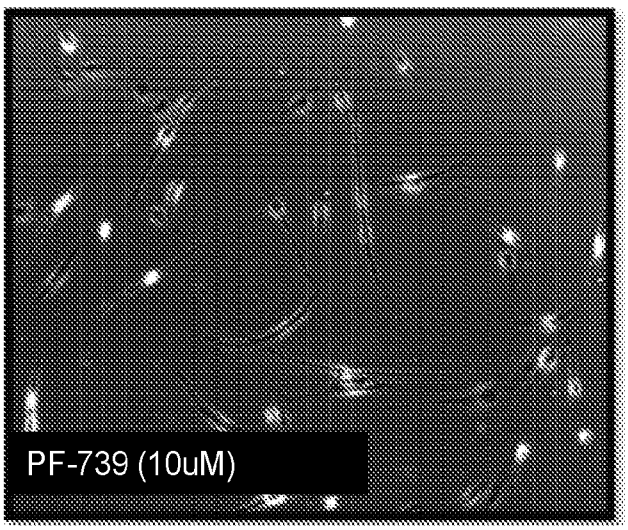

Fig. 3M

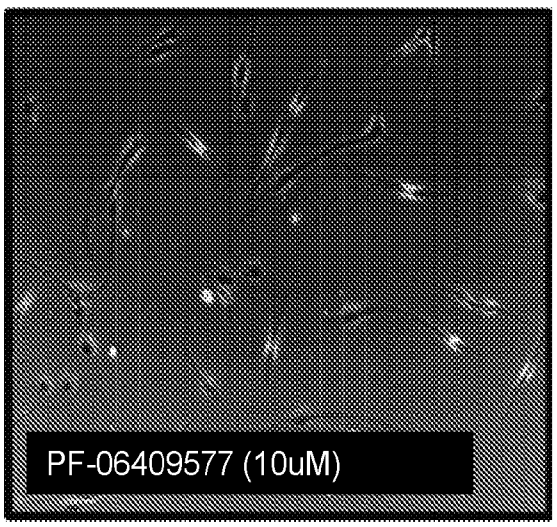

FIG. 3N

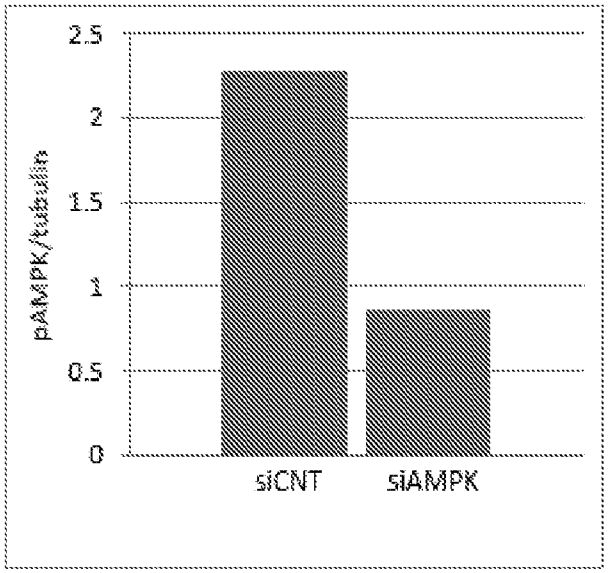

Fig. 4A

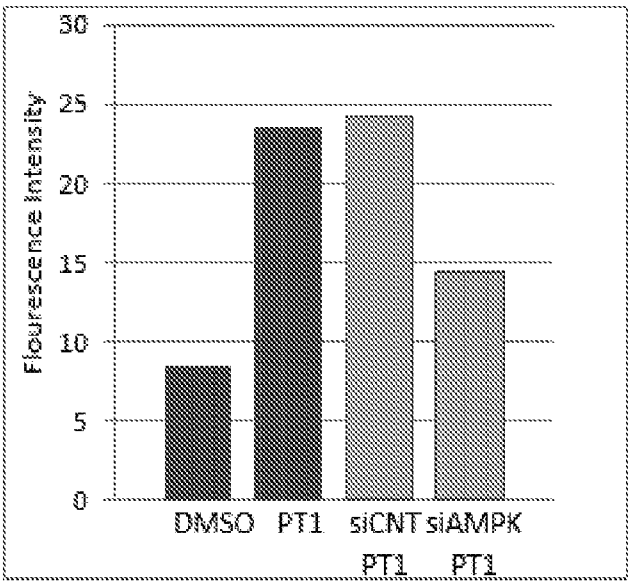

Fig. 4B

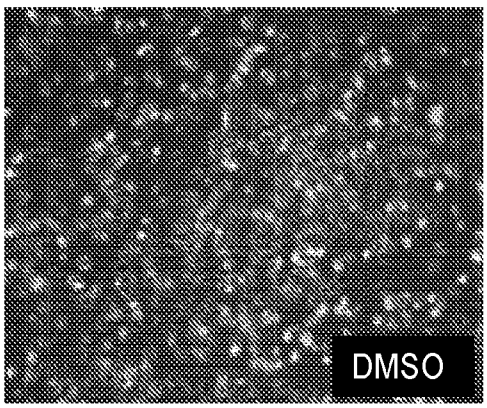

Fig. 4C

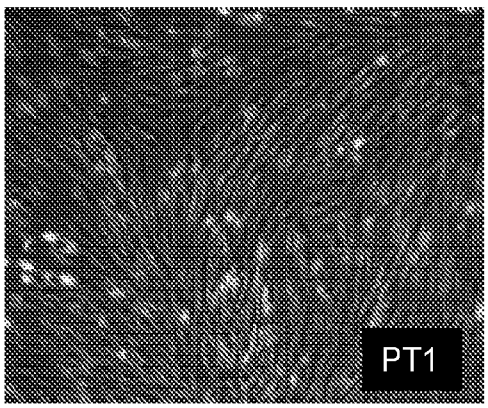

Fig. 4D

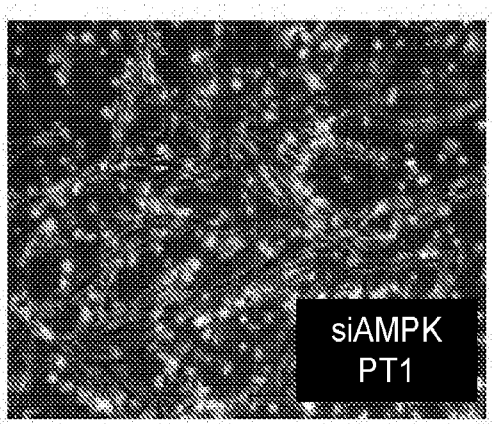

Fig. 4E

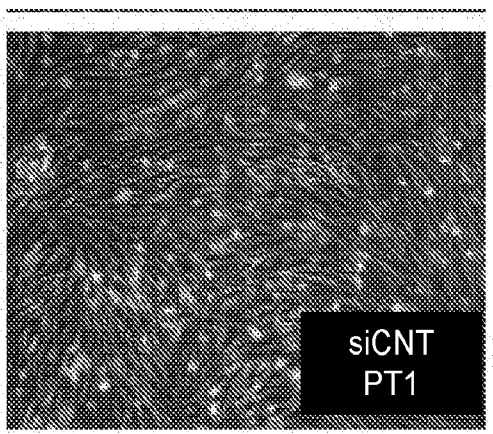

Fig. 4F

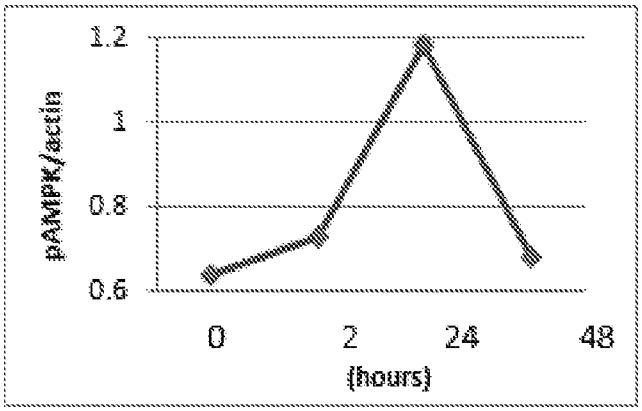

Fig. 5A

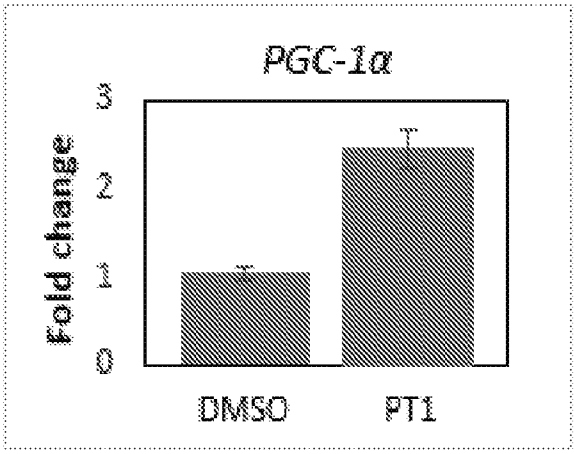

Fig. 5B

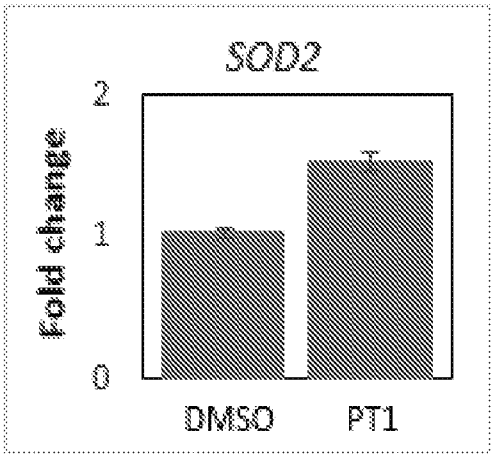

Fig. 5C

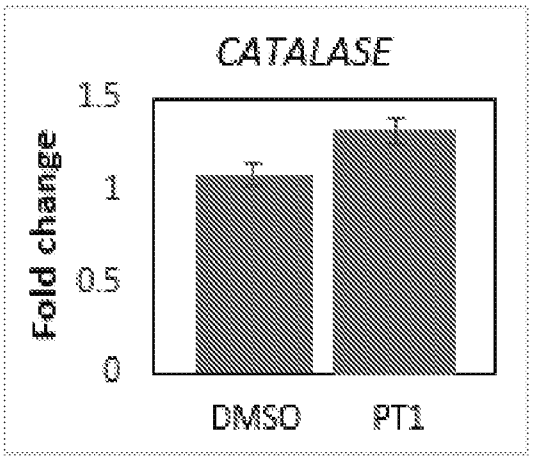

Fig. 5D

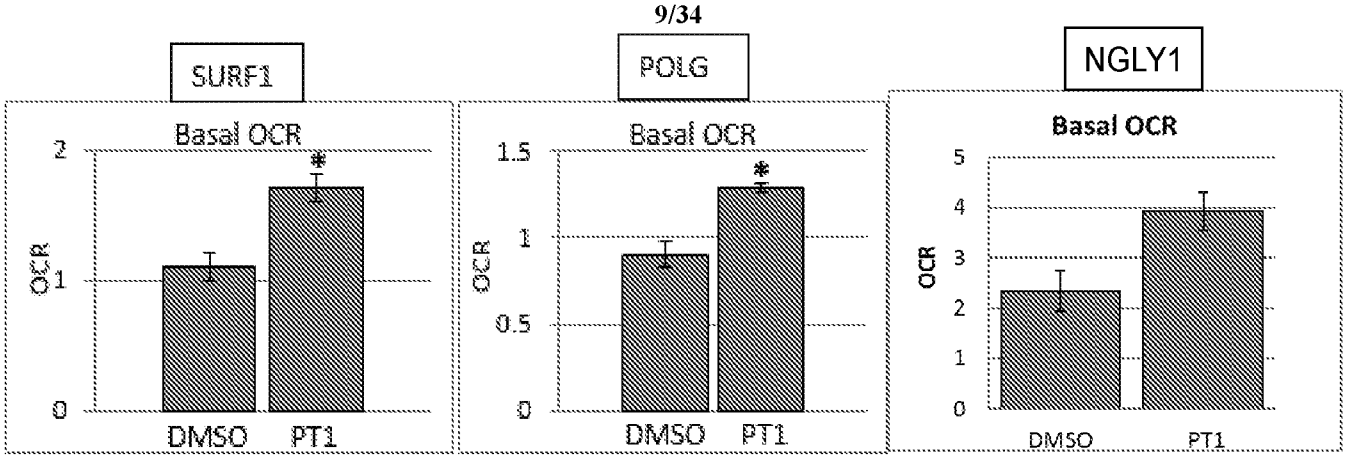

Fig. 6A Fig. 6B Fig. 6C

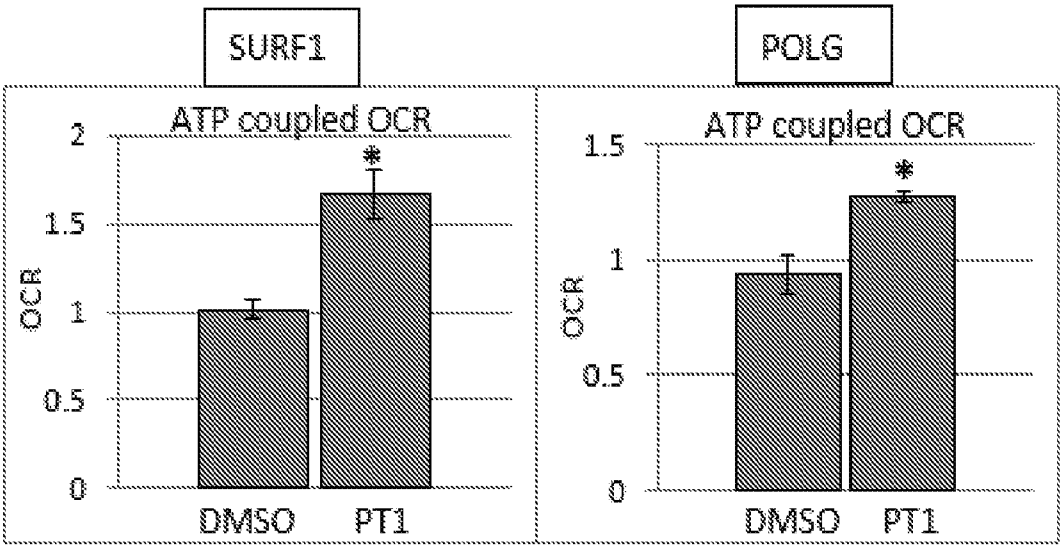

FIG. 6D Fig. 6E

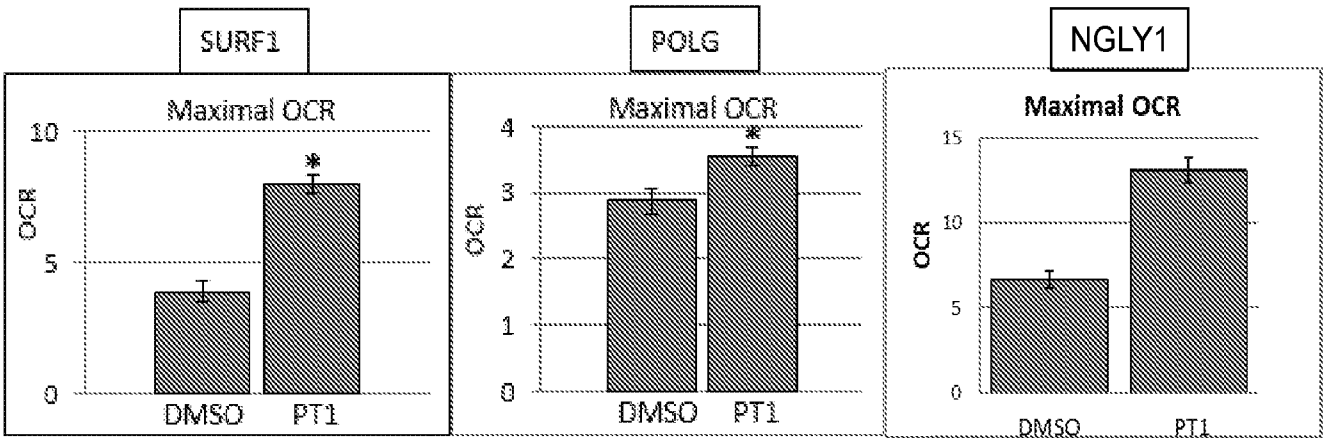

Fig. 6F Fig. 6G FIG. 6H

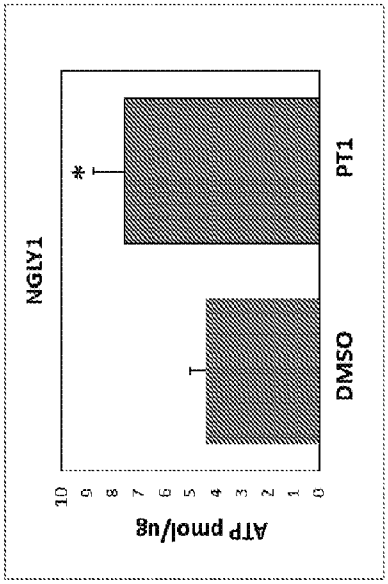

Fig. 7C

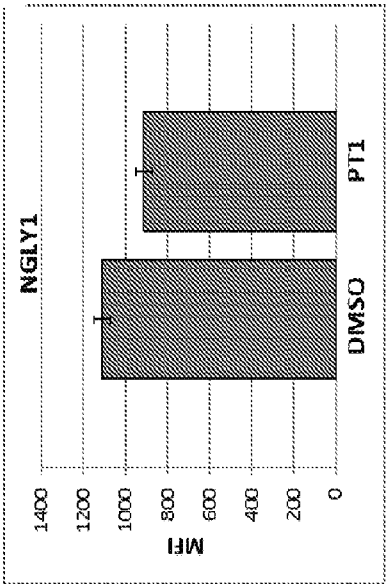

Fig. 7F

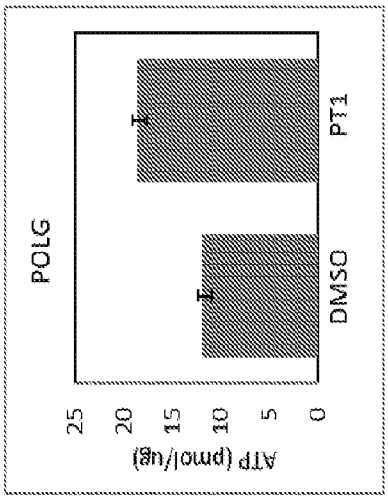

Fig. 7B

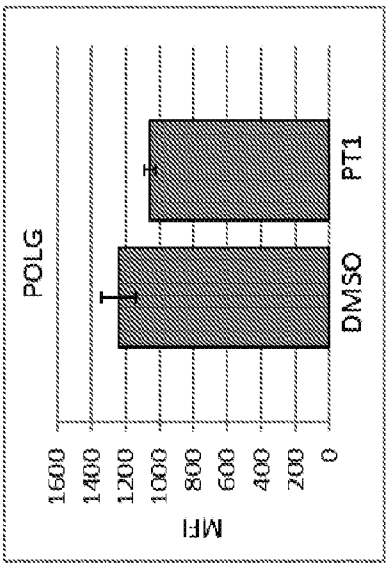

Fig. 7E

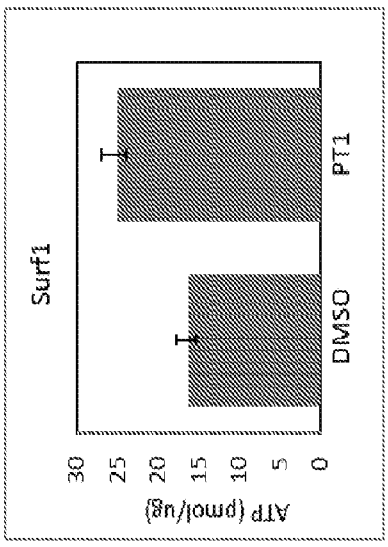

Fig. 7A

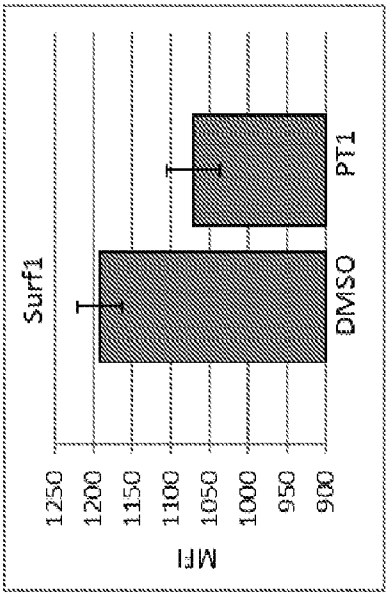

Fig. 7D

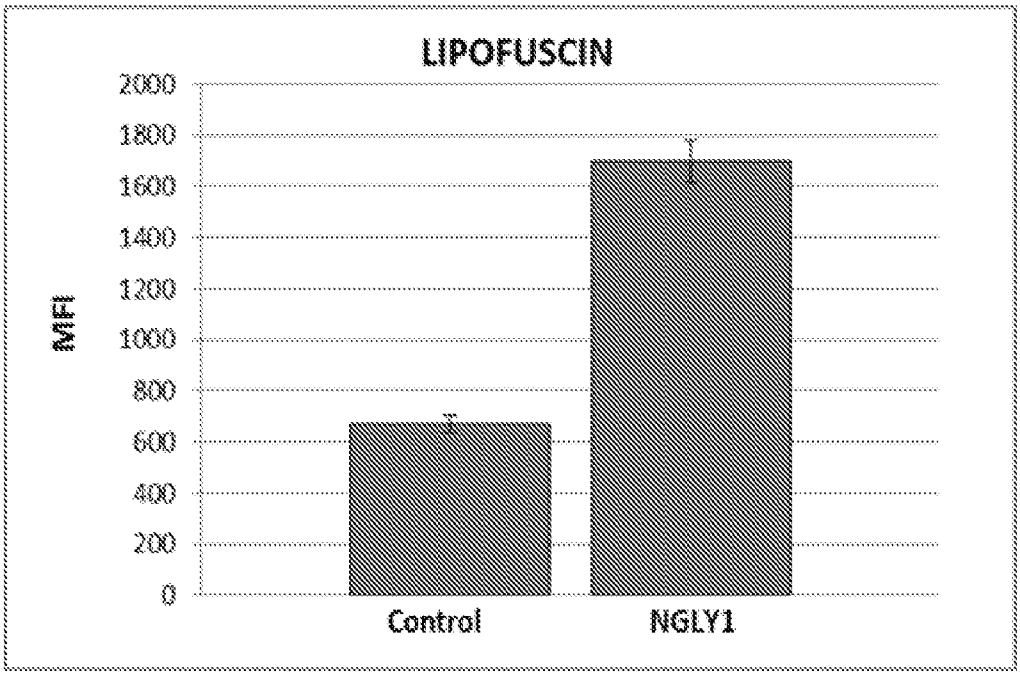
LIPOFUSCIN
MFI
2000
1800
1600
1400
1200
1000
800
600
400
200
0
Control
NGLY1

Fig. 8A

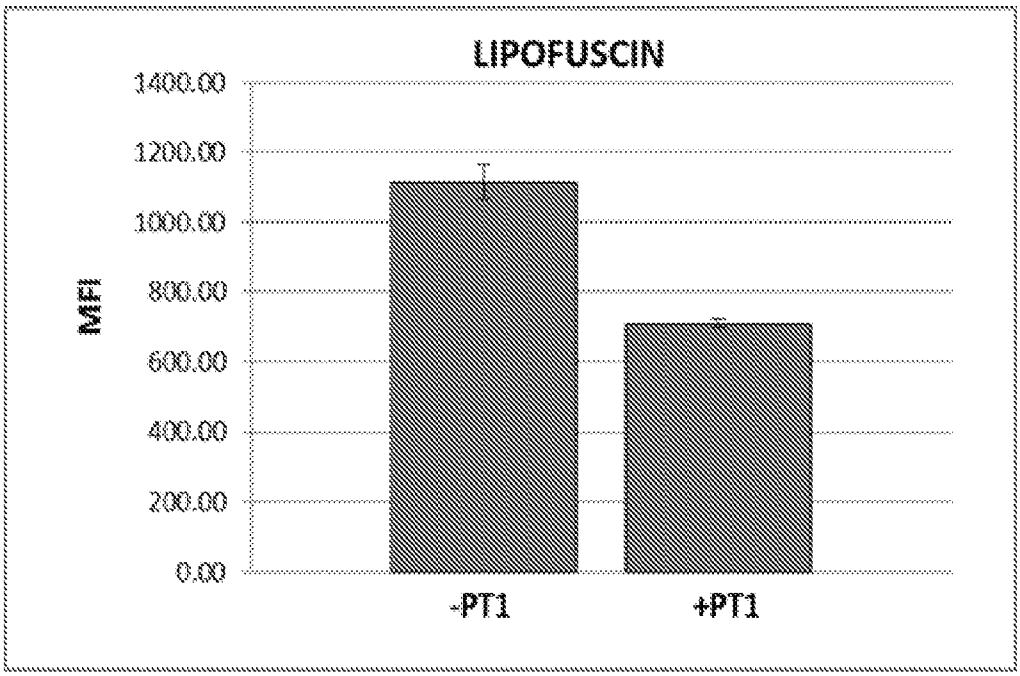
LIPOFUSCIN
MFI
1400.00
1200.00
1000.00
800.00
600.00
400.00
200.00
0.00
-PT1
+PT1

Fig. 8B

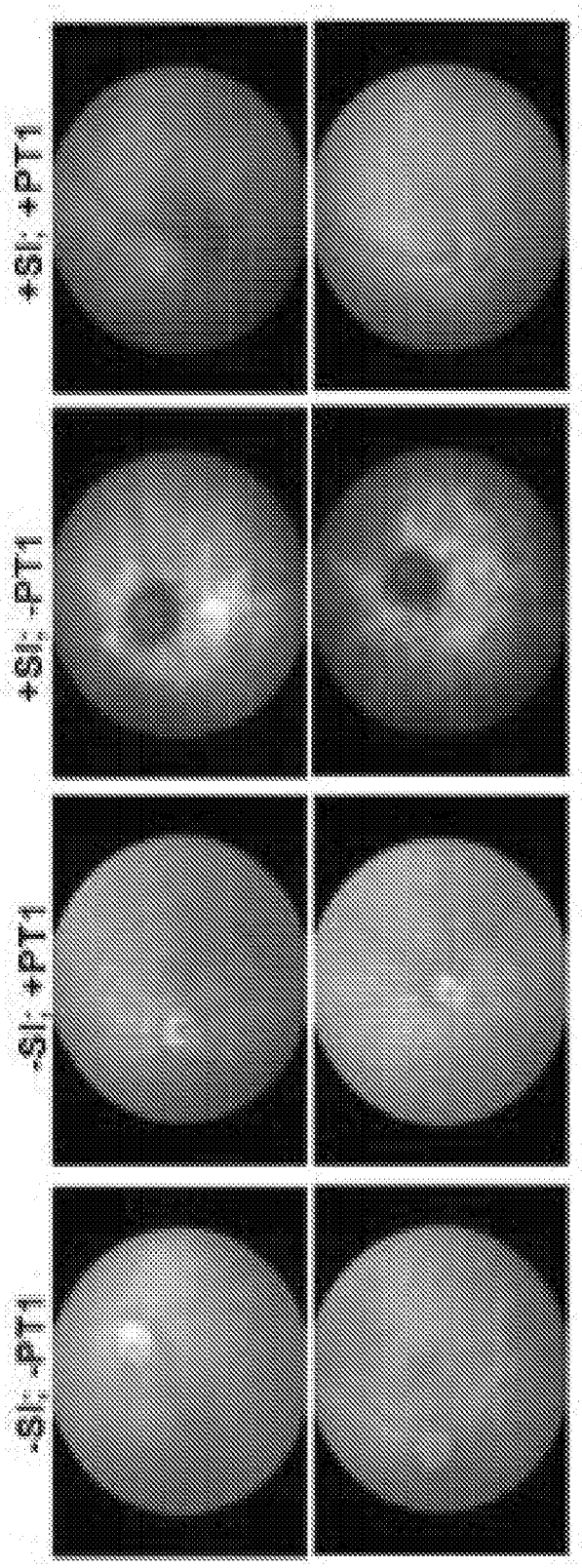

Fig. 9A

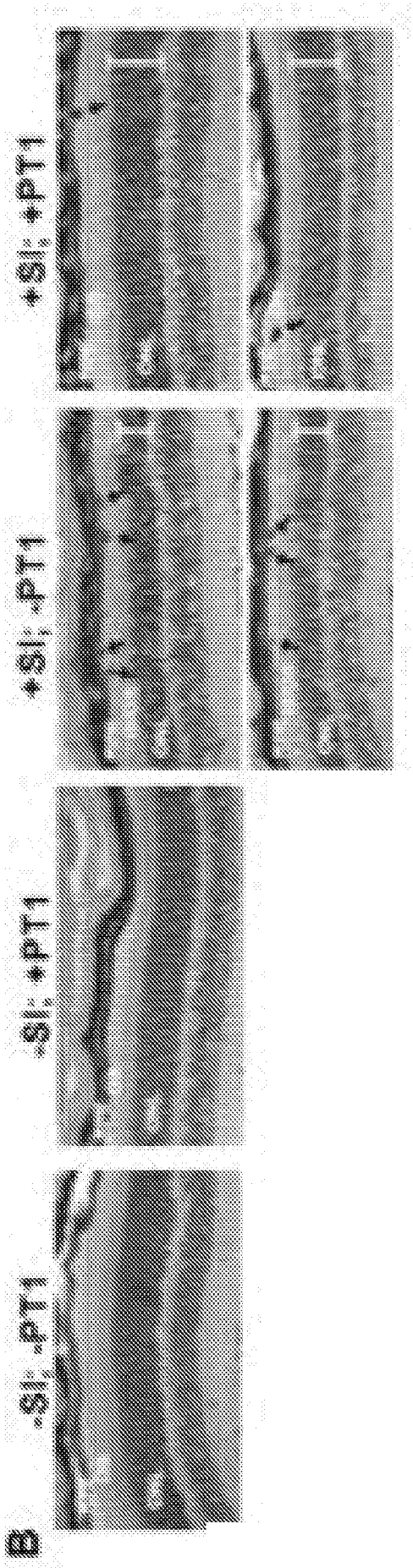
B
-Sl; -PT1
-Sl; +PT1
+Sl; -PT1
+Sl; +PT1

Fig. 9B

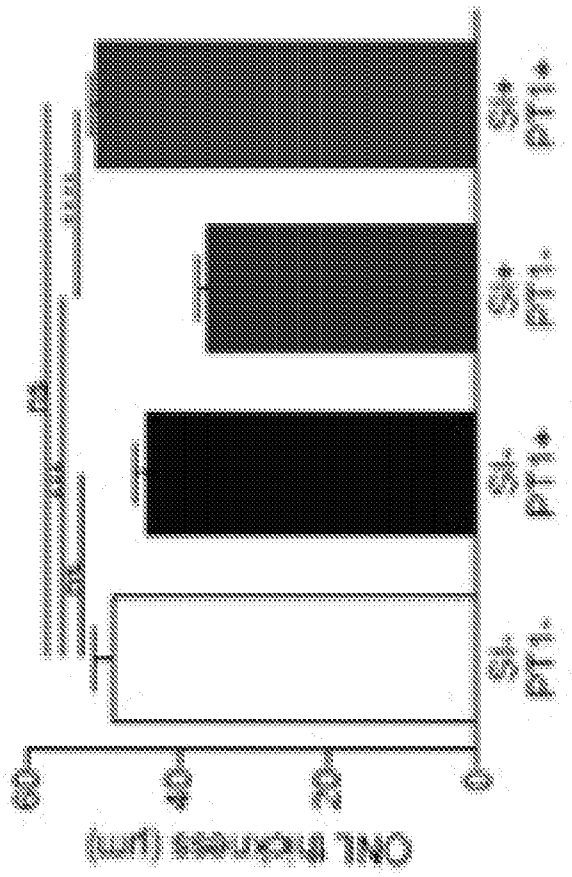
ONL thickness (μm)
60
40
20
0
Sl- PT1-
Sl- PT1+
Sl+ PT1-
Sl+ PT1+

Fig. 9C

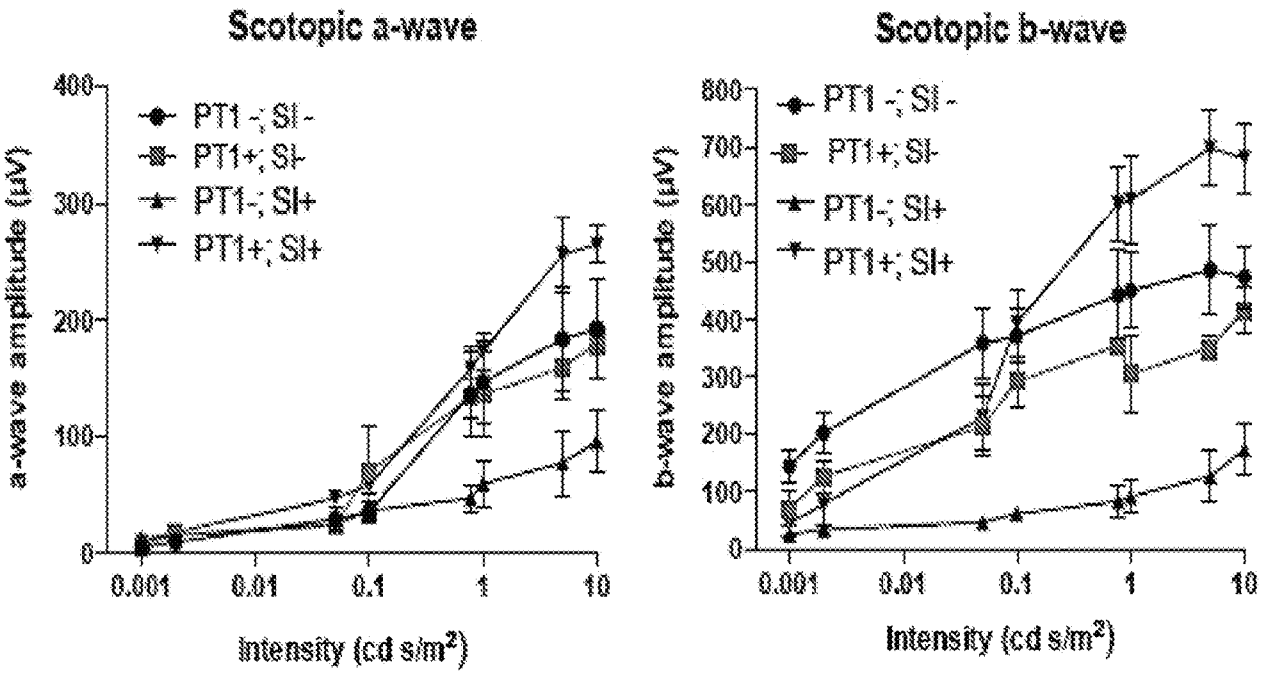

Light Intensity (cd s/m^2)	PT1-; SI- *vs* PT1+; SI-	PT1-; SI- *vs* PT1-; SI+	PT1-; SI- *vs* PT1+; SI+	PT1-; SI+ *vs* PT1+; SI+
Scotopic a-wave amplitude (µV)				
0.001	n.s	n.s	n.s	n.s
0.002	n.s	n.s	n.s	n.s
0.05	n.s	n.s	n.s	n.s
0.1	n.s	n.s	n.s	n.s
0.78	n.s	*	n.s	****
1	n.s	*	n.s	****
5	n.s	**	n.s	****
10	n.s	**	n.s	****
Scotopic b-wave amplitude (µV)				
0.001	n.s	n.s	n.s	n.s
0.002	n.s	n.s	n.s	n.s
0.05	n.s	**	n.s	n.s
0.1	n.s	**	n.s	****
0.78	n.s	***	n.s	****
1	n.s	***	n.s	****
5	n.s	***	n.s	****
10	n.s	*	n.s	****

Fig. 9D

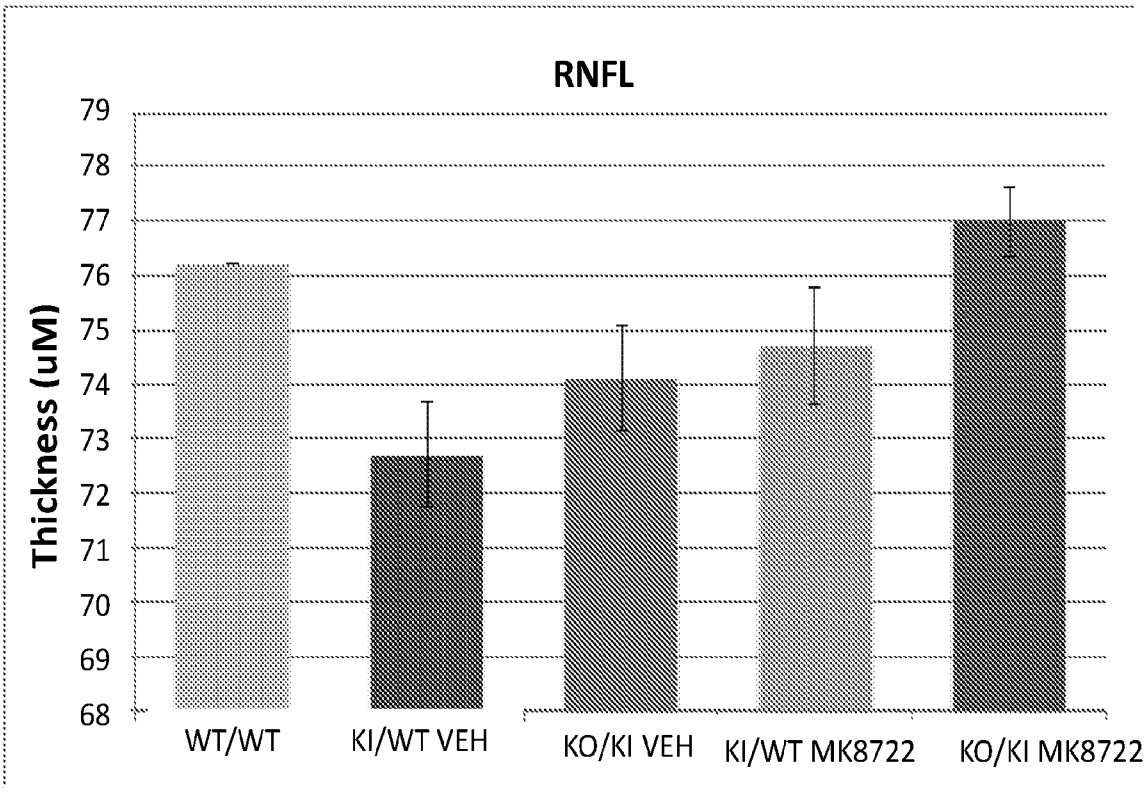
RNFL
Thickness (uM)
79
78
77
76
75
74
73
72
71
70
69
68
WT/WT
KI/WT VEH
KO/KI VEH
KI/WT MK8722
KO/KI MK8722

Fig. 9E

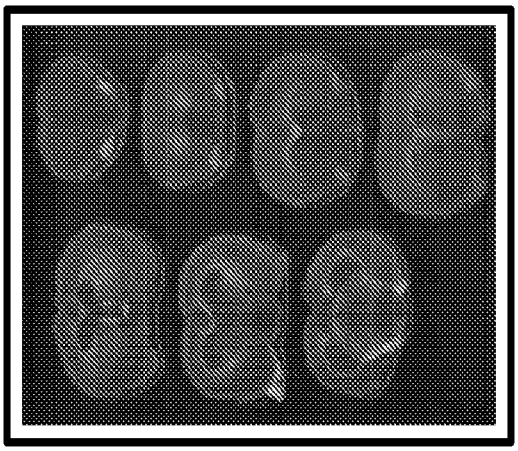

Fig. 10C

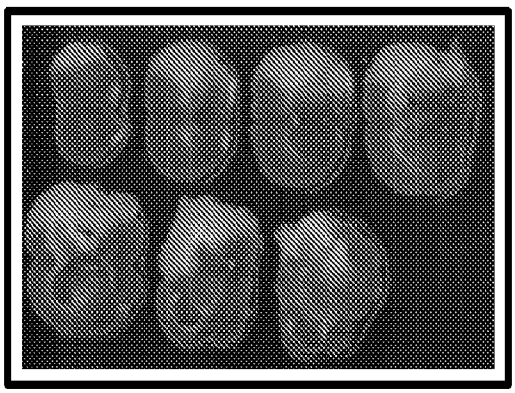

Fig. 10B

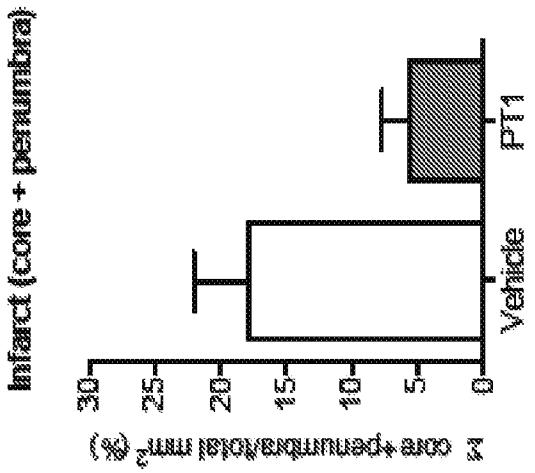

Fig. 10A

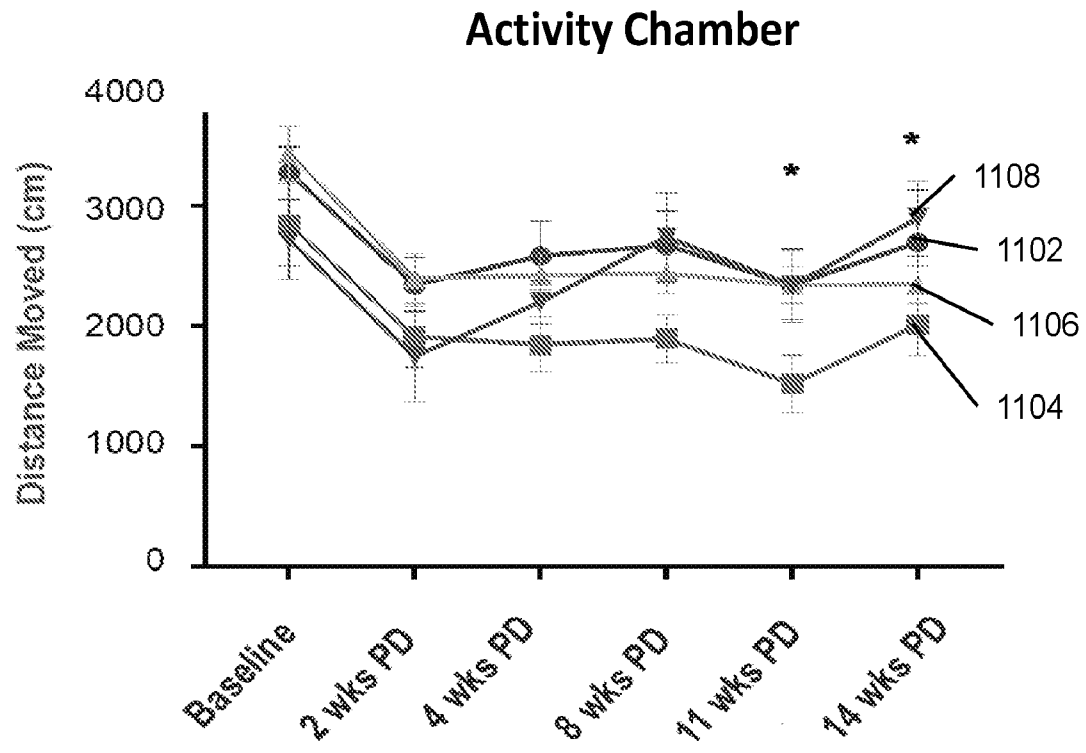

Fig. 11A

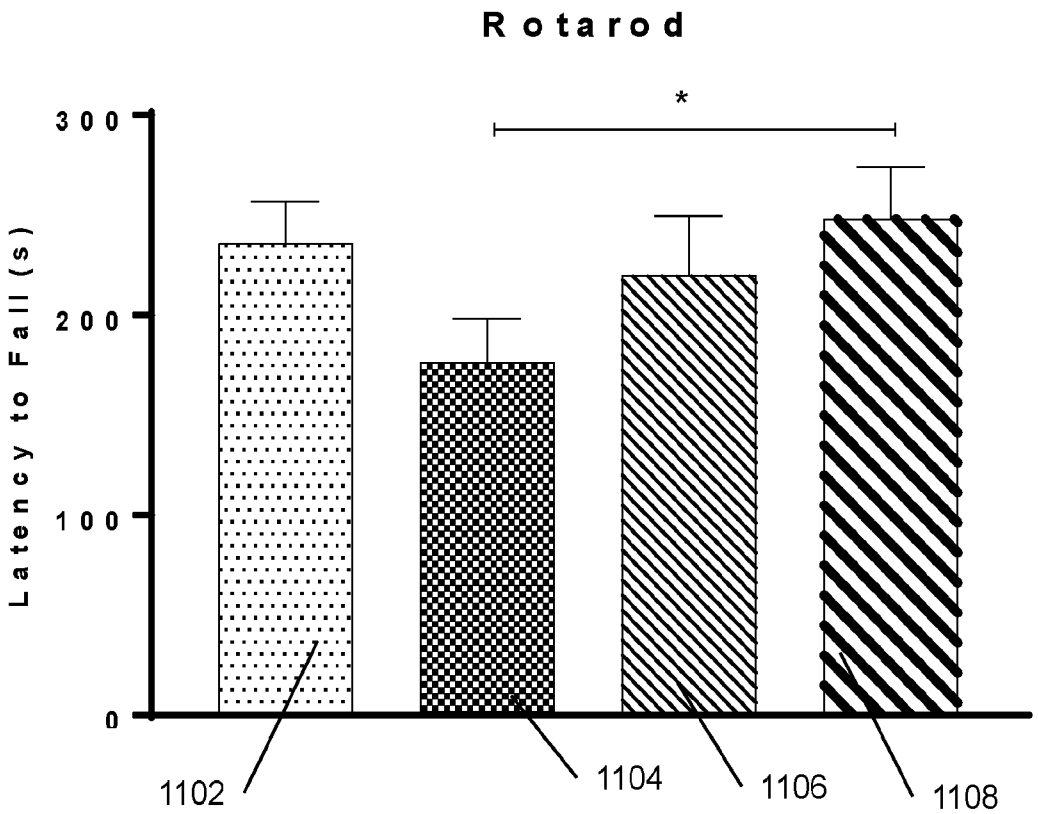

Fig. 11B

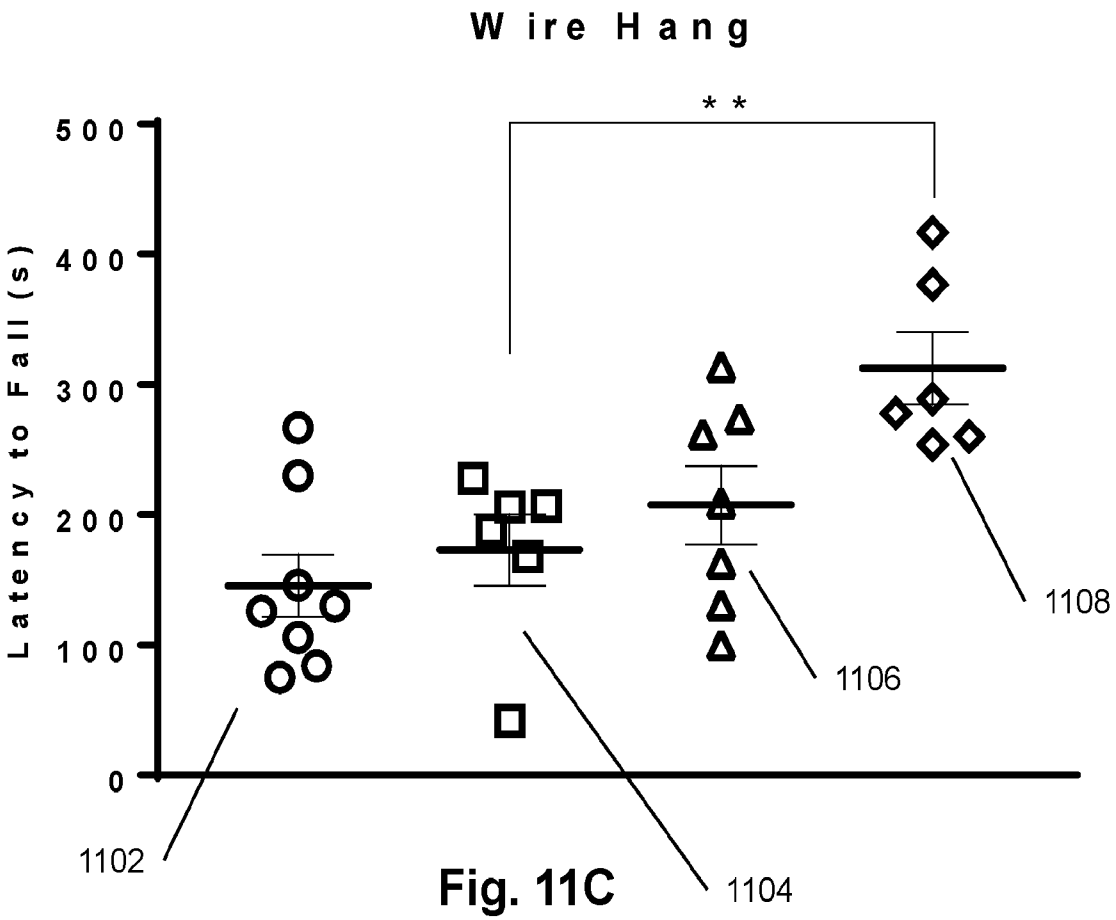
Wire Hang
* *
Latency to Fall (s)
500
400
300
200
100
0
1102
1104
1106
1108

Fig. 11C

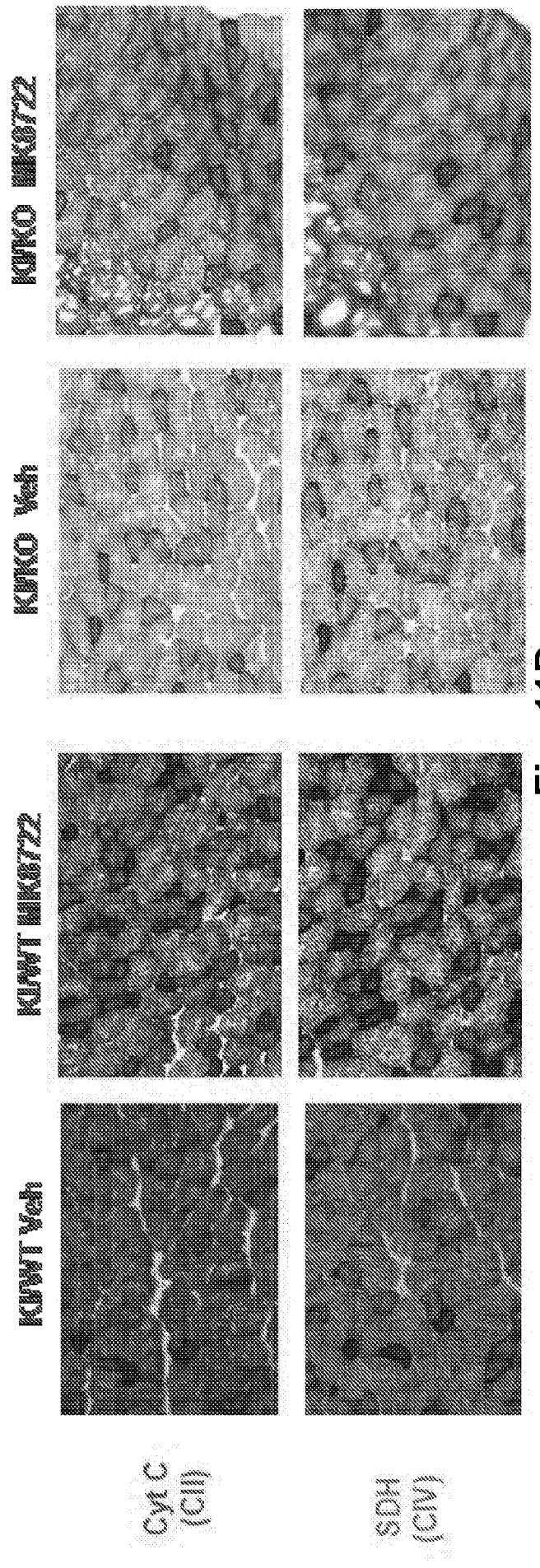

Fig. 11D

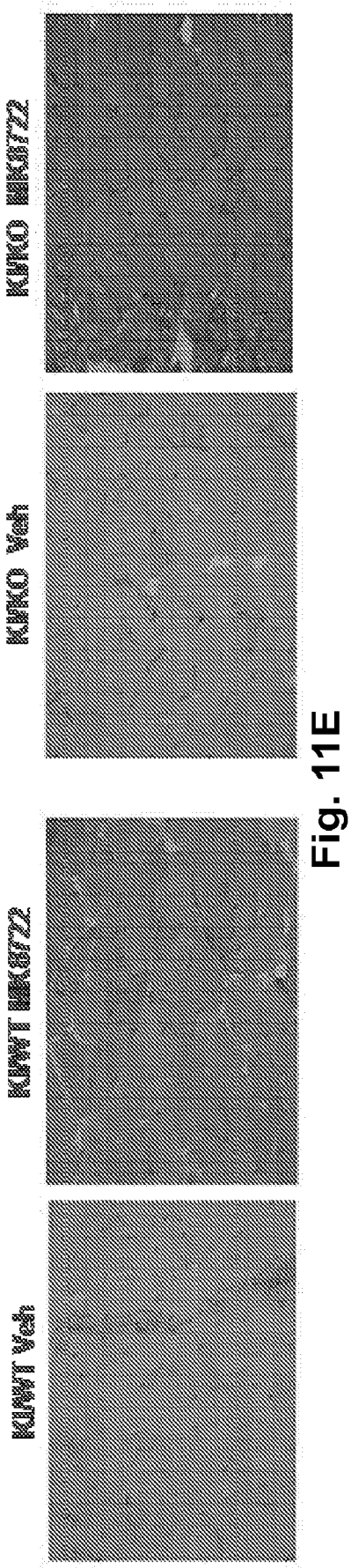

Fig. 11E

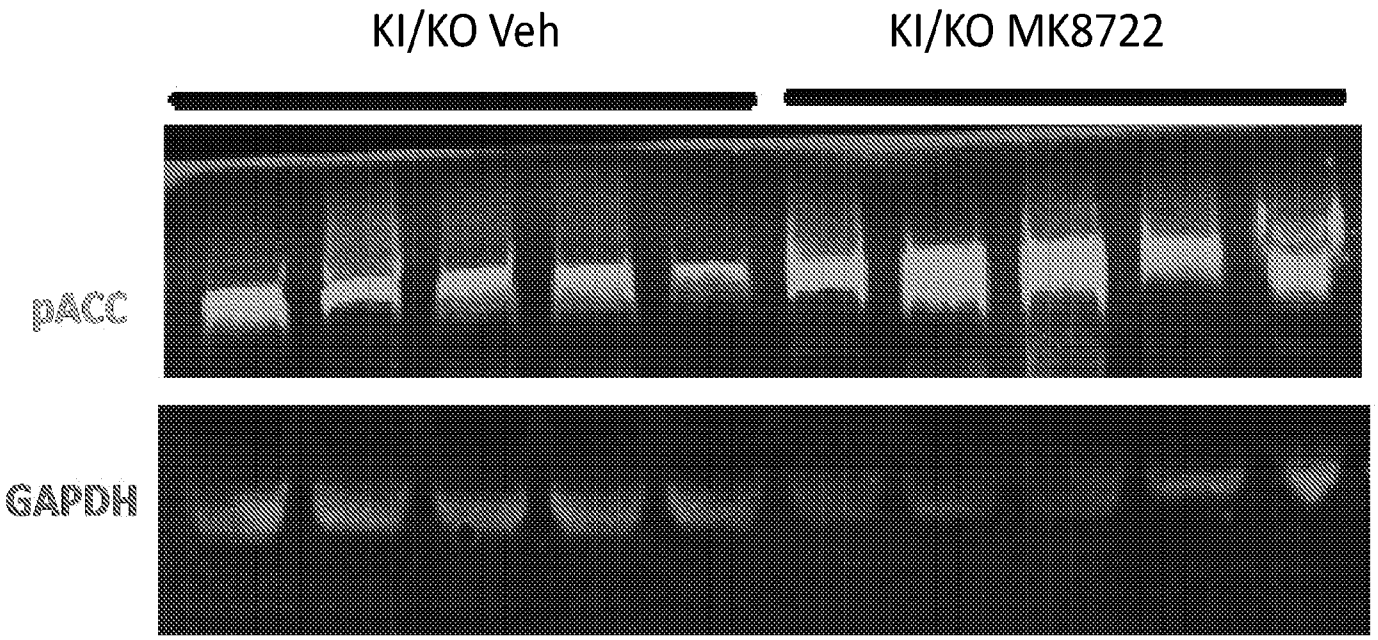

Fig. 11F

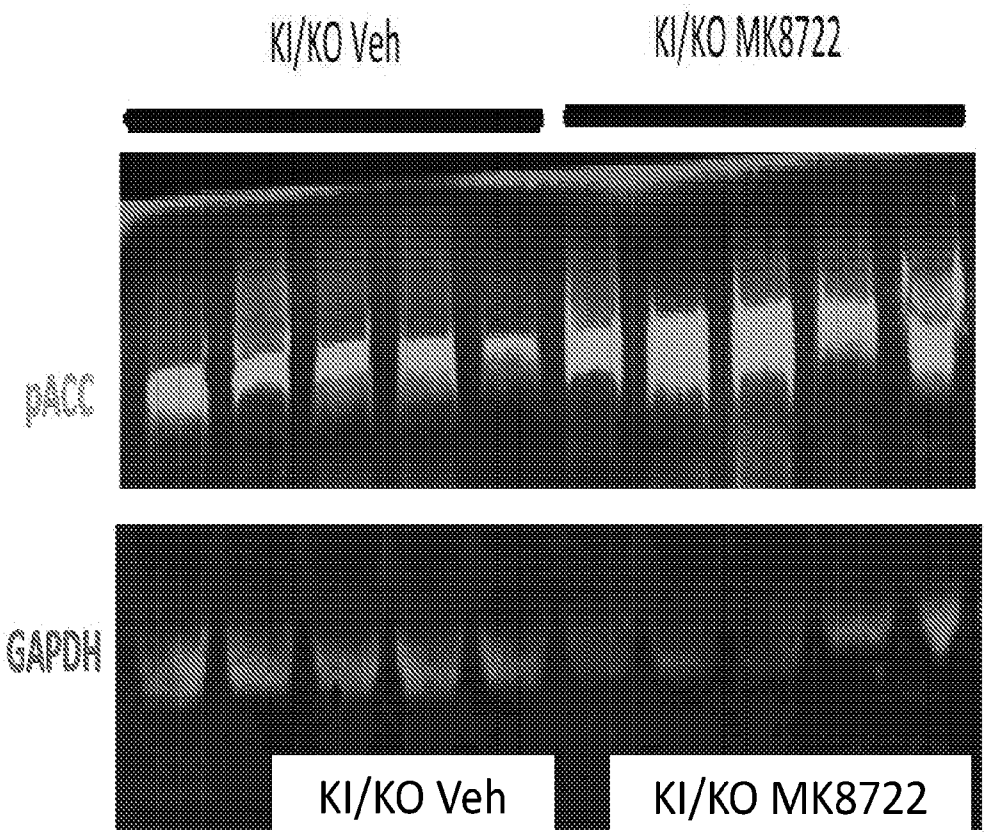

Fig. 11G

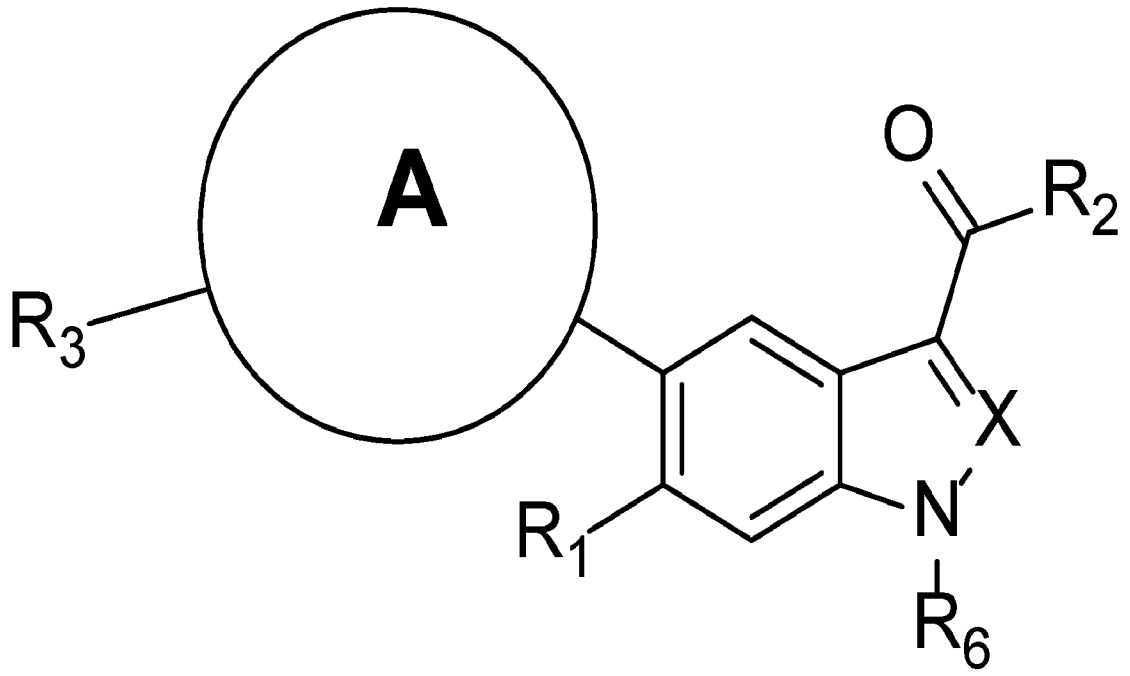

Fig. 12A

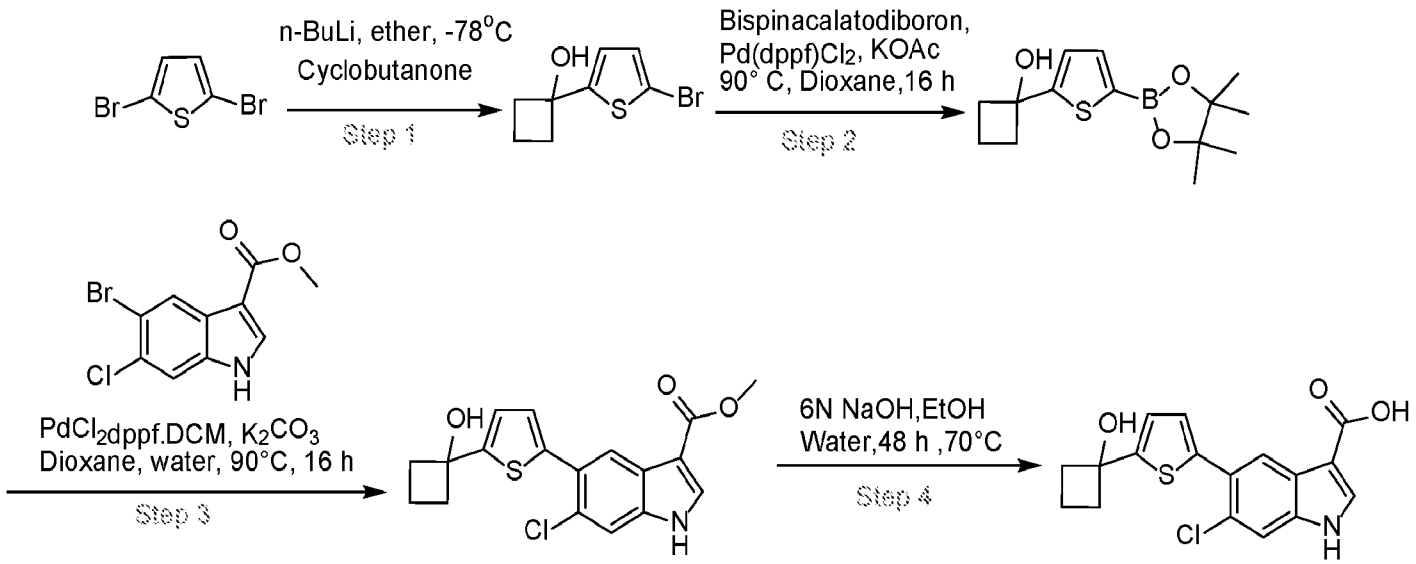

Fig. 12B

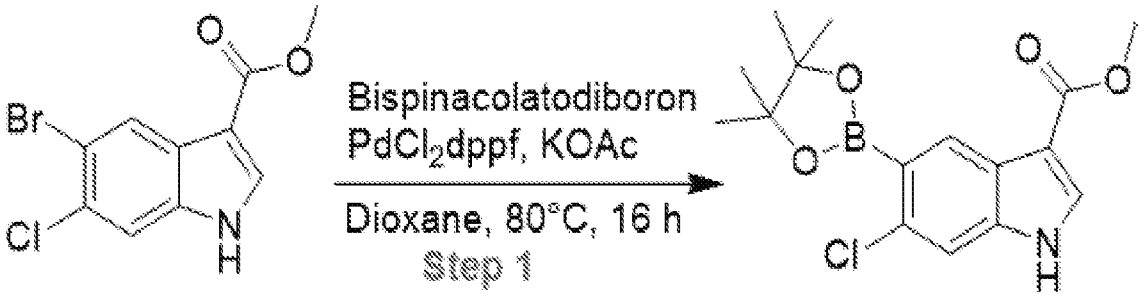
Br
Cl
N
H
O
O
Bispinacolatodiboron
PdCl2dppf, KOAc
Dioxane, 80°C, 16 h
Step 1
B
O
O
Cl
N
H
O
O

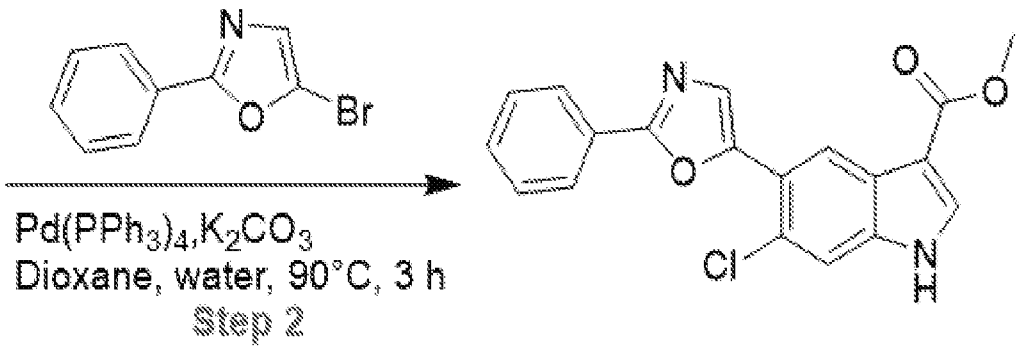
N
O
Br
Pd(PPh3)4,K2CO3
Dioxane, water, 90°C, 3 h
Step 2
N
O
Cl
N
H
O
O

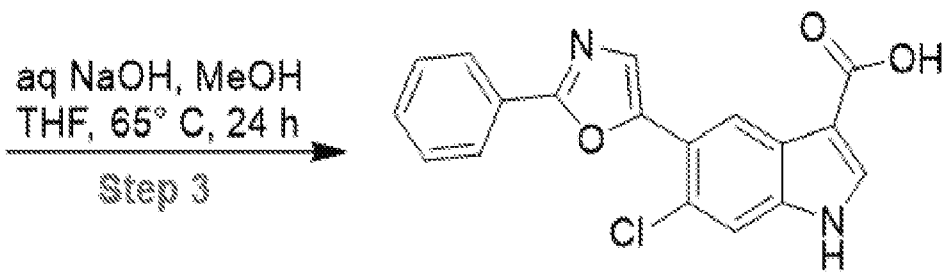
aq NaOH, MeOH
THF, 65° C, 24 h
Step 3
N
O
Cl
N
H
O
OH

Fig. 12C

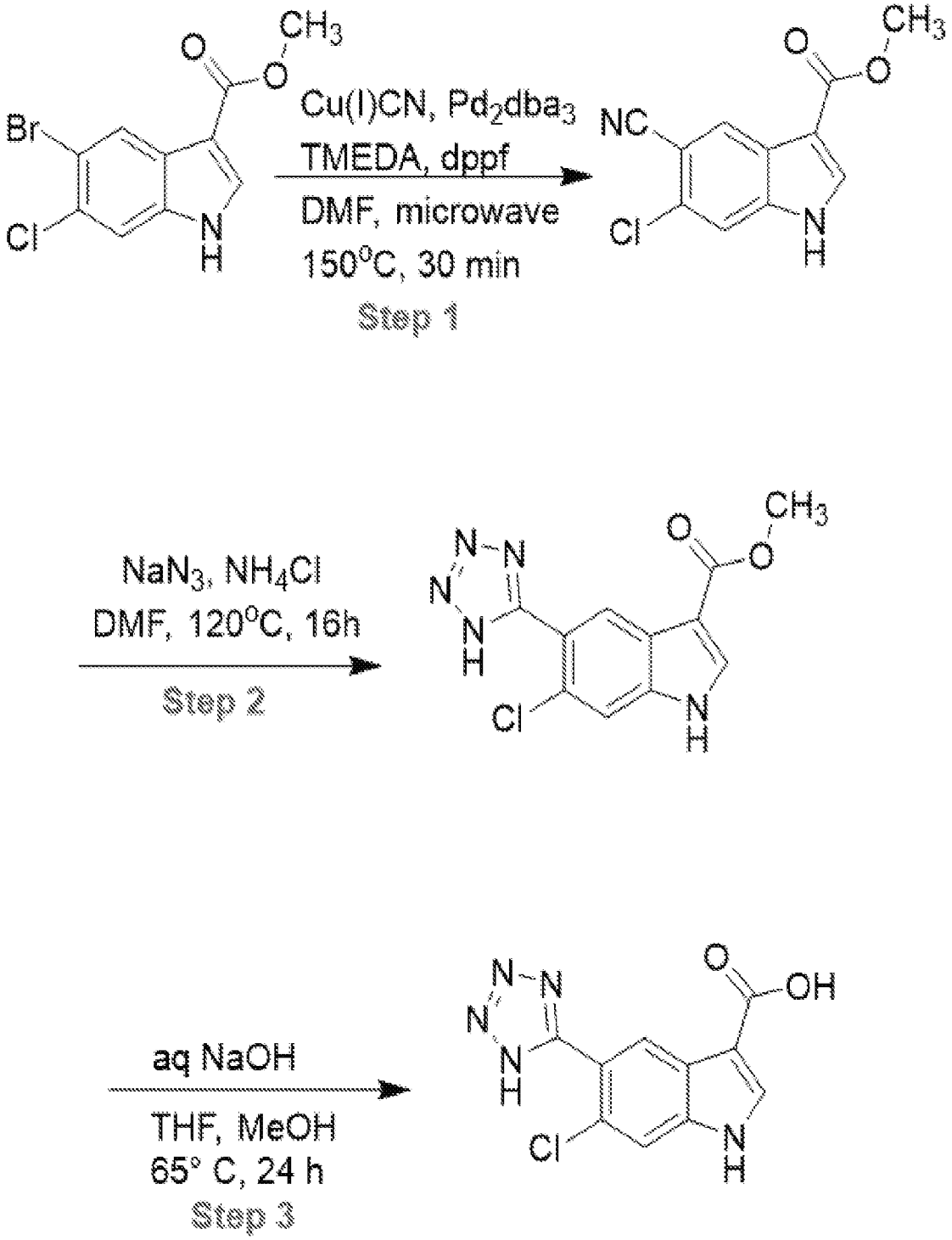
Br
Cl
O
O
CH3
N
H
Cu(I)CN, Pd2dba3
TMEDA, dppf
DMF, microwave
150°C, 30 min
Step 1
NC
Cl
O
O
CH3
N
H
NaN3, NH4Cl
DMF, 120°C, 16h
Step 2
N
N
N
H
Cl
O
O
CH3
N
H
aq NaOH
THF, MeOH
65° C, 24 h
Step 3
N
N
N
H
Cl
O
OH
N
H

Fig. 12D

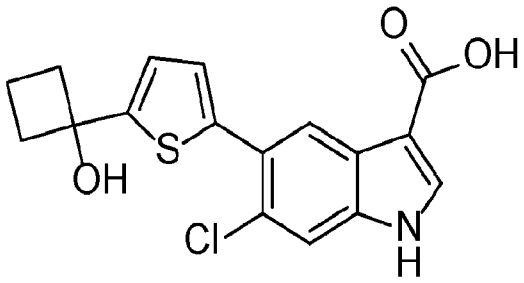

Fig. 13A

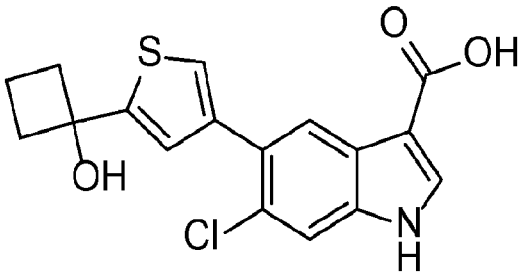

Fig. 13B

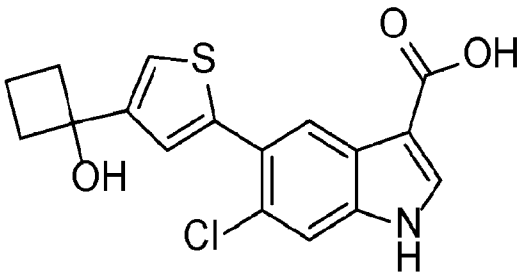

Fig. 13C

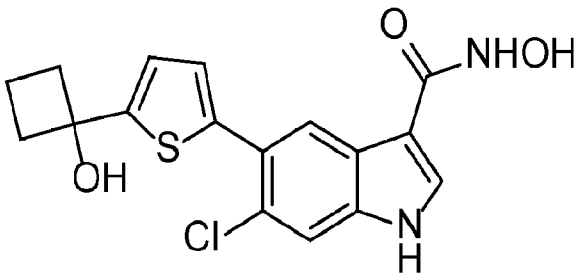

Fig. 13D

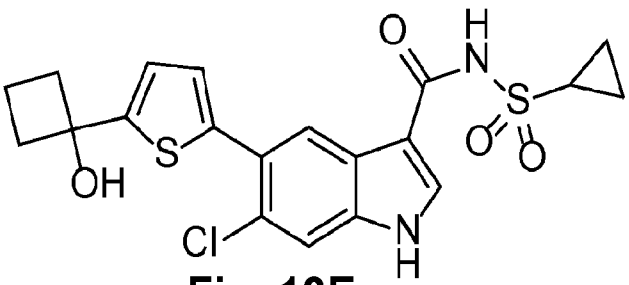

Fig. 13E

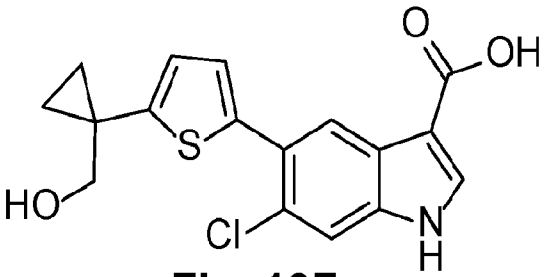

Fig. 13F

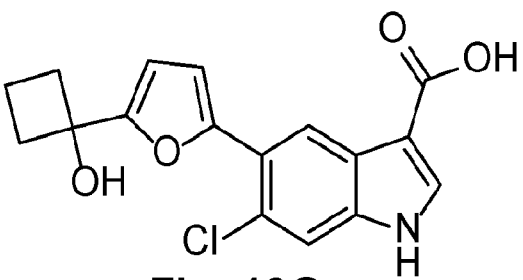

Fig. 13G

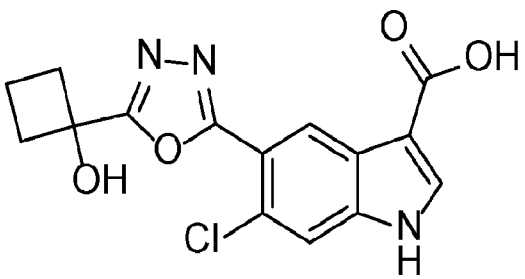

Fig. 13H

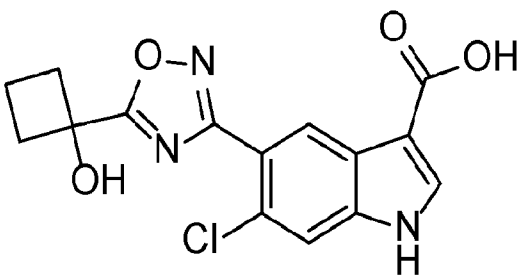

Fig. 13I

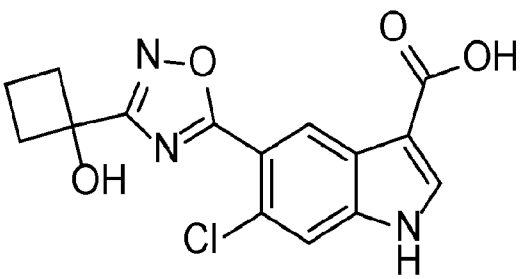

Fig. 13J

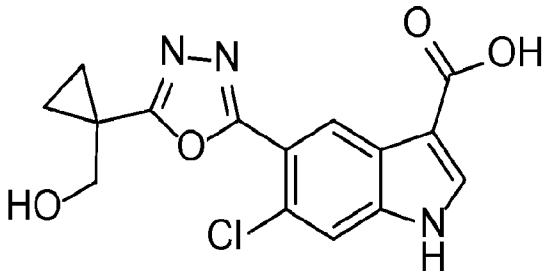

Fig. 13K

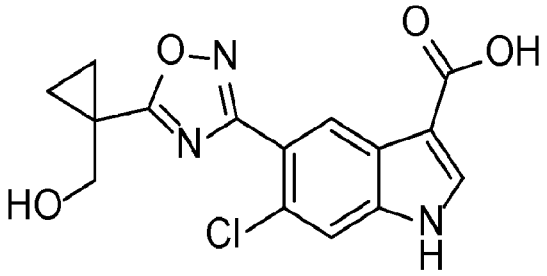

Fig. 13L

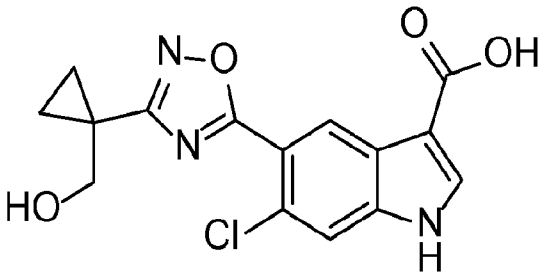

Fig. 13M

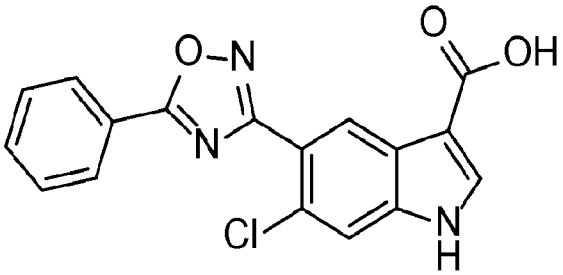

Fig. 13N

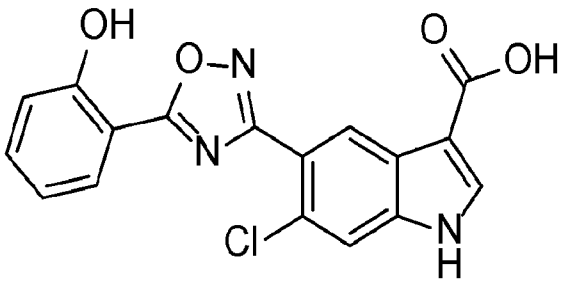

Fig. 13O

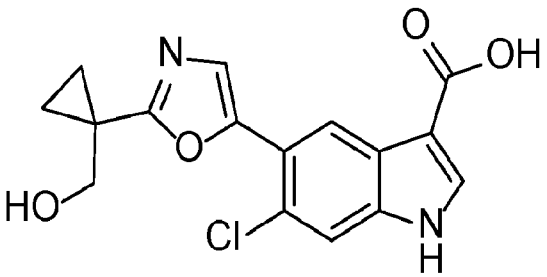

Fig. 13P

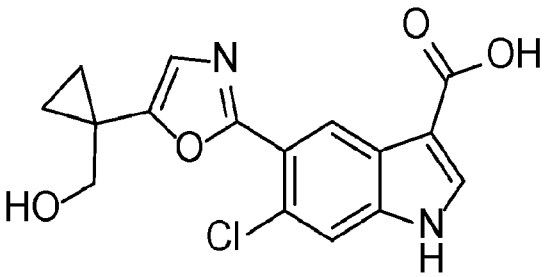

Fig. 13Q

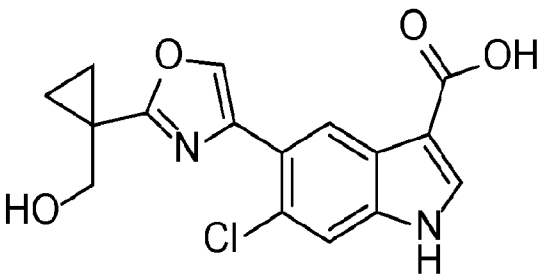

Fig. 13R

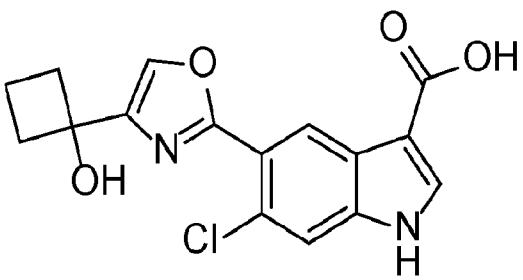

Fig. 13S

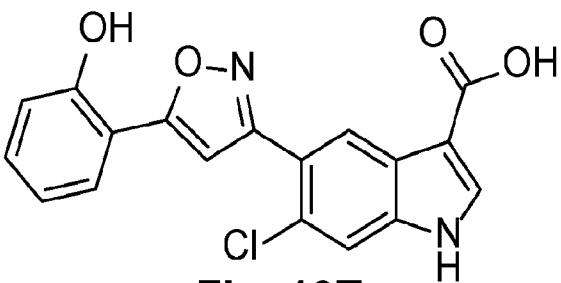

Fig. 13T

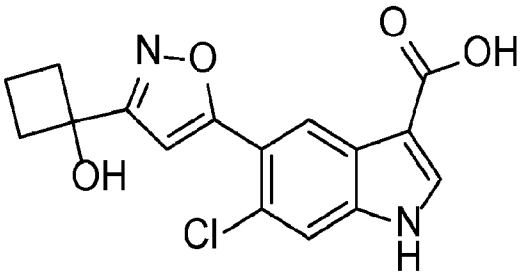

Fig. 13U

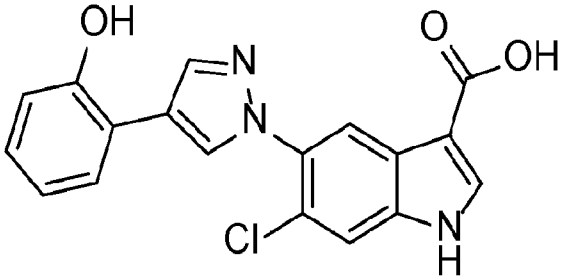

Fig. 13V

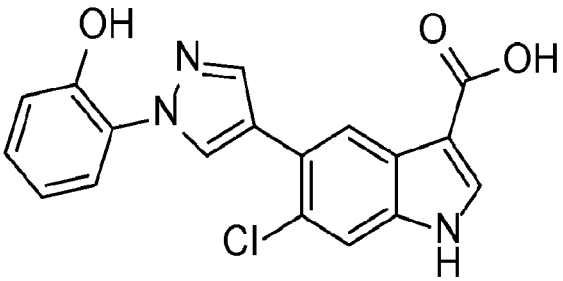

Fig. 13W

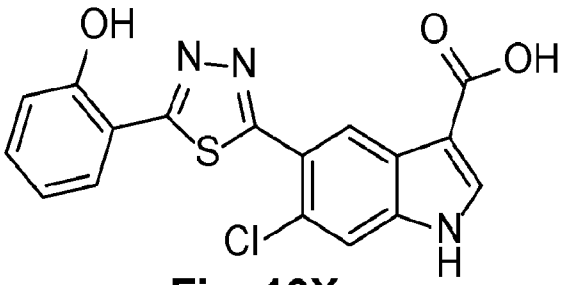

Fig. 13X

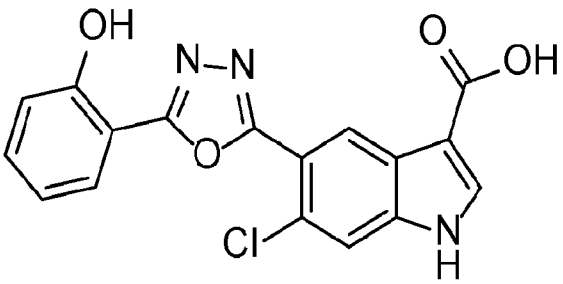

Fig. 13Y

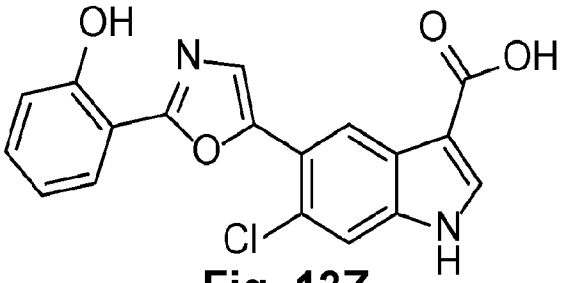

Fig. 13Z

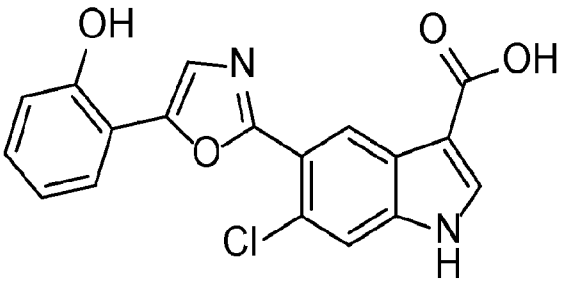

Fig. 14A

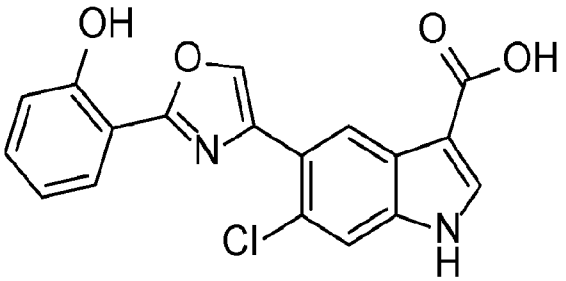

Fig. 14B

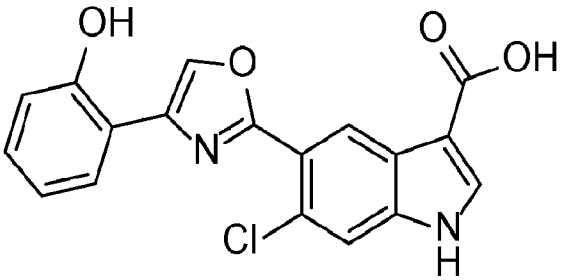

Fig. 14C

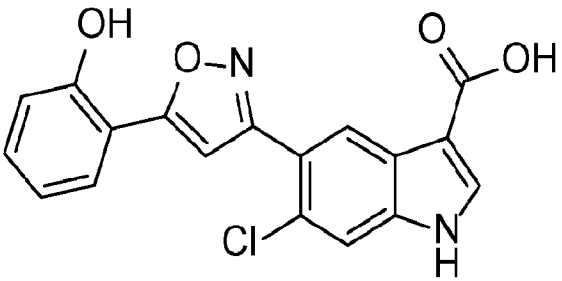

Fig. 14D

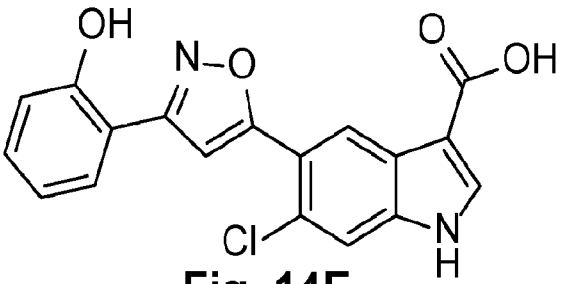

Fig. 14E

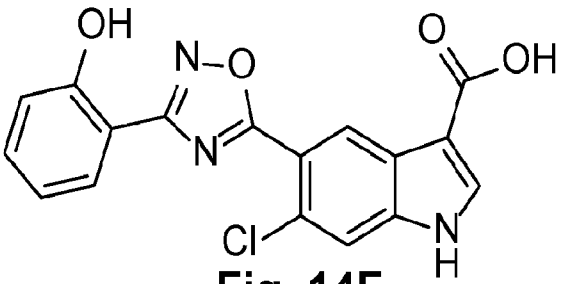

Fig. 14F

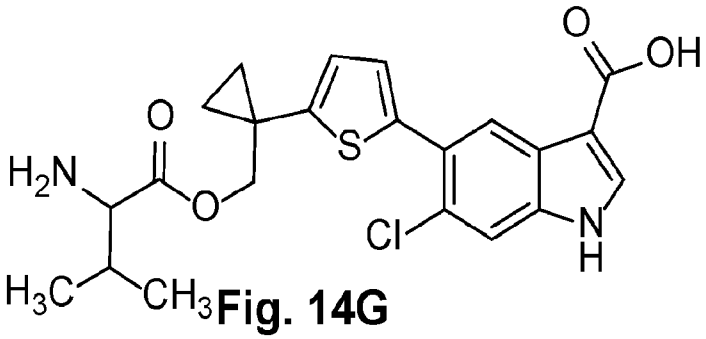

Fig. 14G

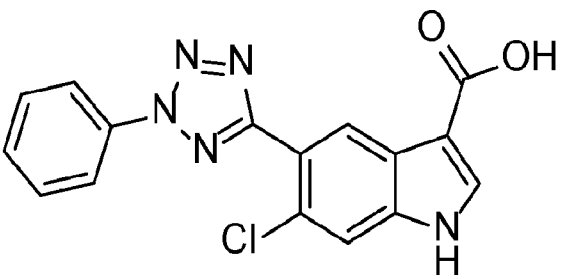

Fig. 14H

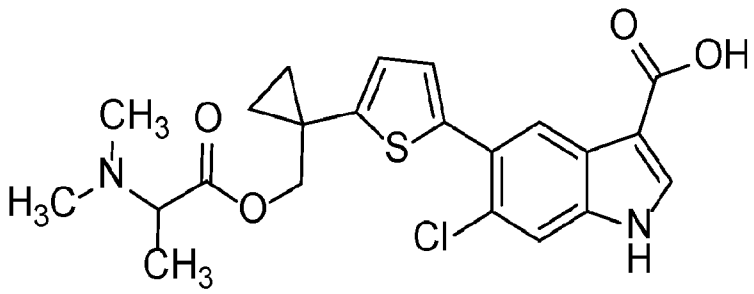

Fig. 14I

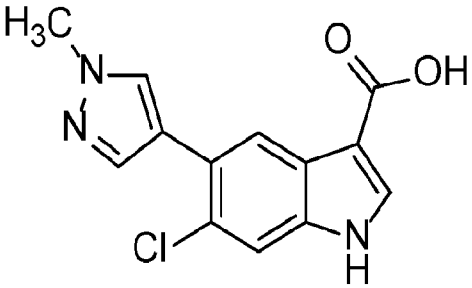

Fig. 14J

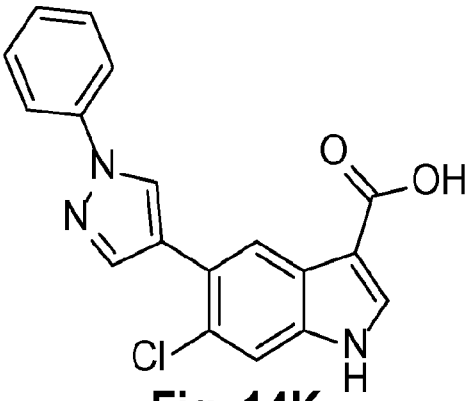

Fig. 14K

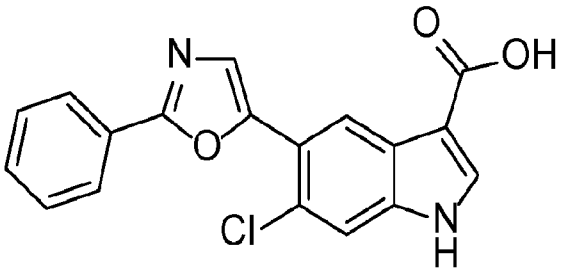

Fig. 14L

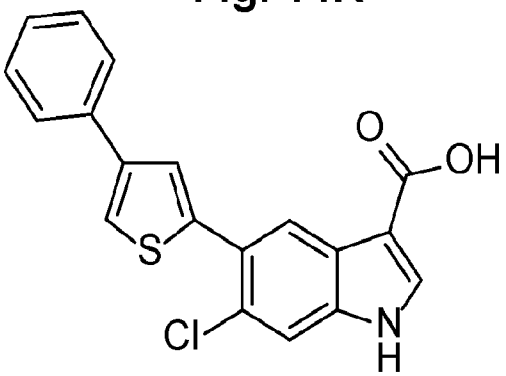

Fig. 14M

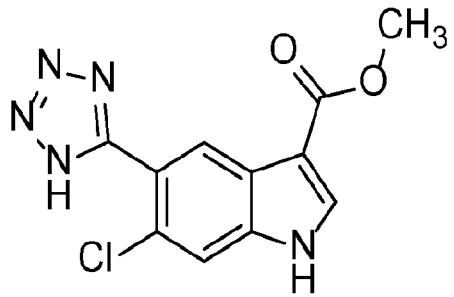

Fig. 14N

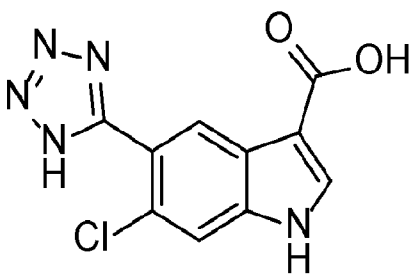

Fig. 14O

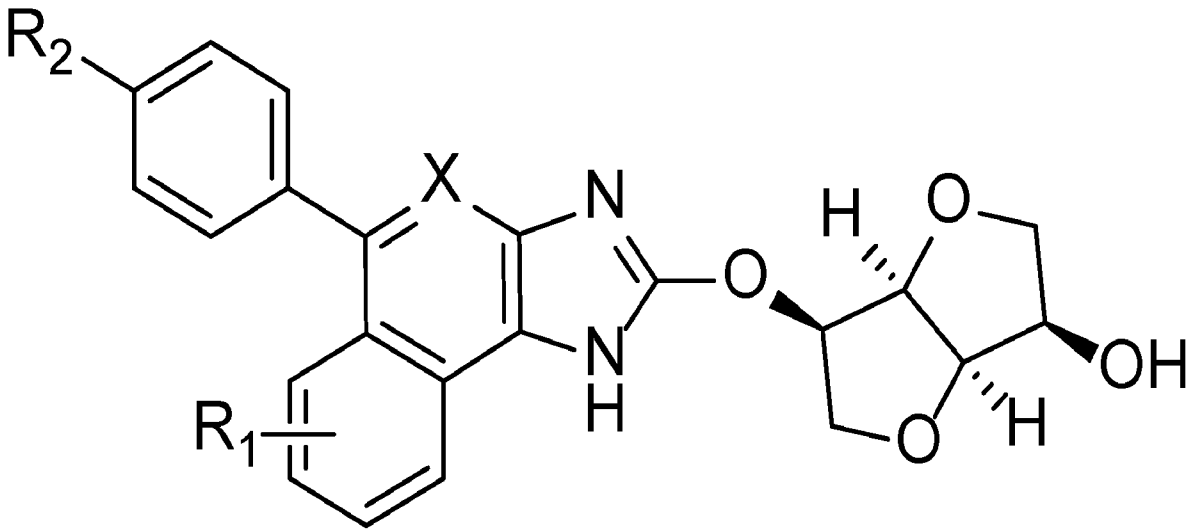

Fig. 15A

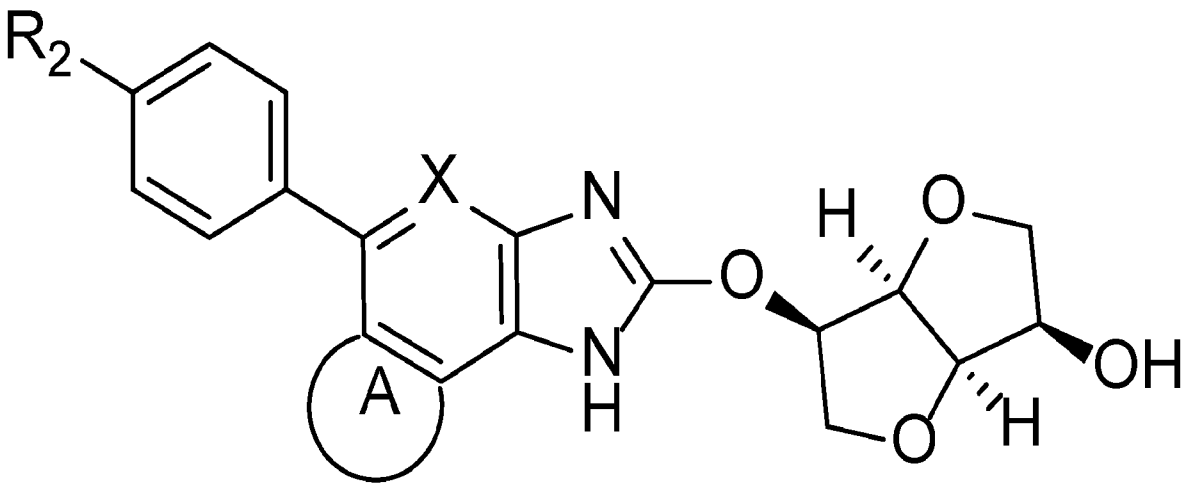

Fig. 15B

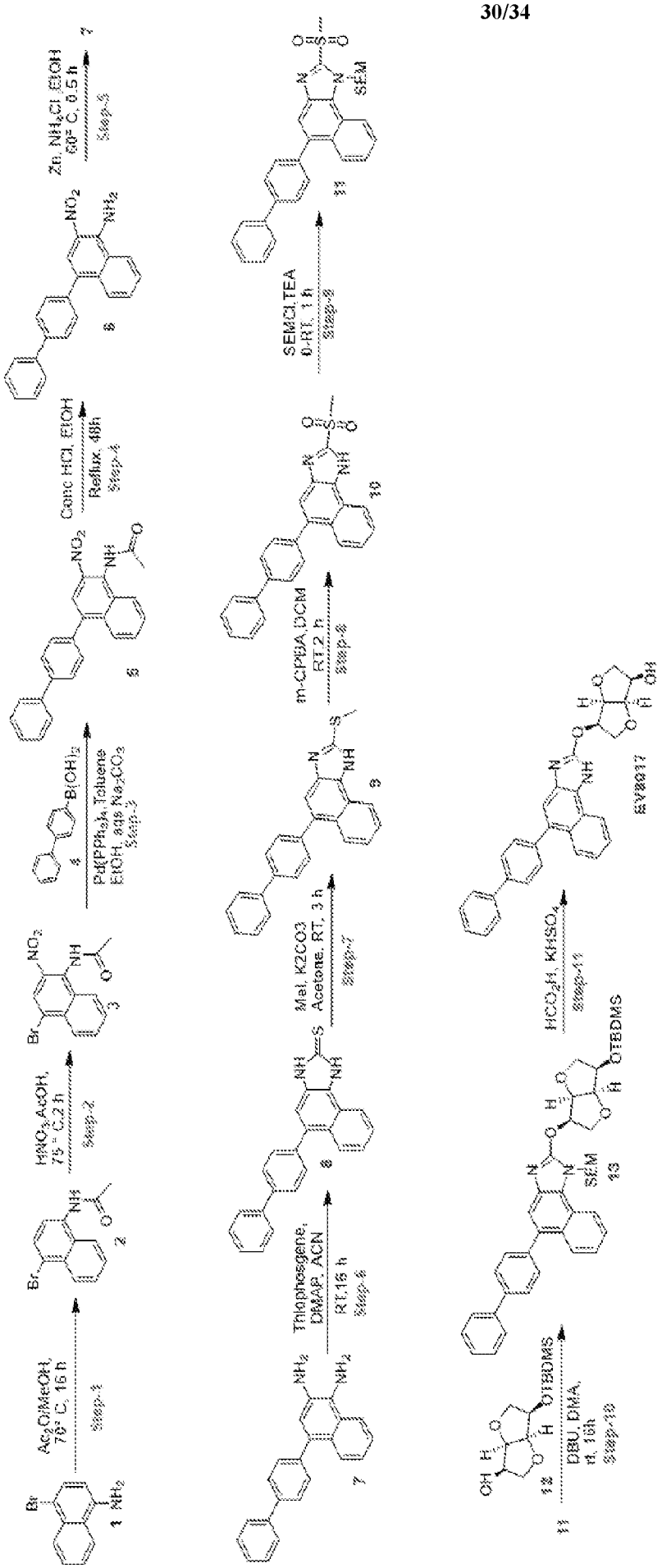

Fig. 15C

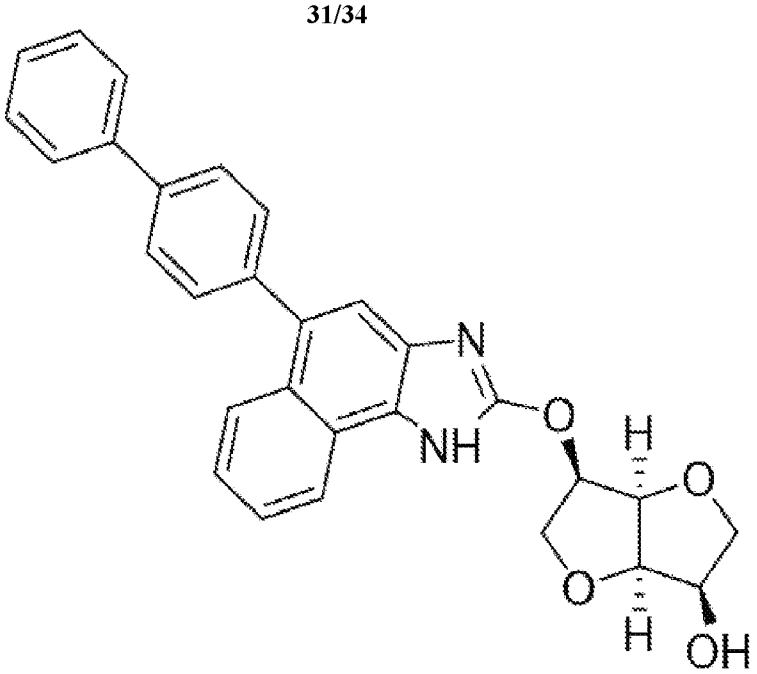

Fig. 15D

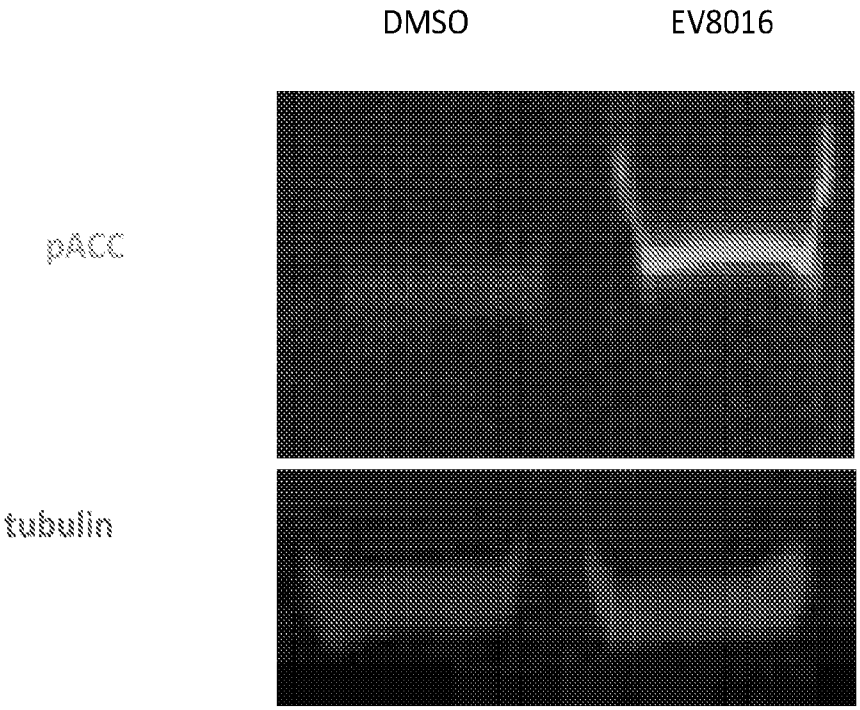

Fig. 16A

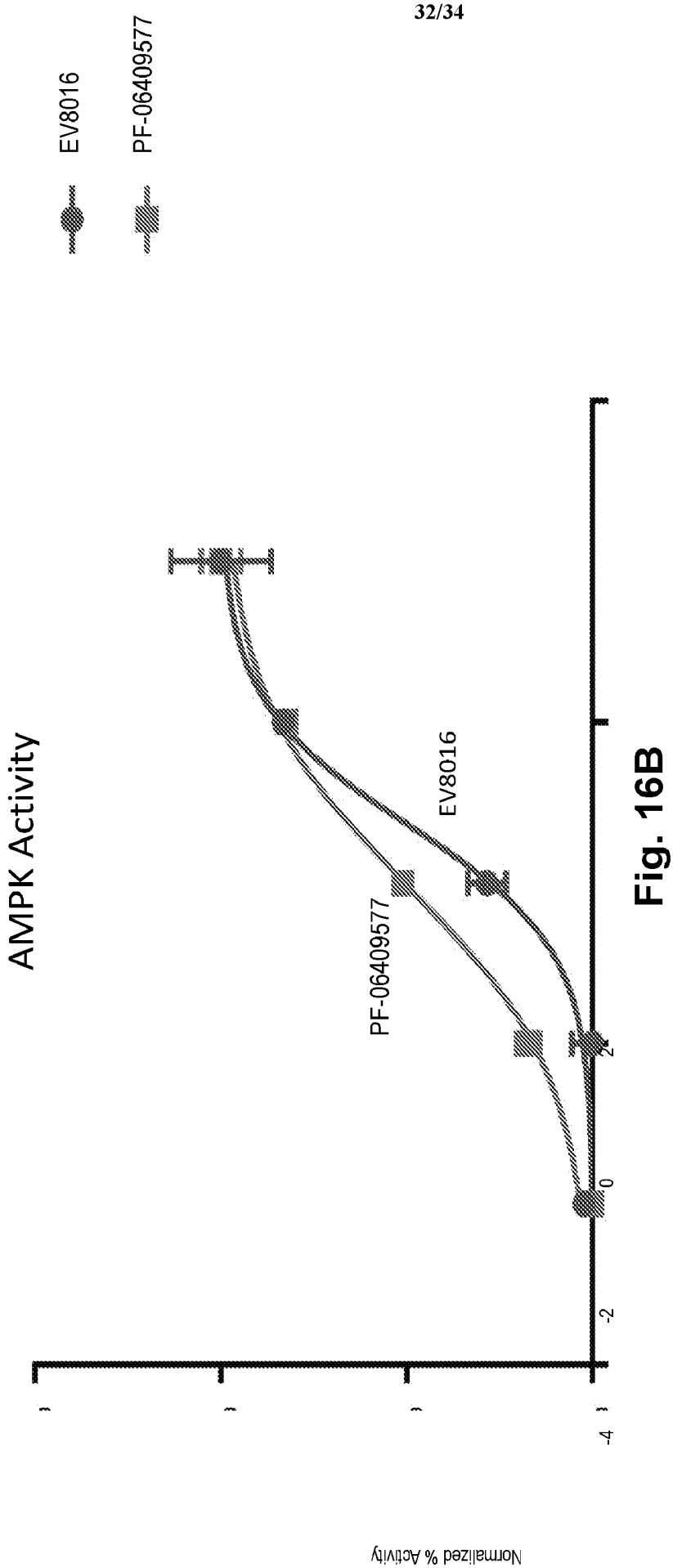
EV8016
PF-06409577
AMPK Activity
EV8016
PF-06409577
2
0
-2
-4
Normalized % Activity

Fig. 16B

1700

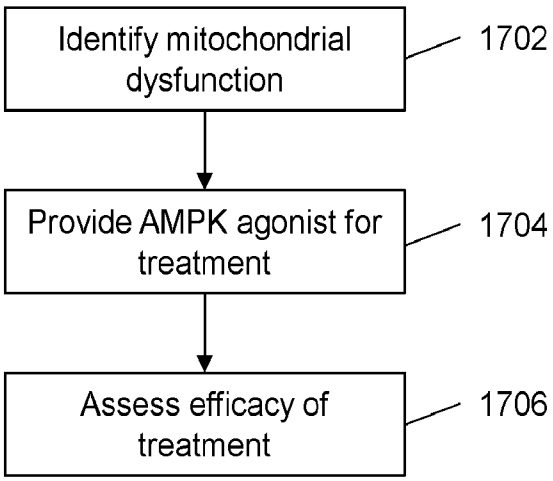
Identify mitochondrial dysfunction
1702
Provide AMPK agonist for treatment
1704
Assess efficacy of treatment
1706

Fig. 17

1800

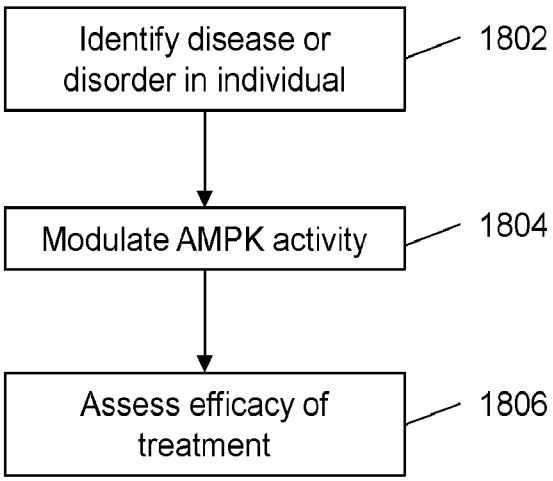
Identify disease or disorder in individual
1802
Modulate AMPK activity
1804
Assess efficacy of treatment
1806

Fig. 18

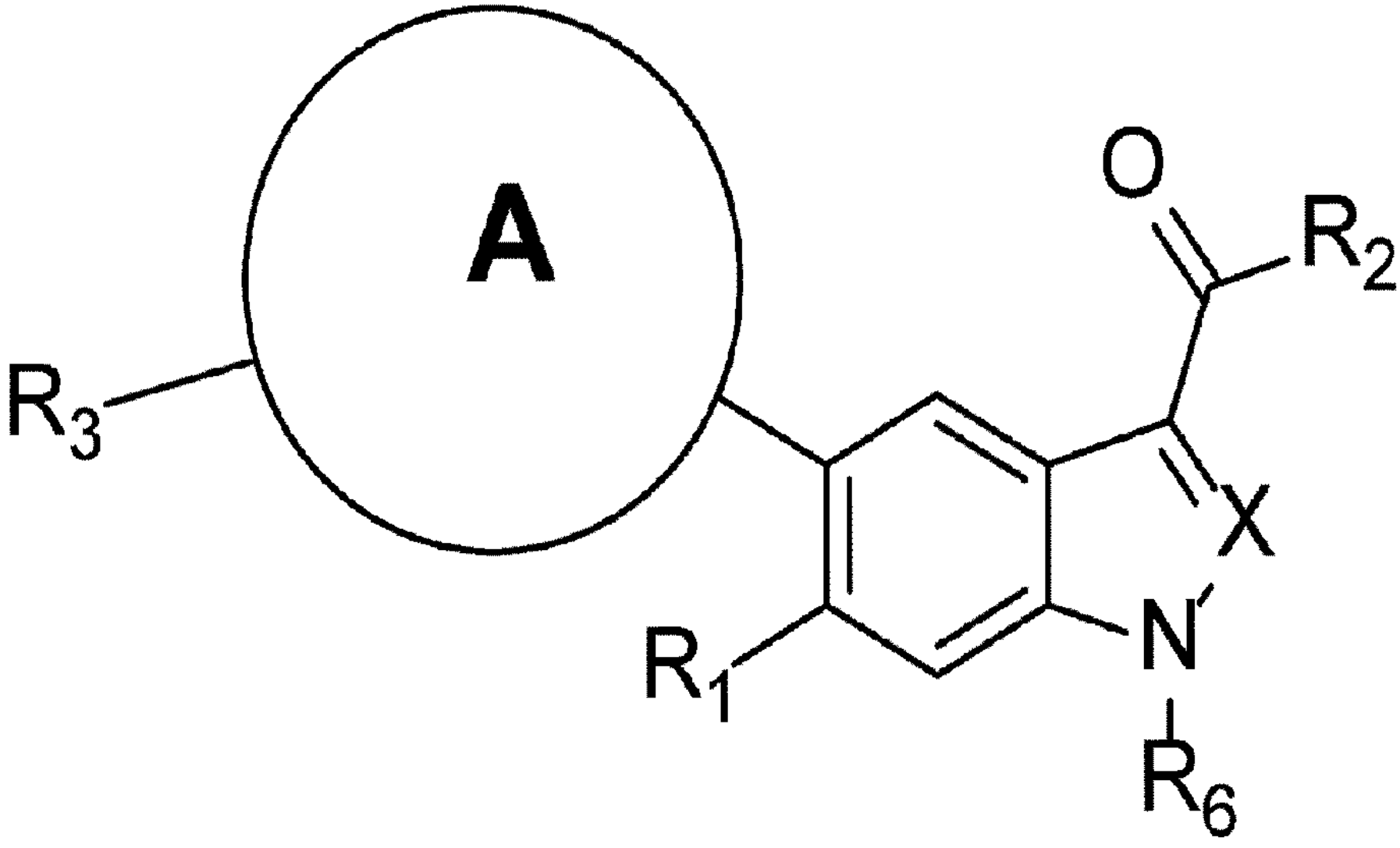

Fig. 12A